



# Preparation of Functional Polymer Surface with Fluorine-containing Groups

Tokuda, Kaya

---

(Degree)

博士 (工学)

(Date of Degree)

2015-03-25

(Date of Publication)

2016-03-01

(Resource Type)

doctoral thesis

(Report Number)

甲第6449号

(URL)

<https://hdl.handle.net/20.500.14094/D1006449>

※ 当コンテンツは神戸大学の学術成果です。無断複製・不正使用等を禁じます。著作権法で認められている範囲内で、適切にご利用ください。



Doctoral Dissertation

博士論文

Preparation of Functional Polymer Surface  
with Fluorine-containing Groups

(含フッ素基を用いた機能性高分子表面の創製)

January, 2015

平成 27 年 1 月

Graduate School of Engineering, Kobe University

神戸大学大学院 工学研究科

Kaya Tokuda

徳田 桂也





# Table of Contents

	page
General Introduction	1
<b>PART I</b>	<b>Surface Properties and Structure of Fluorinated Surfaces</b>
Chapter 1	Simple Way to Lower Surface Energy of Poly(methyl methacrylate) with Fluorinated Reagent
1.1.	Introduction 12
1.2.	Experimental 13
1.3.	Results and discussion 15
1.4.	Conclusions 22
1.5.	References 22
Chapter 2	Surface Structure to Achieve the Surface Free Energy Lower than 10 mJ/m <sup>2</sup>
2.1.	Introduction 26
2.2.	Experimental 28
2.3.	Results and discussion 29
2.4.	Conclusions 34
2.5.	References 34

**PART II      Surface Segregation of Poly(ethylene oxide) Side Chains  
using Perfluoroalkyl Groups and its Properties**

Chapter 3	Effect of Poly(ethylene oxide) Side Chains Length in Surface Modifier on Surface Properties	
	3.1. Introduction	38
	3.2. Experimental	39
	3.3. Results and discussion	43
	3.4. Conclusions	51
	3.5. References	52
Chapter 4	Effect of Poly(ethylene oxide) Side Chains Termini in Surface Modifier on Surface Properties	
	4.1. Introduction	56
	4.2. Experimental	57
	4.3. Results and discussion	60
	4.4. Conclusions	69
	4.5. References	69
Chapter 5	Effect of the Carbon numbers of Perfluoroalkyl groups in Surface Modifier on Surface Properties	
	5.1. Introduction	74
	5.2. Experimental	74
	5.3. Results and discussion	76
	5.4. Conclusions	81
	5.5. References	82

Chapter 6	Low-fouling polymer surface prepared by controlled segregation of poly(ethylene oxide) and its functionalization with biomolecule	
	6.1. Introduction	86
	6.2. Experimental	87
	6.3. Results and discussion	90
	6.4. Conclusions	96
	6.5. References	97
Conclusions		101
List of Achievements		
	Publications	108
	Presentations	110
	Awards	113
Acknowledgement		115







## **General Introduction**

Polymer materials have been used in many fields, from daily necessities to aerospace sciences due to their excellent bulk chemical and physical properties. Compared with other materials, such as metals, ceramics many polymers have good processability. However, polymer materials are inferior to other materials in point of strength, thermal resistance, electric conductivity and so on. To improve these bulk properties, composite materials have been widely studied [1-5].

For surface properties, surface modifications without losing bulk properties are widely performed for high performance of a number of applications such as adhesives, coatings, biomaterials, paints and wrappings. Many surface modification techniques have been developed to achieve desirable and valuable properties to fulfil adhesion property, biocompatibility, and lubricity [6, 7]. These properties directly relate to the surface wettability. Wetting on a solid surface is not only relevant to above properties but also itself an important phenomenon for coating, painting, and so on. The wettings of many kinds of liquids on solid surface have been in the center of attentions over the last few decades [8-15]. These phenomena have been studied both experimentally [16, 17] and theoretically [18, 19]. Focusing on water wettability, some research groups have reported the ultra-water repellent [20-27] and ultra-water wetting surfaces [27-30] through increasing surface roughness. For example, a microstructure, as typified by lotus leaf, was reported to bring about super water repellency to a surface whose contact angle was  $174^\circ$  [21]. McCarthy *et al.* reported more water repellent surface. On the nanostructured surface, a contact angle of water was  $179^\circ$  [31]. They are so-called physical method. On the other hand, controlling of surface free energy by modifying the surface chemical composition is also widely performed. For example, polar functional groups, such as hydroxy, amine, and carboxy groups, are introduced onto the material surfaces, then, the surface becomes hydrophilic by increasing the surface free energy [26-37]. On the other hand, long alkyl chains or fluorinated compounds are used to produce hydrophobic surfaces with low surface free energy. Especially, a fluorinated compound is well known to be effective for its remarkable surface-segregation. It was known to that the unique properties of C-F bounds brought the specific characteristics [38]. Fluorine has a small atomic radius and the biggest electro negativity among atoms. It forms a stable covalent bond with carbon. These bonds impede hydrogen bonding and

dispersion interactions with polar and non-polar liquids. There are a lot of researches about the hydrophobic modifications of polymer surfaces using fluorinated reagents [27, 28, 39-48] and fluorinated polymers [49-60].

Zisman and coworkers reported that the surface chemical species and concentrations of functional groups affects surface free energy, which decreased in the order of  $-\text{CH}_2- > -\text{CH}_3 > -\text{CF}_2- > -\text{CF}_2\text{H} > -\text{CF}_3$  [61].

It should be mentioned that the surface free energy of solid was estimated through the results of contact angle, since it cannot be measured directly. Therefore, several equations, which were combined with the Young equation, have been proposed to evaluate the surface free energy [6]. Hereafter, the surface free energy calculated from the equations is expressed as the  $\gamma_s$  value in this thesis.

Nishino and Ueda groups reported the surface of the vapor deposited *n*-perfluoroeicosane ( $\text{C}_{20}\text{F}_{42}$ ) film [62]. Single-like crystallites of  $\text{C}_{20}\text{F}_{42}$  were epitaxially grown with the molecular axis perpendicular to the substrate surface. The terminal  $-\text{CF}_3$  groups were completely organized in a hexagonally closest packing on the surface, which showed  $6.7 \text{ mJ/m}^2$ . It was the lowest  $\gamma_s$  value on solid surface.

The very low  $\gamma_s$  value was similarly obtained using fluorinated reagent. In 1999, Nakamae *et al.* demonstrated hydrophobizing poly(vinyl alcohol) surface by lowering surface free energy,  $10 \text{ mJ/m}^2$ , with a fluorinated silane coupling reagent. An original poly(vinyl alcohol) (PVA) surface is very hydrophilic and less resistant to water. After fluorination, the surface showed high water repellency whose contact angle of water was  $105^\circ$ . Compared with the original PVA surface, the fluorinated PVA surface showed low swelling ratio. This indicated that fluorinated PVA had resistance to water derived from fluorine on the surface [63].

Lowering  $\gamma_s$  value is achieved both by the surface coverage of  $-\text{CF}_3$  and  $-\text{CF}_2-$  groups, and by the ordered structures of the fluorinated compound [33-40]. Especially, self-assembled monolayers (SAMs) contained perfluoroalkylated ( $\text{CF}_3(\text{CF}_2)_n-$ ) compounds are well known to be effective. Nakamae and Nishino studied the structures and the  $\gamma_s$  values of fluorinated polymers, random and diblock copolymers of methyl

methacrylate and 2-perfluorooctylethyl methacrylate (PMMA-*r*-PFEMA and PMMA-*b*-PFEMA, respectively). They found that the  $\gamma_s$  value of the PMMA-*b*-PFEMA surface was lower than that of PMMA-*r*-PFEMA, because the PMMA-*b*-PFEMA surface was thoroughly covered with the -CF<sub>3</sub> groups while -CF<sub>2</sub>- groups and methacrylate backbones were likely to be exposed on the PMMA-*r*-PFEMA surface [64].

Fluorinated component plays an important role not only in lowering  $\gamma_s$  value but also in surface-segregating of hydrophilic component. Jannasch looked into the surface compositions of poly(styrene(S)-*block*-ethylene oxide (EO)) and poly(S-*graft*-EO) films. He reported that S segments having the PEO chain ends terminated by hydroxy groups were segregated on the copolymer surface, while EO segments were dominated on the film surface for the copolymers with fluorinated poly(ethylene oxide) (PEO) chain ends. These shows hydrophilic EO unit can be surface-segregated against the request of surface enrichment of hydrophobic segments under some conditions [65]. These fluorinated polymer surfaces were more hydrophilic than poly(S-*graft*-EO) surface and surface-segregated components affected its properties. The effect of a surface-segregated component on the property has been studied using many methods, because of the contribution for surface properties [66]. By using fluorine-containing groups as a driving force for surface-segregation, surface-segregated components were able to be controlled and multifunctional surfaces were easily designed.

The first aim of the present work is to show how to achieve a low energy surface through very simple method, by using fluorinated reagent. A poly(methyl methacrylate) (PMMA) surface was fluorinated by simply immersing it into 3-(perfluoro-7-methyloctyl)-1,2-epoxypropene, as shown in Figure 1, followed by heat treatment at 120°C. As describe earlier, fluorinated reagent have been used to make hydrophobic surfaces [29, 30, 40-49]. So far, these methods are effective in only case of there being reactive functional groups, such as hydroxy groups. Then, introduction of functional groups is necessary to use fluorinated reagent for polymer surface without functional groups, such as PMMA.

The fluorinated PMMA surface showed low  $\gamma_s$  value, 10 mJ/m<sup>2</sup>. In this way, for most

surface fluorination, the  $\gamma_s$  value down to  $10 \text{ mJ/m}^2$  was reported. To reach the  $\gamma_s$  value less than  $10 \text{ mJ/m}^2$ , the ordered structures of the fluorinated compound are essential. In this thesis, the relationship between inclination of perfluoroalkyl ( $R_f$ ) groups and  $\gamma_s$  value on the fluorinated surface was also observed.

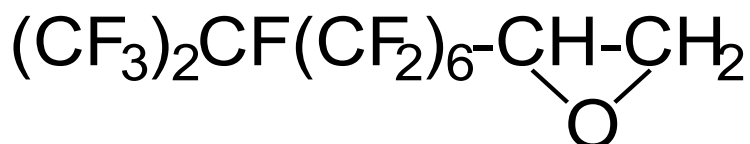


Figure 1 Chemical structure of 3-(perfluoro-7-methyloctyl)-1, 2-epoxypropane.

The second aim of the present work is to investigate the surface properties of polymer surface modified by MMA terpolymer containing both perfluoroalkyl ( $R_f$ ) groups and PEO chains as side chain, shown in Figure 2. As mentioned above, even hydrophilic component could be surface-segregated by using fluorine. Then, investigating the optimum condition of surface-segregation of hydrophilic components is of great importance to utilize them through easy method.

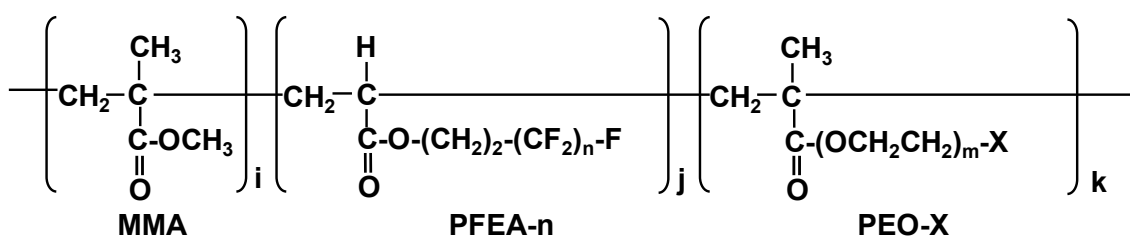


Figure 2 Chemical structure of P(MMA/PFEA-n/PEO-X).

This thesis consists of following two parts that have been subdivided into six chapters to fulfill the above aims.

**Part I** is concerned with the preparation of low energy surface using fluorine, and the effect of orientation of surface  $R_f$  groups on  $\gamma_s$  value. This part contains two chapters. In

**Chapter 1**, properties of fluorinated PMMA surface prepared by simple method were evaluated. In **Chapter 2**, *n*-perfluoroeicosane (C<sub>20</sub>F<sub>42</sub>) thin films were vapor deposited on glass. The  $\gamma_s$  value of these surfaces was measured, and the effect of the orientation of R<sub>f</sub> groups on the  $\gamma_s$  value was investigated. **Part II** is concerned the surface-segregation of PEO side chains promoted by R<sub>f</sub> groups which are involved in a single molecule. In **Chapter 3**, polymer surfaces were modified using mixture of following three polymers; methacrylate-based terpolymers (surface modifier) containing both R<sub>f</sub> groups and PEO as side chains in a single molecule, PMMA, and fluorinated copolymer. The structure and properties of the terpolymer modified surfaces were evaluated. The effect of PEO side chain length and the composition of matrix resin, which was composed PMMA and fluorinated polymer, on surface-segregation of PEO side chain was discussed. In **Chapter 4**, the PEO termini in terpolymer were changed and its surface properties were investigated. **Chapter 5** described the adhesion property of terpolymer modified surface which had different carbon numbers of R<sub>f</sub> groups. In **Chapter 6**, low-fouling properties of terpolymer modified surface were observed using several accretions. Moreover, the covalent immobilization of a functional biomolecule on the low-fouling surfaces was attempted.

## References

- [1] Morimune, S.; Kotera, M.; Nishino, T.; Goto, K.; Hata, K. *Macromolecules*, 2011, 44, 4415.
- [2] Morimune, S.; Nishino, T.; Goto, K. *ACS Appl. Mater. Interfaces*, 2012, 4, 3596.
- [3] Beese, A. M.; Sarkar, S.; Nair, A.; Naraghi, M.; An, Z.; Moravsky, A.; Loutfy, R. O.; Buehler, M. J.; Nguyen, S. T.; Espinosa, H. D. *ACS NANO*, 2013, 7, 3434.
- [4] Irin, F.; Das, S.; Atore, F. O.; Green, M. J. *Langmuir*, 2013, 29, 11449.
- [5] Xu, L.; McGraw, J.; Gao, F.; Grundy, M.; Ye, Z.; Gu, Z.; Shepherd, J. L. *J. Phys. Chem.*, 2013, 117, 10730.
- [6] Garbassi, F.; Morra, M.; Occhiello, E. *Polymer Surfaces : From Physics to Technology*, John Wiley & Sons, Chichester, 1988.
- [7] Feast, W. J.; Munro, H. S.; Richards, R. W., eds. *Polymer Surface and Interface II*, Wiley, Chichester, 1993.

- [8] de Gennes, P. G. *Rev. Mod. Phys.*, 1985, 57, 827.
- [9] Nakajima, K.; Nakagawa, Y.; Furuta, T.; Sakai, M.; Isobe, T.; Matsushita, S. *Langmuir*, 2013, 29, 9269.
- [10] Furmidge, C. G. L. *J. Colloid Sci.* 1962, 17, 309.
- [11] Carre, A.; Shanahan, M. E. R. *J. Adhes.* 1995, 49, 177-185.
- [12] Yoshimitsu, Z.; Nakajima, A.; Watanabe, T.; Hashimoto, K. *Langmuir*, 2002, 18, 5818.
- [13] Zhang, X.; Cai, Y.; Mi, Y. *Langmuir*, 2011, 27, 9630.
- [14] Richard, D.; Quere, D. *Europhys. Lett.*, 1999, 48, 286.
- [15] Dettre, R. H.; Johnson, R. E. Jr. *Advances in Chemistry Series*; American Chemical Society: Washington, DC, 1964, Vol. 43, pp 136.
- [16] Heslot, F.; Cazabat, A. M.; Levinson, P.; Fraysee, N. *Phys. Rev. Lett.*, 1990, 65, 599.
- [17] Heslot, F.; Cazabat, A. M.; Fraysee, N.; Levinson, P. *Adv. Colloid Interface Sci.*, 1992, 39, 129.
- [18] Li, X.; Hu, Y.; Wang, H. *J. Appl. Phys.*, 2006, 39, 24905.
- [19] De Coninck, J. *J. Colloid Surf., A.*, 1996, 114, 155.
- [20] Watanebe, N.; Tei, Y. *Kagaku*, 1991, 46, 477.
- [21] Onda, T.; Shibuichi, S.; Satoh, N.; Tsujii, K. *Langmuir*, 1996, 12, 2125.
- [22] Zhai, L.; Cebeci, F. C.; Cohen, R. E.; Rubner, M. F. *Nano Lett.*, 2004, 4, 1349.
- [23] Riekerrink, M. B. O.; Terlingen, G. A. J.; Egbers, G. H. M.; Feigen, J. *Langmuir*, 1999, 15, 4847.
- [24] Youngblood, J. P.; McCarthy, T. J. *Macromolecules*, 1999, 32, 6800.
- [25] Chen, W.; Fadeev, A. Y.; Hsieh, M. C.; Oner, D.; Youngblood, J.; McCarthy, T. J. *Langmuir*, 1999, 15, 3395.
- [26] Coulson, S. R.; Woodward, I. S.; Badyal, J. P. S. *Chem. Mater.*, 2000, 12, 2031.
- [27] Teshima, K.; Sugimura, H.; Inoue, Y.; Takai, O.; Takano, A. *Langmuir*, 2003, 19, 10624.
- [28] Tadanaka, K.; Morinaga, J.; Matsuda, A.; Minami, T. *Cham. Mater.*, 2000, 12, 590.
- [29] Minko, S.; Muller, M.; Motornov, M.; Nichke, M.; Grundke, K.; Stamm, M. *J. Am. Chem. Soc.*, 2003, 125, 3896.
- [30] Feng, X.; Feng, L.; Jin, M.; Zhai, J.; Jiang, L.; Zhi, D. *J. Am. Chem. Soc.*, 2004, 126,



62.

- [31] Gao, L.; McCarthy, T. M. *J. Am. Chem. Soc. Commun.*, 2006, 128, 9052.
- [32] Sogiv, J.J. *Am. Chem. Soc.* 1980, 102, 92.
- [33] Tillman, N.; Ulman, A.; Penner, T. L. *Langmuir*, 1989, 5 101.
- [34] Wasserman, S. R.; Tao, Y. T.; Whitesides, G. M. *Langmuir*, 1989, 5, 1074.
- [35] Terlingen, G. A. J.; Hoffman, A. S.; Feijen, J. *J. Appl. Polym. Sci.*, 1994, 50, 1529.
- [36] Terlingen, G. A. J.; Takens, G. A. J.; van der Gaag, F. J.; Hoffman, A. S.; Feijen, J. *J. Appl. Polym. Sci.*, 1994, 52, 39.
- [37] Hyum, J. *Polymer*, 2001, 42, 6473.
- [38] Zisman, W. A. *Advance in Chemistry*, 1964, 43, Washington, DC, p. 1.
- [39] Abe, K.; Takiguchi, H.; Tamada, K. *Langmuir*, 2000, 16, 2394.
- [40] Ederth, T.; Tamada, K.; Claesson, P. M.; Valiokas, R.; Colorado Jr., R.; Graupe, M.; Shmakova, O. E.; Lee, T. R. *J. Colloid Interface Sci.* 2001, 235, 391.
- [41] Colorado Jr., R.; Lee, T. R. *Langmuir*, 2003, 19, 3288.
- [42] Jia, X.; McCarthy, T. J. *Langmuir*, 2002, 18, 683.
- [43] Pellerite, M. J.; Wood, E. J.; Jones, V. W. *J. Phys. Chem. B*, 2002, 106, 4746.
- [44] Genzer, J.; Efimenko, K. *Science*, 2000, 290, 2130.
- [45] Thanawala, S. K.; Chaudhury, M. K. *Langmuir*, 2000, 16, 1256.
- [46] Winter, R.; Nixon, P. G.; Grad, G. L.; Graham, D. J.; Castner, D. G.; Holcomb, N. R.; Grainger, D. W. *Langmuir*, 2004, 20, 5776.
- [47] Guo, Y.; Di, C.; Liu, H.; Zheng, J.; Zhang, L.; Yu, G.; Liu, Y. *ACS NANO*, 2010, 4, 5749.
- [48] Durand, N.; Gaveau, P.; Silly, G.; Améduri, B.; Boutevin, B. *Macromolecules*, 2011, 4 6249.
- [49] Li, K.; Wu, P.; Han, Z. *Polymer*, 2002, 43, 4079.
- [50] Ha, J. W.; Park, I. J.; Kim, D. K.; Kim, J. H.; Lee, S. B. *Surf. Sci.*, 2003, 328, 532-535.
- [51] Berret, J-F.; Calvet, D.; Collet, A.; Viguier, M. *Current Opinion in Colloid and Interface Sci.*, 2003, 8, 296.
- [52] Ito, H.; Imae, T.; Nakamura, T.; Sugiura, M.; Oshibe, Y. *J. Colloid Interface Sci.*, 2004, 276, 290.
- [53] Tsibouklis, J.; Nevell, T. G. *Adv. Mater.*, 2003, 15, 647.

- [54] Borkar, S.; Jankova, K.; Siesler, H. W.; Hvilsted, S. *Macromolecules*, 2004, 37, 788.
- [55] McCloskey, C. K.; Yip, C. M.; Santerre, J. P. *Macromolecules*, 2002, 35, 924.
- [56] Tan, H.; Xie, X.; Li, J.; Zhong, Y.; Fu, Q. *Polymer*, 2004, 45, 1495.
- [57] Bertolucci, M.; Galli, G.; Chiellini, E.; Wynne, K. J. *Macromolecules*, 2004, 37, 3666.
- [58] van Ravenstein, L.; Ming, W.; van de Grampel, R. D.; de With, G.; Loontjens, T.; Thune, P. C.; Niemantsverdriet, J. W. *Macromolecules*, 2004, 37, 408.
- [59] Tervoort, T.; Vigjager, J.; Graf, B.; Smith, P. *Macromolecules*, 2000, 33, 6460.
- [60] Scherirs, J., ed. *Modern Fluoropolymers*, John Wiley & Sons, Chichester, 1997.
- [61] Schulman, F.; Zisman, W. A. *J. Colloid Sci.*, 1952, 7, 465.
- [62] Nishino, T.; Meguro, M.; Nakamae, K.; Matsusima, M.; Ueda, Y. *Langmuir*, 1999, 15, 4321.
- [63] Nishino, T.; Meguro, M.; Nakamae, K. *Int. J. Adhes.*, 1999, 19, 39.
- [64] Nishino, T.; Urushihara, Y.; Meguro, M.; Nakamae, K. *J. Colloid Interface Sci.*, 2004, 279, 364.
- [65] Jannasch, P. *Macromolecules*, 1998, 31, 1341.
- [66] Hook, A. L., Chang, C., Yang, J., Luckett, J., Cockayne, A., Atkinson, S., Mei, Y., Bayston, R., Irvine, D. J., Langer, R., Anderson, D. G., Williams, P., Davies, M. C., Alexander, M. R. *Nat. Biotechnol.* 2012, 30, 868.



# **Part I**

## **Surface Properties and Structure of Fluorinated Surfaces**



## **Chapter 1**

# **Simple Way to Lower Surface Energy of Poly(methyl methacrylate) with Fluorinated Reagent**

## 1.1. Introduction

Surface fluorination is matchlessly effective to achieve desirable surface properties such as low adhesive property, lubricity and hydrophobicity without changing bulk properties [1-3]. Typical and easy fluorinated methods use using coupling reagent containing fluorine [4-6]. For example, the hydroxy groups on a poly(vinyl alcohol) surface were able to be fluorinated using a fluorinated silane coupling reagent, which brought about a hydrophobic surface with the  $\gamma_s$  value of  $10 \text{ mJ/m}^2$ . Durand *et al.* reported hydrophobic silica surface by radical addition of tetrafluoroethylene [7]. Nyström *et al.* reported that a super water repellent and self cleaning cellulose surface was obtained via grafting of glycidyl methacrylate to hydroxy groups followed by fluorination [8]. These methods need reactive functional groups, such as hydroxy groups on a substrate surface. Then, these methods are easy but can be applied to limited substrates.

Poly(methyl methacrylate) (PMMA) is a typical amorphous polymer and possess several desirable bulk properties such as high strength, dimensional stability, optical transparency and high wear resistance. Because of the high transparency, PMMA has been utilized widely for optical instruments [9]. For producing hydrophobicity on a PMMA surface, a coupling reagent method can not be applied to the surface, because PMMA potentially has no special reactive group which reacts with a fluorinated coupling reagent.

In this chapter, PMMA was purposely selected as a substrate whose surface potentially has no functional groups for fluorination. However, a ring-opened glycidyl group shows very high reactivity and might be introduced to a PMMA surface. The surface of PMMA was fluorinated with the fluorinated reagent containing glycidyl and perfluoroalkyl groups. The low-fouling properties and anti-fouling property of the fluorinated PMMA surface against fingerprints were examined through albumin adsorption, thrombogenesis, and wettability of oleic acid.

## 1.2. Experimental

### 1.2.1. Sample preparation

PMMA, commercially called Acrypet VH and kindly supplied by Mitsubishi Rayon Co. Ltd. (Tokyo, Japan), was used in this study. The number average molecular weight ( $M_n$ ) and the polydispersity index  $M_w/M_n$  ( $M_w$  is the weight average molecular weight) from gel permeation chromatography were  $7.6 \times 10^4$  and 3.1, respectively. PMMA was twice purified by reprecipitation from acetone solution to 10 times the volume of methanol. The PMMA film was achieved by casting on a polyethylene (PE) sheet from 0.05 g/mL chloroform solution at room temperature. The cast film was dried in air for 24 h and under vacuum at 40°C for 24 h. PMMA film was rinsed with cyclohexane for 5 min after being immersed in 3-(perfluoro-7-methyloctyl)-1, 2-propyleneoxide [Figure 1-1, Wako Pure Chemical Industries, Ltd., Osaka, Japan] for 30 min at 25°C. Then, the film was air dried and heat-treated at 120°C for 24 h.

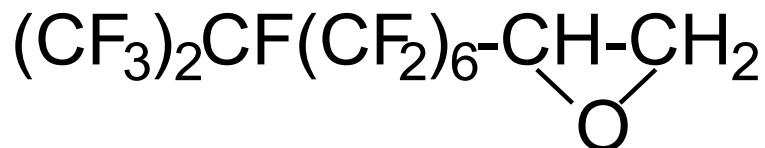


Figure 1-1 Chemical structure of 3-(perfluoro-7-methyloctyl)-1, 2-epoxypropane.

### 1. 2. 2. Characterization

X-ray photoelectron spectroscopy (XPS) measurements were carried out using a Shimadzu ESCA-850 to investigate the surface composition and bindings.  $\text{MgK}\alpha$  radiation, generated at 8 kV, 30 mA, was irradiated on the films, and then the XPS spectra were collected at 90° of the take-off angle between the sample and the analyzer. The pressure in the instrumental chamber was less than  $1.0 \times 10^{-5}$  Pa. No radiation damage was observed during the data collection.

The dynamic contact angles of distilled water and diiodomethane were measured at room temperature [10-12]. The advancing contact angle ( $\theta_a$ ) and the receding contact angle ( $\theta_r$ )



were measured when the droplet enlarged (< 2 mm diameter) and shrunk, respectively. The average contact angle ( $\theta_{av}$ ) was calculated as

$$\theta_{av} = \cos^{-1} \left\{ (1/2)(\cos \theta_a + \cos \theta_r) \right\}. \quad (1)$$

The surface free energy  $\gamma_s$  of the polymer solid was calculated using the contact angles by Eqs. (2) and (3), which were proposed by Owens and Wendt [12] who extended the Fowkes concept [13].

$$\gamma_s^d + \gamma_s^p = \gamma_s, \quad (2)$$

$$(1 + \cos \theta) \gamma_l = 2(\gamma_s^d \gamma_l^d)^{1/2} + 2(\gamma_s^p \gamma_l^p)^{1/2}, \quad (3)$$

where  $\gamma_l$  is the surface free energy of the liquid, and  $\gamma_l^d$  and  $\gamma_l^p$  are its dispersion and polar components, respectively. The  $\gamma_l^d$  and  $\gamma_l^p$  values of water are 21.8 and 51.0 mJ/m<sup>2</sup> and those of diiodomethane are 48.5 and 2.3 mJ/m<sup>2</sup>, respectively [12]. To evaluate the  $\gamma_s$  value from the contact angles, several equations have been proposed. In this study, the Young–Owens equation was used to simplify the evaluation, because the polar component contributed negligibly little to the total  $\gamma_s$  value in this study, as shown below. In addition, the static contact angle of oleic acid was also measured at room temperature to estimate the anti-fouling property against the fingerprint model on the surface.

Moreover, to estimate the stability of fluorinated PMMA surface, the sample was immersed into distilled water at 50°C for 4 days, then the static contact angle of water was measured. Bovine serum albumin (BSA, Sigma Co., St Louis, MO) was used for the protein adsorption test on the fluorinated PMMA surface. The films were immersed in BSA solution (2 mg/mL, in phosphate buffered saline (PBS)) for 24 h at 37°C and then rinsed with PBS three times to remove protein weakly adsorbed on the surface. The amount of adsorbed BSA on the surface was evaluated using the bicinchoninic acid (BCA) method [14], where the absorbance change in the solution at 562 nm was measured using UV-vis spectrophotometer (Hitachi Ltd., U-2000, Tokyo, Japan). The amounts of BSA adsorbed on polytetrafluoroethylene (PTFE), polyurethane (PU, Pellethane 2363-91AE, Dow Chemical Company, Midland, MI), poly(ethylene terephthalate) (PET), and PMMA were also

measured as references. In addition, the fluorinated films were immersed in distilled water at 37°C for a prescribed time to estimate the stability of the fluorinated PMMA surface in water.

Square films ( $1 \times 1 \text{ cm}^2$ ) of the fluorinated PMMA, original PMMA, and PTFE were immersed in fresh human whole blood for 20 min at 37°C and then rinsed with PBS three times to remove clots weakly attached to the film. Then the films were immersed in glutaraldehyde solution (Nacalai Tesque Inc., Kyoto, Japan) at 37°C for 24 h to fix blood attached to the surface. After 24 h, the films were observed using an optical microscope (Nikon Co., E950, Tokyo, Japan). Fresh human whole blood supplied from a health donor was collected at the medical center for student health, Kobe University. All samples were obtained in accordance with ethical committee regulations of Kobe University.

### 1. 3. Results and discussion

#### 1. 3. 1. Fluorinated PMMA surface

Figure 1-2 shows the XPS wide spectra and  $C_{1s}$  spectra of the PMMA and the fluorinated PMMA film, respectively. After fluorination, a  $F_{1s}$  peak, clearly identified around 680.0 eV, originating from the perfluoroalkyl groups, appeared on the film surface. The  $C_{1s}$  spectrum for the fluorinated PMMA surface could be a curve-resolved into five peaks: at 294.1 eV ( $-CF_3$ ), 291.8 eV ( $-CF_2-$ ), 288.8 eV ( $-C=O$ ), 286.5 eV ( $C-O$ ), and 285.0 eV ( $-CH_n$ ). The  $C_{1s}$  spectrum for the PMMA surface, on the other hand, has no peak assigned to the perfluoroalkyl group ( $-CF_2-$  and  $-CF_3$ ). After fluorination, the O/C ratio was reduced from 0.43 to 0.27. The high F/C (2.34) value of the fluorinated PMMA surface reveals that the fluorinated PMMA surface was almost covered with  $R_f$  groups. PMMA has the surface without functional groups which can be reacted with glycidyl groups of fluorinated reagent. However, the methoxycarbonyl groups of PMMA slightly change to carboxylic acid [15]. Then, it is assumed that the carboxylic acid plays a role of the foothold of the surface reaction. One of the plausible fluorination mechanisms of PMMA through the reaction between PMMA and glycidyl groups is as follows:

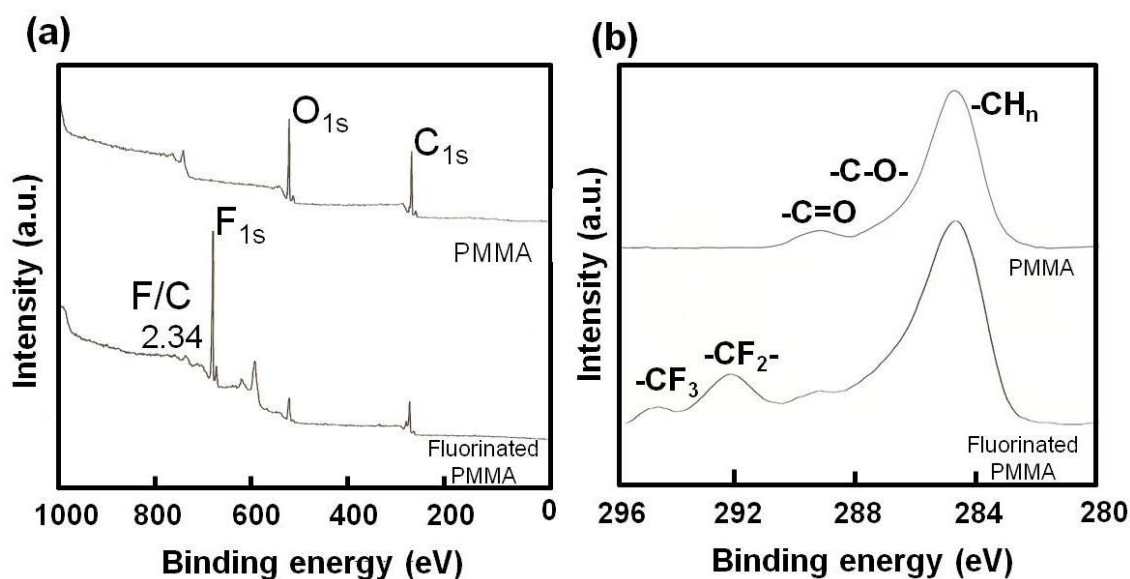
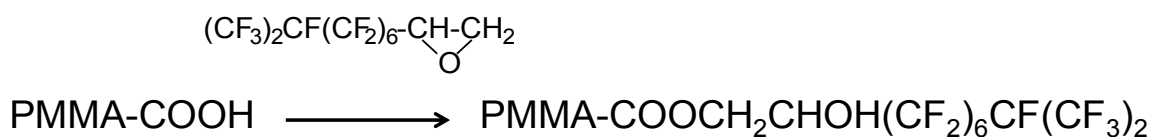


Figure 1-2 (a) XPS wide spectra of PMMA and fluorinated PMMA, (b) C<sub>1s</sub> core level spectra of PMMA and fluorinated PMMA. Incident angle of X-ray is 90°.

Once epoxy groups of fluorinated reagent react to a little carboxy groups on PMMA surface, a next fluorinated reagent reacts to it. As a result, fluorine was assumed to be introduced to a PMMA surface one after another.

Figure 1-3 shows photographs of water droplets on (a) the PMMA and (b) the fluorinated PMMA films. The PMMA surface clearly changed to a water repellent one by being simply immersed in the fluorinated reagent followed by heat treatment. The photographs superimposed on each upper-right corner reveal high optical transparency, originating from PMMA, was maintained after fluorination. Table 1-1 lists the dynamic contact angles and the  $\gamma_s$  values of the PMMA and the fluorinated PMMA films. The  $\theta_{av}$  value of water on the PMMA film changed from 67° to 111° and the  $\gamma_s$  value decreased from 42.8 mJ/m<sup>2</sup> to

10.0 mJ/m<sup>2</sup> by fluorination. The low value of  $\gamma_s$  after fluorination corresponds to the fact the PMMA surface was mostly covered with fluorinated components as revealed by XPS measurement. Moreover the  $\gamma_s$  of 10 mJ/m<sup>2</sup> achieved by this fluorination technique is much lower than those of other hydrophobic polymers, such as polyethylene (36 mJ/m<sup>2</sup>), polypropylene (32 mJ/m<sup>2</sup>), and PTFE (22 mJ/m<sup>2</sup>) [10]. The fluorinated PMMA in this study showed higher water repellency than other hydrophobizing methods such as plasma treatment followed by fluorination with silane coupling treatment [8, 16]. In contrast, the value is much higher than that (6.7 mJ/m<sup>2</sup>) based on -CF<sub>3</sub> groups with a hexagonally close packed surface, which was reported as the lowest  $\gamma_s$  value of any solid at room temperature [11]. This is because -CF<sub>2</sub>- groups were exposed on the surface besides -CF<sub>3</sub> groups.

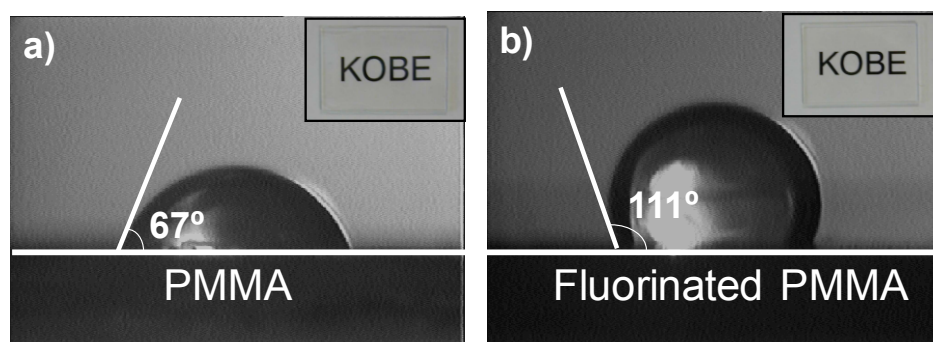


Figure 1-3 Photographs of water droplet on (a) PMMA and (b) fluorinated PMMA. Film transparency is shown in upper-right corners.

Table 1-1 Contact angle  $\theta$  and surface free energy  $\gamma_s$  of PMMA and fluorinated PMMA films.

	Contact angle of water (degree)				Contact angle of CH <sub>2</sub> I <sub>2</sub> (degree)				$\gamma_s^d$	$\gamma_s^p$ (mJ/m <sup>2</sup> )	$\gamma_s$
	$\theta_{av}$	$\theta_a$	$\theta_r$	$\Delta\theta$	$\theta_{av}$	$\theta_a$	$\theta_r$	$\Delta\theta$			
PMMA	67	75	56	19	43	47	39	8	30.9	11.9	42.8
Fluorinated PMMA	111	121	101	20	99	108	90	18	7.4	2.6	10.0

Figure 1-4 shows the static contact angle of water on the fluorinated PMMA after being immersed in water at 50°C for the designated time. Even after 4 days, the static contact angle of water was maintained at 112°. This result indicates that the fluorinated PMMA coating is stable against heated and wet conditions.

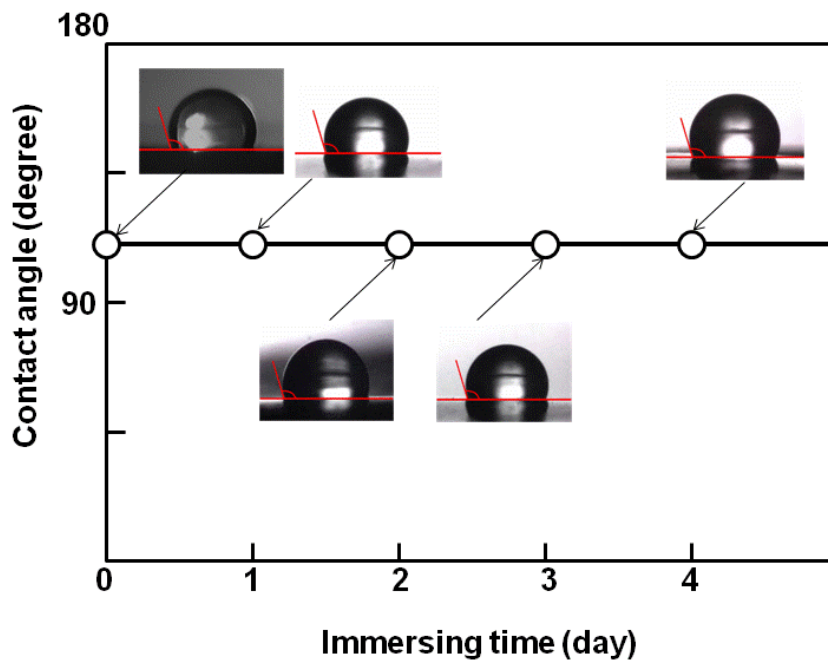


Figure 1-4 Relationship between the contact angle of water on the fluorinated PMMA after immersing in distilled water at 50°C for 1, 2, 3 and 4 days.

### 1. 3. 2. Application of the fluorinated PMMA

Figure 1-5 shows the photographs of (left) PMMA and (right) fluorinated PMMA films with lines drawn with a permanent marker. Unlike the original PMMA surface, the oily felt pen resin was repelled on the fluorinated PMMA surface.

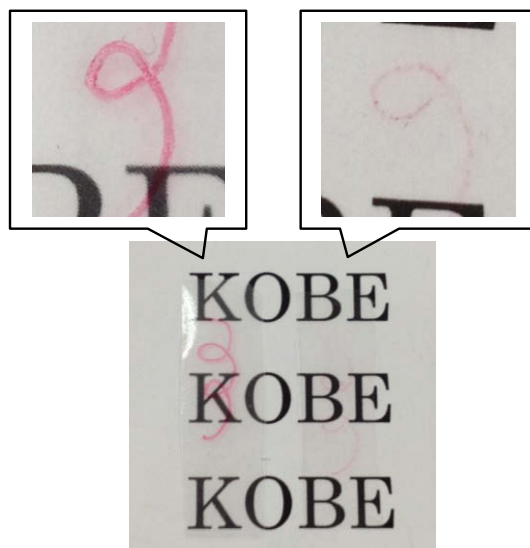


Figure 1-5 Photographs of (left) PMMA and (right) fluorinated PMMA films. Lines were drawn with permanent marker.

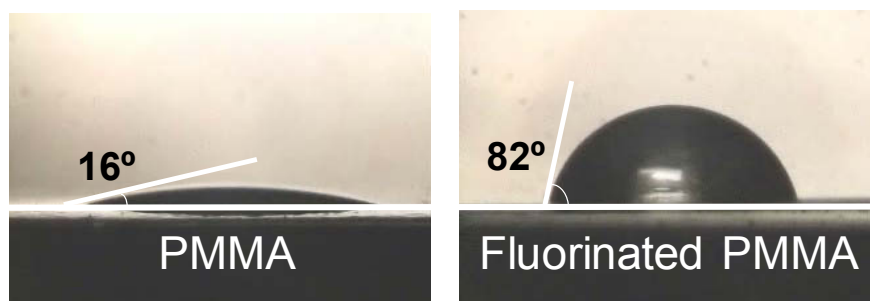


Figure 1-6 Photographs of oleic acid droplet on (left) PMMA and (right) fluorinated PMMA films.

Figure 1-6 shows the droplet of oleic acid on PMMA film before and after fluorination. Oleic acid is known as the main component of sebum. The contact angle of oleic acid on the PMMA film was dramatically changed from  $16^\circ$  to  $82^\circ$  by fluorination. The results in Figures 1-5 and 1-6 indicate the fluorinated surface has anti-fouling property and the potential to be an anti-fingerprint application.

Figure 1-7a shows the amount of BSA adsorbed on various polymer films. Tamada and Ikeda reported that protein adsorption was reduced on a very hydrophobic surface [17]. Compared with other conventional polymers such as PTFE, PU, PET, and PMMA, the fluorinated PMMA surface showed reduced BSA adsorption.

Figure 1-7b shows the amount of BSA adsorbed on fluorinated PMMA surfaces before and after being immersed in water at  $37^\circ\text{C}$  for several days. The amount of BSA adsorbed on fluorinated PMMA was maintained at a low value even after four-day immersion of the film in water. This reveals that the fluorinated film was stable in water without losing its protein repellent characteristic.

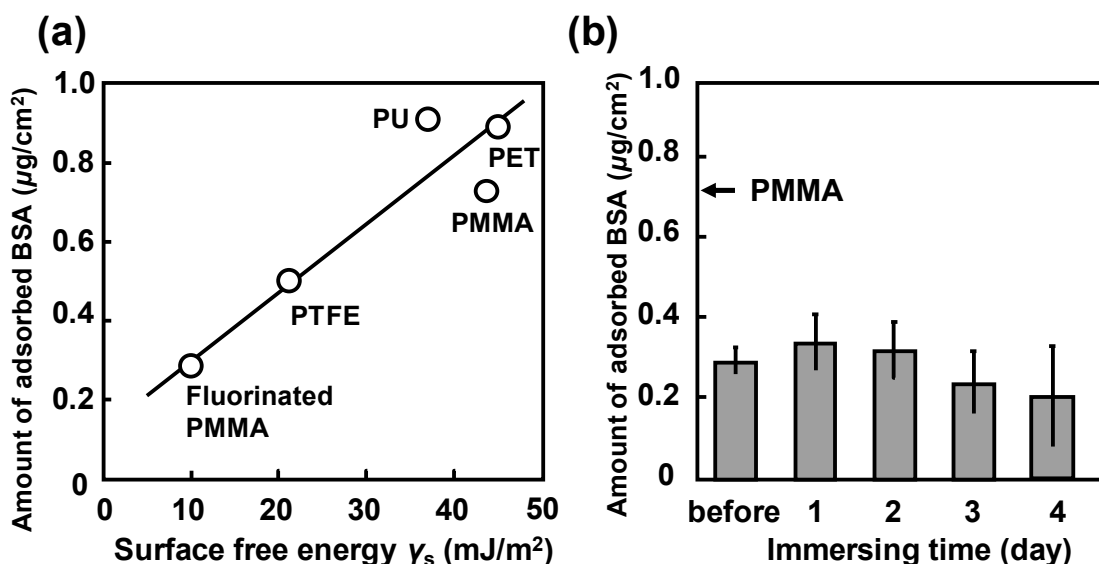


Figure 1-7 (a) Amount of BSA adsorbed on various polymer surfaces. PTFE: polytetrafluoroethylene, PU: polyurethane, PET: poly(ethylene terephthalate). (b) Amount of BSA adsorbed on fluorinated PMMA surfaces before and after immersed in water for several days. Amount of BSA adsorbed on PMMA surface was also superimposed on the figure with arrow.

Figure 1-8 shows the photographs of (a) PMMA, (b) PTFE, and (c) fluorinated PMMA films after being immersed in whole human blood then rinsed. On the PMMA and PTFE films, clotting took place, while no clots were observed on the fluorinated PMMA. This originated from the protein repellent characteristics of the fluorinated PMMA surface, because when materials came into contact with blood, proteins were rapidly adsorbed onto the surfaces, which triggers the clotting. This result demonstrates that the fluorinated PMMA had weak affinity with platelets and is a good candidate for an antithrombogenic material.



**(a) PMMA**



**(b) PTFE**



**(c) Fluorinated PMMA**

Figure 1-8 Photographs of (a) PMMA, (b) PTFE, (c) fluorinated PMMA films after immersion in whole blood for 20 minutes at 37°C.



#### 1.4. Conclusions

The PMMA surface was fluorinated by simply immersing it into a fluorinate reagent followed by heat-treatment. The contact angle of water for the fluorinated PMMA increased to 111°. This corresponds to the surface free energy of 10 mJ/m<sup>2</sup>, which is much lower than that of PTFE and stable under wet and heated conditions. In addition, fluorinated PMMA surface showed high resistance to BSA adsorption, thrombogenesis, and anti-fouling properties against fingerprints. This fluorination technique simply and effectively lowers the surface free energy of PMMA.

#### 1.5. References

- [1] Chen, L.; Geissler, A.; Bonaccorso, E.; Zhang, K. *ACS Appl. Mater. Interfaces*, 2014, 6, 6969.
- [2] Barthwal, S.; Kim, Y. S.; Lim, S. *Langmuir*, 2013, 29, 11966.
- [3] Chu, E.; Sidorenko, A. *Langmuir*, 2013, 29, 12585.
- [4] Guo, Y.; Di, C.; Liu, H.; Zheng, J.; Zhang, L.; Yu, G.; Liu, Y. *ACS NANO*, 2010, 4, 5749.
- [5] Nishino, T.; Meguro, M.; Nakamae, K. *Int. J. Adhes.*, 1999, 19, 399.
- [6] Ly, B.; Belgacem, M. N.; Bras, J.; Brochier Salon, M. C. *Mater. Sci. Eng. C*, 2010, 30, 343.
- [7] Durand, N.; Gaveau, P.; Silly, G.; Améduri, B.; Boutevin, B. *Macromolecules*, 2011, 44, 6249.
- [8] Nyström, D.; Lindqvist, J.; Östmark, E.; Antoni, P.; Carlmark, A.; Hult, A.; Malmström, E. *ACS Appl. Mater. Interfaces*, 2009, 1, 816.
- [9] Tsutsumi, N.; Ono, T.; Kiyotsukuri, T. *Macromolecules*, 1993, 26, 5447.
- [10] Sumiya, K.; Taii, T.; Nakamae, K.; Matsumoto, T. *J. Adhes. Soc. Jpn.*, 1982, 18, 345.
- [11] Nishino, T.; Meguro, M.; Nakamae, K.; Matsushita, M.; Ueda, Y. *Langmuir*, 1999, 15, 4321.
- [12] Owens, D. K.; Wendt, R. C. *J. Appl. Polym. Sci.*, 1969, 13, 1741.
- [13] Fowkes, S. M. *J. Phys. Chem.*, 1963, 67, 2538.

- [14] Smith, P. K.; Krohn, R. I.; Hermanson, G. T.; Mallia, A. K.; Gartner, F. H.; Provenzano, M. D.; Fujimoto, E. K.; Geoke, N. M.; Olson, B. J.; Klenk, D. C. *Anal. Biochem.*, 1985, 150, 76.
- [15] McCarley, R. L.; Vaidya, B.; Wei, S.; Smith, A. F.; Patel, A. B.; Feng, J. *J. Am. Chem. Soc.*, 2005, 127, 842.
- [16] Tsougeni, K.; Tserepi, A.; Constantoudis, V.; Gogolides, E. *Langmuir*, 2010, 26, 13883.
- [17] Tamada, Y.; Ikeda, Y. *J. Colloid Interface Sci.*, 1993, 155, 334.



**Chapter 2**  
**Surface Structure to Achieve**  
**the Surface Free Energy Lower than  $10 \text{ mJ/m}^2$**

## 2.1. Introduction

For satisfaction of high performance of adhesives, paints, coatings and biomaterials, the control of the surface free energy is needed. A low free energy surface possesses a variety of useful properties for these applications [1-4]. In fact, polymer surface with low surface free energy ( $\gamma_s$ ) showed water and oil repellencies, biocompatibility in Chapter 1. In regards to lowering  $\gamma_s$  value, Zisman *et al.* reported that the surface chemical species and concentrations of functional groups affects  $\gamma_s$ , which decreased in the order of  $-\text{CH}_2- > -\text{CH}_3 > -\text{CF}_2- > -\text{CF}_2\text{H} > -\text{CF}_3$  [5]. From this view point, the  $\gamma_s$  value can be much more reduced, compared with that ( $18 \text{ mJ/m}^2$ ) [6] of PTFE which is composed of  $-\text{CF}_2-$ . Nishino *et al.* previously reported the lowest  $\gamma_s$  of  $6.7 \text{ mJ/m}^2$  for *n*-perfluoroeicosane ( $\text{C}_{20}\text{F}_{42}$ ), epitaxially grown surface, on which the closest hexagonally packed  $-\text{CF}_3$  groups exposure [7]. The determination of the lowest  $\gamma_s$  plays an important role in the practical achievement in a process aimed at obtaining materials with the low  $\gamma_s$ . Table 2-1 summarizes the endeavors to lower the  $\gamma_s$  value in the literatures [8-21]. In a large numbers of cases, the  $\gamma_s$  values down to  $10 \text{ mJ/m}^2$  were reported, and only a few polymers with perfluorinated side chains could reach to the  $\gamma_s$  value less than  $10 \text{ mJ/m}^2$ . These suggest that strict control of surface structure is needed to approach the low  $\gamma_s$  value.

In this chapter, the vapor deposition of  $\text{C}_{20}\text{F}_{42}$  thin film was performed, and the dynamic contact angle was measured. Then the effect of structure of  $\text{C}_{20}\text{F}_{42}$  thin film on the  $\gamma_s$  value was investigated.

Table 2-1 Surface free energy reported in the literatures.

Fluorine compound	Substrate	Surface free energy (mJ/m <sup>2</sup> )	References
Surface treatment			
CF <sub>3</sub> (CF <sub>2</sub> ) <sub>7</sub> (CH <sub>2</sub> ) <sub>2</sub> SiCl <sub>3</sub>	PVA	10	8
CF <sub>3</sub> (CF <sub>2</sub> ) <sub>6</sub> COCl	PVA	18	9
CF <sub>3</sub> (CH <sub>2</sub> ) <sub>2</sub> Si(OCH <sub>3</sub> ) <sub>3</sub>	Cellulose	26.7	10
CF <sub>3</sub> (CF <sub>2</sub> ) <sub>5</sub> (CH <sub>2</sub> ) <sub>2</sub> Si(OCH <sub>3</sub> ) <sub>3</sub>	Cellulose	19.9	10
(CF <sub>3</sub> ) <sub>2</sub> CF(CF <sub>2</sub> ) <sub>6</sub> CHOCH <sub>2</sub>	PMMA	10.0	11
Polymers with perfluorinated side chains			
H <sub>2</sub> C=C(CH <sub>3</sub> )CO <sub>2</sub> CH <sub>2</sub> CH <sub>2</sub> (CF <sub>2</sub> ) <sub>5</sub> CF <sub>3</sub>	PMMA	10.2	12
H <sub>2</sub> C=CHCO <sub>2</sub> (CH <sub>2</sub> ) <sub>2</sub> (CF <sub>2</sub> ) <sub>3</sub> CF <sub>3</sub>		9	13
H <sub>2</sub> C=CHCO <sub>2</sub> (CH <sub>2</sub> ) <sub>2</sub> (CF <sub>2</sub> ) <sub>6</sub> CF <sub>3</sub>	-	18.4	14
H <sub>2</sub> C=CHCO <sub>2</sub> (CH <sub>2</sub> ) <sub>2</sub> (CF <sub>2</sub> ) <sub>7</sub> CF <sub>3</sub>	-	7.8	15
H <sub>2</sub> C=CHCO <sub>2</sub> (CH <sub>2</sub> ) <sub>2</sub> (CF <sub>2</sub> ) <sub>7</sub> CF <sub>3</sub>	-	10	16
H <sub>2</sub> C=C(CH <sub>3</sub> )(CH <sub>2</sub> ) <sub>2</sub> CO(CH <sub>2</sub> ) <sub>10</sub> (CF <sub>2</sub> ) <sub>6</sub> H	-	20.5	17
H <sub>2</sub> C=C(CH <sub>3</sub> )(CH <sub>2</sub> ) <sub>2</sub> CO(CH <sub>2</sub> ) <sub>10</sub> (CF <sub>2</sub> ) <sub>10</sub> H	-	16.5	17
H <sub>2</sub> C=C(CH <sub>3</sub> )CO <sub>2</sub> CH <sub>2</sub> (CF <sub>2</sub> ) <sub>2</sub> CF <sub>3</sub>	-	12.0	18
H <sub>2</sub> C=C(CH <sub>3</sub> )CO <sub>2</sub> CH <sub>2</sub> (CF <sub>2</sub> ) <sub>4</sub> H	-	18.0	18
H <sub>2</sub> C=C(CH <sub>3</sub> )CO <sub>2</sub> CH <sub>2</sub> CH <sub>2</sub> (CF <sub>2</sub> ) <sub>5</sub> CF <sub>3</sub>	-	12.6	9
H <sub>2</sub> C=C(CH <sub>3</sub> )CO <sub>2</sub> (CH <sub>2</sub> ) <sub>2</sub> (CF <sub>2</sub> ) <sub>7</sub> CF <sub>3</sub>	LB <sup>a</sup>	7.3	19
H <sub>2</sub> C=C(CH <sub>3</sub> )CO <sub>2</sub> (CH <sub>2</sub> ) <sub>2</sub> (CF <sub>2</sub> ) <sub>7</sub> CF <sub>3</sub>	-	7.8	20
H <sub>2</sub> C=C(CH <sub>3</sub> )CO <sub>2</sub> (CH <sub>2</sub> ) <sub>2</sub> (C <sub>3</sub> H <sub>3</sub> N <sub>2</sub> )CH <sub>3</sub> ·N(SO <sub>2</sub> CF <sub>3</sub> ) <sub>2</sub> -		26.9	21

<sup>a</sup>Langmuir film on Si wafer deposited at surface pressure of 5.5 mN/m from chloroform solution.

## 2. 1. Experimental

### 2. 1. 1. Sample preparation

Slide glass was used as a substrate. To alter the surface property of the glass, a substrate was immersed in 0.5% wt/wt aqueous solution containing distearyl dimethyl ammonium chloride (SMA) or dialkyl sulfosuccinic acid, followed by rinsing with distilled/deionized water and drying. The former (SMA) treatment gives the surface hydrophobicity, but the latter (ASS) treatment brings it hydrophilicity. C<sub>20</sub>F<sub>42</sub> (PCR Chemicals Inc.) was heated at 47°C under 10<sup>-4</sup> Pa and vapor deposited onto the each pretreated slide glass with the deposition rate of 10 Å/min. During deposition, the substrate was cooled to -30°C. Total thickness of vapor deposited layer was 1000 Å, being monitored by a quartz crystal microbalance.

### 2. 1. 2. Characterization

The dynamic contact angle was measured with the same method described in Chapter 1.

The X-ray diffraction measurement was performed by symmetrical reflection geometry with CuK $\alpha$  radiation generated at 40 kV, 20 mA.

The degree of crystallite orientation,  $f$ , in the thin films was determined by calculating the Herman's orientation function [22] from the relationship between the X-ray diffraction intensity and the angle of inclination for the (006) plane of C<sub>20</sub>F<sub>42</sub> along the Debye-Scherrer ring.

$$f = \frac{3\langle \cos^2 \phi \rangle - 1}{2} \quad (1)$$

$$\langle \cos^2 \phi \rangle = \frac{\int_0^{\pi/2} I(\phi) \cos^2 \phi \sin \phi d\phi}{\int_0^{\pi/2} I(\phi) \sin \phi d\phi} \quad (2)$$

where  $I(\phi)$  is the intensity at the inclination angle  $\phi$ .

### 1. 3. Results and discussion

#### 1. 3. 1. Surface structure of $C_{20}F_{42}$ vapor deposited on as-received and ASS treated glass

Figure 2-1 shows the X-ray diffraction profiles of the  $C_{20}F_{42}$  thin films vapor-deposited on a) as-received glass and b) ASS treated glass. Several sharp diffractions were observed with overlapping to amorphous halo of the glass around  $2\theta$  of  $25^\circ$ . Judging from the crystal structure (rhombohedral lattice system,  $a = b = 5.70 \text{ \AA}$ ,  $c = 85.0 \text{ \AA}$ ,  $\beta = 120^\circ$ ) of  $C_{20}F_{42}$ , these could be indexed as shown in Figure 2-1. There observed the meridional  $00l$  reflections, which reveal that the fluoroalkyl chains stand with their  $c$ -axis perpendicular to both of the glass surface. In addition to these meridional reflections, for the profile on a) as-received glass, equatorial  $100/010$  reflection appeared. This result indicates that some molecules laid parallel to the surface, then some  $-CF_2-$  groups were exposed on the as-received glass surface. This contrasted with the case for the  $C_{20}F_{42}$  thin films vapor deposited on SMA treated glass, where most of the surface was covered with  $-CF_3$  groups.

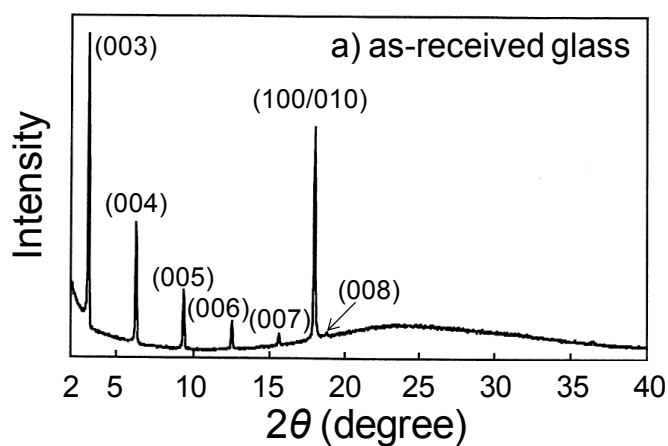


Figure 2-1 X-ray diffraction profiles of the  $C_{20}F_{42}$  thin films vapor deposited on a) as-received glass and b) ASS treated glass.

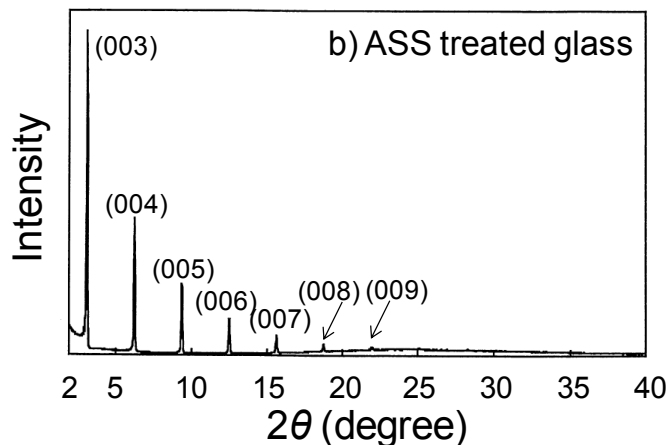




Figure 2-2 shows the relationship between the X-ray diffraction intensity and the angle of inclination for the (006) plane of  $C_{20}F_{42}$  along the Debye-Scherrer ring. From the integral width of the curve, the  $f$  value of the crystallite orientation was valued as shown in Figure 2-2. In both cases, very high  $f$  values indicate that the  $C_{20}F_{42}$  molecules are almost standing on the substrate. In particular, the  $f$  value for  $C_{20}F_{42}$  deposited on as-received glass was higher than that on the ASS treated glass. The glass surface may be roughened by the ASS treatment. The molecular alignment of  $C_{20}F_{42}$  against substrate will be disturbed for this reason.

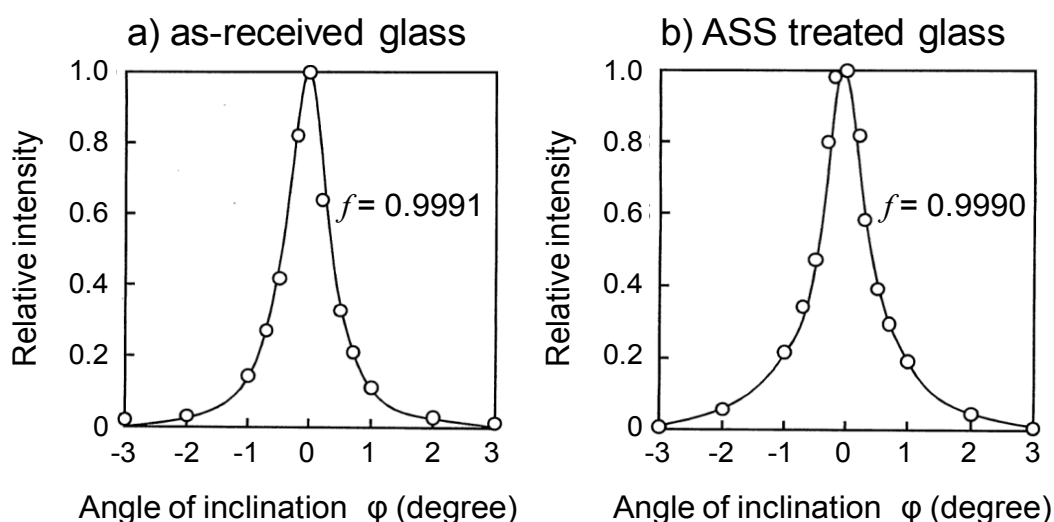


Figure 2-2 Relationship between the X-ray diffraction intensity and the angle of inclination for the (006) plane of  $C_{20}F_{42}$  along the Debye-Scherrer ring. Thin film was vapor deposited on a) as-received glass and b) ASS treated glass.

Table 2-2 Dynamic contact angle  $\theta_{av}$  of H<sub>2</sub>O, CH<sub>2</sub>I<sub>2</sub>, the surface free energy  $\gamma_s$  of vapor deposited C<sub>20</sub>F<sub>42</sub>.

Glass	Contact angle		Surface free energy
	Water	CH <sub>2</sub> I <sub>2</sub>	
	degree		mJ/m <sup>2</sup>
As-received	91	84	19
ASS treated	112	106	8.1

Table 2-2 shows the dynamic contact angle  $\theta_{av}$  of H<sub>2</sub>O, CH<sub>2</sub>I<sub>2</sub>, the  $\gamma_s$  value of vapor deposited C<sub>20</sub>F<sub>42</sub> on as-received and ASS treated glasses. The  $\theta_{av}$  and the  $\gamma_s$  values for the C<sub>20</sub>F<sub>42</sub> thin film on the as-received glass almost correspond to those of PTFE [18]. On the other hand, the  $\theta_{av}$  value was higher, and the  $\gamma_s$  value was lower for C<sub>20</sub>F<sub>42</sub> vapor deposited on the ASS treated glass. These results indicate that the lack of -CF<sub>2</sub>- groups and -CF<sub>3</sub> total coverage of the surface are more important for the low (<10 mJ/m<sup>2</sup>)  $\gamma_s$ .

### 2. 3. 2. Time dependence of surface structure

Figure 2-3 shows the X-ray diffraction profiles of C<sub>20</sub>F<sub>42</sub> thin film on SMA treated glass at a) just after deposition, b) 3 days after deposition, and c) 30 days after deposition. The profile a) and b) were intrinsically as same as that observed in Figure 2-1b. However, the profile c) showed that the thin film became amorphous state after 30 days. This indicates that crystalline state is unstable, and C<sub>20</sub>F<sub>42</sub> thin film is intrinsically amorphous at room temperature.

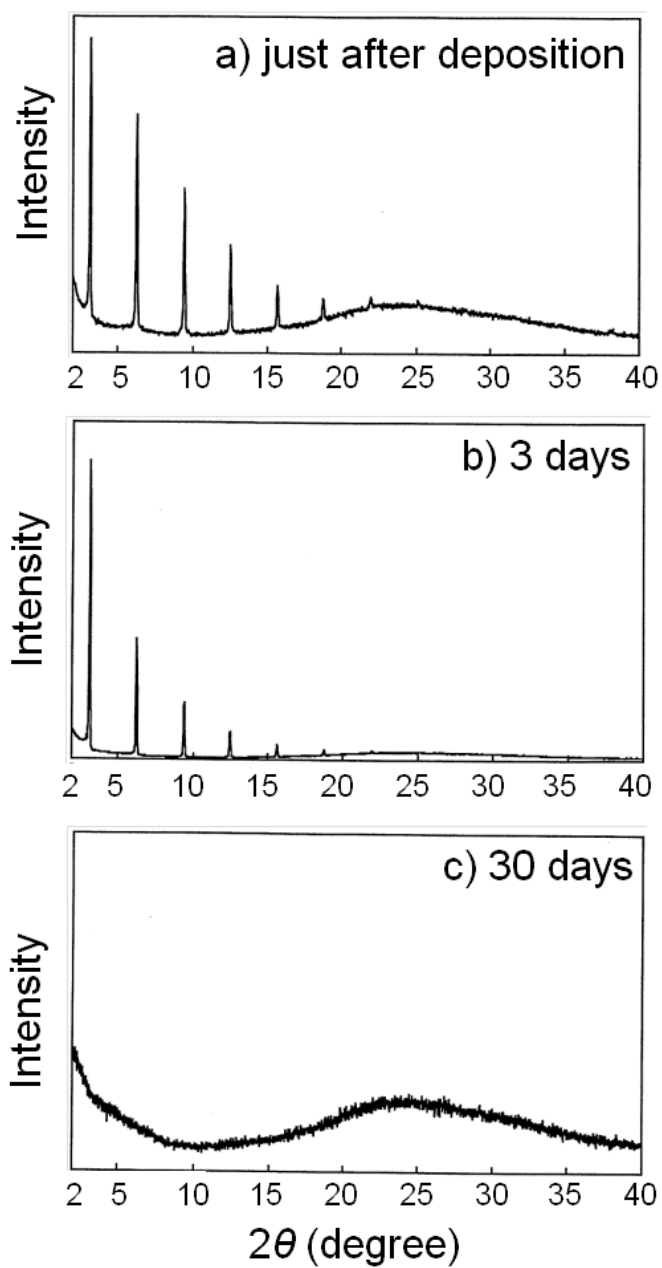


Figure 2-3 X-ray diffraction profiles of  $C_{20}F_{42}$  thin film on SMA treated glass at a) just after deposition, b) 3 days after deposition, and c) 30 days after deposition.

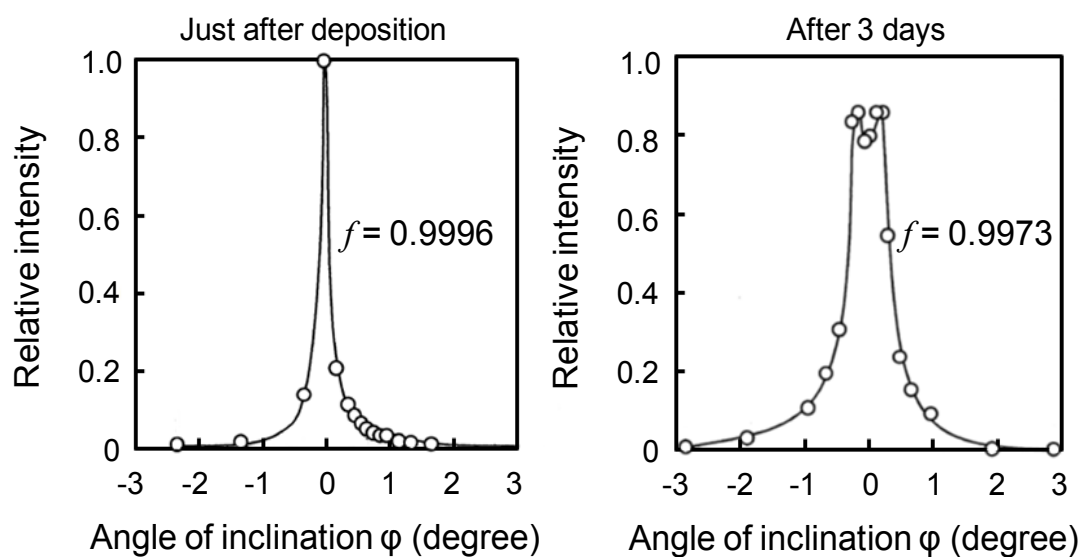


Figure 2-4 Time dependence for the relationship between the X-ray diffraction intensity and the angle of inclination for the (006) plane of  $C_{20}F_{42}$  vapor deposited on SMA treated surface along the Debye-Scherrer ring.

Table 2-3 Dynamic contact angle  $\theta_{av}$  of  $H_2O$ ,  $CH_2I_2$ , the surface free energy  $\gamma_s$  together with schematic representation of the orientation of  $C_{20}F_{42}$  molecule on SMA treated glass just after deposition, 3 days and 1 month.

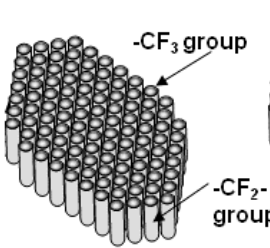
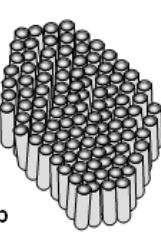
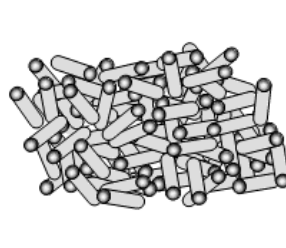
	Just after	3 days	30 days
Contact angle (deg.)			
Water	119	113	79
$CH_2I_2$	107	100	59
Surface free energy ( $mJ/m^2$ )	6.7	9.1	33
			

Figure 2-4 shows the time dependence for the relationship between the X-ray diffraction intensity and the angle of inclination for the (006) plane of C<sub>20</sub>F<sub>42</sub> vapor deposited on SMA treated surface along the Debye-Scherrer ring. Just after deposition, very high crystallite orientation was observed. On the other hand, the distribution peak was split into two peaks after 3 days stored at room temperature. The  $\theta_{av}$  and  $\gamma_s$  values were shown in Table 2-3 together with schematic representation of the orientation of C<sub>20</sub>F<sub>42</sub> molecule on SMA treated glass. Just after deposition, C<sub>20</sub>F<sub>42</sub> molecules were strictly standing on the substrate, which brought the lowest  $\gamma_s$  value to the surface. After stored for 3 days at room temperature, the molecules started to incline, and the  $\gamma_s$  value increase to 9.1 mJ/m<sup>2</sup> from 6.7 mJ/m<sup>2</sup>. This result reveals that ca.0.2° distortion of chain orientation caused the increase of 2.5 mJ/m<sup>2</sup> for the  $\gamma_s$  value. After one month, the chain orientation was totally lost and both -CF<sub>2</sub>- and -CF<sub>3</sub> groups exposed on the surface, and the  $\gamma_s$  value increased very much.

#### 2. 4. Conclusion

While with large number of papers appeared, many reported the  $\gamma_s$  value down to 10 mJ/m<sup>2</sup>, and only a few reported the  $\gamma_s$  value lower than 10 mJ/m<sup>2</sup>. To examine this reason, the microstructure and surface properties of C<sub>20</sub>F<sub>42</sub> thin film vapor deposited under various conditions were investigated. Surface exposure of -CF<sub>2</sub>- group, instead of -CF<sub>3</sub> group, increased the  $\gamma_s$  value. In addition, slight inclination of the perfluoroalkyl groups also increased the  $\gamma_s$  value. As a result, in order to reach to the lowest  $\gamma_s$  value, precise control of the surface structure, especially total coverage of the surface with -CF<sub>3</sub> groups is necessary.

#### 2. 5. References

- [1] Park, D.; Weinman, C. J.; Finlay, J. A.; Fletcher, B. R.; Paik, M. Y.; Sundaram, H. S.; Dimitriou, M. D.; Sohn, K. E.; Callow, M. E.; Callow, J. A.; Handlin, D. L.; Willis, C. L.; Fischer, D. A.; Kramer, E. J.; Ober, C. K. *Langmuir*, 2010, 26, 9772.
- [2] Kessman, A. J.; Cairns, D. R. *Langmuir*, 2011, 27, 5968.
- [3] Booth, B. D.; Vilt, S. G.; Lewis, J. B.; Rivera, J. L.; Buehler, E. A.; McCabe, C.; Jennings, G. K. *Langmuir*, 2011, 27, 5090.
- [4] Klein, R. J.; Fischer, D. A.; Lenhart, J. L. *Langmuir*, 2011, 27, 12423.

- [5] Schulman, F.; Zisman, W. A. *J. Colloid Sci.*, 1952, 7, 465.
- [6] Sumiya, K.; Taii, T.; Nakamae, K.; Matsumoto, T., *J. Adhes. Soc. Jpn.*, 1982, 18, 345.
- [7] Nishino, T.; Meguro, M.; Nakamae, K.; Matsushita, M.; Ueda, Y. *Langmuir*, 1999, 15, 4321.
- [8] Nishino, T.; Meguro, M.; Nakamae, K. *Int. J. Adhes.*, 1999, 19, 399.
- [9] Nishino, T.; Nakahara, S.; Nakamae, K. *J. Adhes. Soc. Jpn.*, 1999, 35, 138.
- [10] Ly, B.; Belgacem, M. N.; Bras, J.; Brochier Salon, M. C. *Mater. Sci. Eng. C Biomimetic Mater. Sens. Syst.*, 2010, 30, 343.
- [11] Tokuda, K.; Ogino, T.; Kotera, M.; Nishino, T. *Polymer Journal*, accepted in 31 August 2014.
- [12] Park, I. J.; Lee, S.; Choi, C. K. *Macromolecules*, 1998, 31, 7555.
- [13] Kim, J.; Efimenko, K.; Genzer, J.; Carbonell, R. G. *Macromolecules*, 2007, 40, 588.
- [14] Ishikawa, T.; Kobayashi, M.; Takahara, A. *ACS Appl. Mater.*, 2010, 2, 1120.
- [15] Honda, K.; Morita, M.; Otsuka, H.; Takahara, A. *Macromolecule*, 2005, 38, 5699.
- [16] Yang, S.; Wang, J.; Ogino, K.; Valiyaveetil, S.; Ober, C. K. *Chem. Mater.*, 2000, 12, 33.
- [17] Hayakawa T.; Wang, J.; Xiang, M.; Li, X.; Ueda, M.; Ober, C. K.; Genzer, J.; Sivaniah, E.; Kramer, E. J.; Fischer, D. A. *Macromolecules*, 2000, 33, 8012.
- [18] Urushihara, Y.; Nishino, T. *Langmuir*, 2005, 21, 2614.
- [19] Nishino, T.; Urushihara, Y.; Meguro, M.; Nakamae, K. *J. Colloid Interface Sci.*, 2004, 279, 364.
- [20] Nishino, T.; Urushihara, Y.; Meguro, M.; Nakamae, K. *J. Colloid and Interface Sci.*, 2005, 283, 533.
- [21] Miyata, T.; Yamada, H.; Uragami, T. *Macromolecules*, 2001, 34, 8026.
- [22] Hermans, P. H. "Contribution to the Physics of Cellulose Fibres, ch. VI", Elsevier, New York, 1946.



## **Part II**

### **Surface Segregation of Poly(ethylene oxide) Side Chains using Perfluoroalkyl Groups and its Properties**





## **Chapter 3**

# **Effect of Poly(ethylene oxide) Side Chains Length in Surface Modifier on Surface Properties**

### 3.1. Introduction

Surface property is important for high performance of adhesives, paints, coatings, biomaterials, and lubrications. For many applications, a lot of hydrophobic surface modifications have been reported, because a hydrophobic surface, in other words, a low-free-energy surface, brings useful surface properties. As mentioned in General introduction, the use of fluorine is well known to be effective for achievement of a low-free-energy surface and there has been a great deal of studies on fluoropolymers for lowering the surface free energy. A typical and first example is polytetrafluoroethylene (PTFE), it is widely utilized in many fields such as coating, biomaterials, and soil-resistant and breathable textiles. However, fully fluorinated polymers have disadvantages from the viewpoint of mechanical properties, processing, and cost [1-3]. For industrial applications, a surface modifier is commonly used to change surface properties without losing bulk properties. In order to overcome the disadvantages of using fully-fluorinated polymers, copolymers with smaller amounts of fluorine-containing comonomers have potential applications as surface modifiers. This is because that the fluorine-containing moieties tend to be segregated at the air/polymer interface to lower the surface free energy, so polymers with perfluoroalkyl ( $R_f$ ) side chains were reported to show very low surface free energy. Enrichment of the low surface free energy component at the surface has been observed experimentally [1, 2, 4-6] and demonstrated theoretically [3, 7, 8]. It brought the surface high water repellency and low adhesive strength simultaneously.

Fluorine-containing groups are also used for surface-segregation of hydrophilic components, which is hard to be segregated on a surface. Jannasch investigated the surface compositions of poly(styrene(S)-*block*-ethylene oxide (EO)) and poly(S-*graft*-EO) films. He presented that S segments were segregated on the film surface of the copolymer having the EO chain ends with hydroxy groups, while EO segments dominated the surface by the fluorine termination of the EO chain ends. These shows hydrophilic EO units can be surface-segregated against the request of surface enrichment of hydrophobic segments under some conditions [9]. This method brought unique properties, which could not be achieved using only fluorine-containing groups, on modified surface.

In this chapter,  $R_f$  group and poly(ethylene oxide) (PEO) were used as fluorine-containing group and a hydrophilic component, respectively. As a surface modifier, methacrylate-based terpolymers containing both  $R_f$  group and poly(ethylene oxide) (PEO) as side chains were synthesized. The PEO side chain length was changed to observe the effect on the surface properties. Then the surface structure and properties of these terpolymers were investigated, and the surface composition was found. Then, I revealed the factors affecting the surface-segregation of PEO side chains.

## 3. 2. Experimental

### 3. 2. 1. Materials

Methyl methacrylate (MMA, Nacalai Tesque, Inc., Kyoto, Japan) was distilled under reduced pressure before use. 2, 2'-Azobisisobutyronitrile (AIBN, Nacalai Tesque, Inc., Kyoto, Japan) was recrystallized from methanol. Fluorine-containing monomer, 2-(perfluorooctyl) ethyl acrylate (PFEA-8, Clariant Corp., Tokyo, Japan), and several macromonomers with PEO side chains with different lengths (PEO-OMe: BLEMMER PME-100, 400, 1000, 2000 and 4000, NOF Co. Tokyo, Japan) were used as received. The PEO side chain lengths ( $n$ ) in PEO-OMe were 2, 9, 22, 45, and 90. The termini of the PEO side chain were methoxy group. Poly(methyl methacrylate) (PMMA) (Acrypet VH, Mitsubishi Rayon Co. Ltd.,  $M_n = 41,100$ , Tokyo, Japan) was purified by reprecipitation from methyl ethyl ketone (MEK) solution into methanol. Vinylidene fluoride (VdF) - tetrafluoroethylene (TFE) copolymer (P(2F-4F),  $(CH_2CF_2)_{80}(CF_2CF_2)_{20}$ , Kynar SL, Atfina Chemicals Inc.,  $M_n = 69,300$ ) was used as received.

### 3. 2. 2. Sample preparation

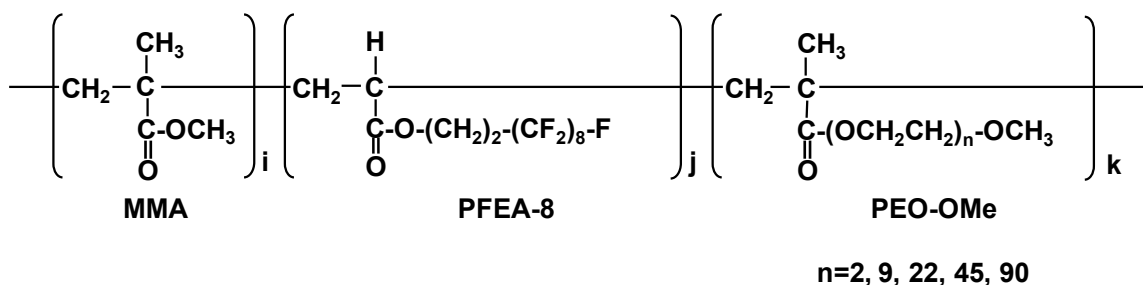


Figure 3-1 Chemical formulae of terpolymers, P(MMA/PFEA-8/PEO-OMe)s.

The chemical formulae of terpolymer, P(MMA/PFEA-8/PEO-OMe)s, used in this study are shown in Figure 3-1. P(MMA/PFEA-8/PEO-OMe)s were synthesized by free-radical polymerization in ethyl acetate at 75°C for 16 h using AIBN as an initiator (0.5% w/w vs. monomers). The sum of the monomer concentrations was 30% w/w. After polymerization, an excess of *n*-hexane/*n*-butanol mixture (*n*-hexane/*n*-butanol = 4/1 v/v) was poured into the reactant solution at 55°C, then the terpolymers were obtained as precipitates. The resultant terpolymer was used as the surface modifier after being dried at 60°C under vacuum. To evaluate the PEO side chain content in the terpolymer, nuclear magnetic resonance analysis (<sup>1</sup>H-NMR, DPX-250, Bruker BioSpin K. K., Kanagawa, Japan, 250. 63 MHz) was performed at 60°C using deuterated chloroform (EURISO-TOP Co., Les Algorithmes, France) as a solvent. The fluorine content was evaluated by the lanthanum alizarin complexone method followed by being resolved through oxygen flask combustion method [10, 11]. The weight average molecular weight ( $M_w$ ), number average molecular weight ( $M_n$ ) were measured using gel permeation chromatography (GPC, Waters Co., Ltd., Model 410) equipped with reflective index detector and connected four columns (HR0.5, HR1, HR2, HR4, Waters Co., Ltd.). Tetrahydrofuran and polystyrene were used as an

eluent, and molecular weight standards, respectively. The actual monomer compositions and molecular weight of the terpolymers were shown in Table 3-1.

A mixture of PMMA and P(2F-4F) was used as a matrix resin of the modifier. The mixture of PMMA, P(2F-4F) and each surface modifier was co-dissolved in methyl ethyl ketone/methyl isobutyl ketone (MIBK) = 7/3 w/w to prepare 10% w/w clear solution. After stirring for overnight, the solution was dip-coated on a poly(ethylene terephthalate) (PET) film, followed by annealing at 140°C for 1 h. The coated surface is hereafter a terpolymer modified surface.

Table 3-1 Monomer compositions of P(MMA/PFEA-8/PEO-OMe)s.

n		2	9	22	45	90
Actual composition (mol ratio)	MMA	1000	1000	1000	1000	1000
	PFEA-8	166	151	128	139	140
	PEO-OMe	110	107	339	390	401
Average molecular weight	$M_n (10^3)$	21.8	-	23.7	19.9	12.7
	$M_w (10^3)$	58.2	-	65.8	61.3	68.9
	$M_w/M_n$	2.7	-	2.8	3.1	5.4

### 3. 2. 3. Characterization

X-ray photoelectron spectroscopy (XPS) measurements were carried out with a Kratos AXIS-HS to investigate the surface composition. The radiation source was monochromated X-ray gun (LMX-30, Shimadzu Co., Kyoto, Japan). AlK $\alpha$  radiation, generated at 15 kV, 10 mA, was irradiated on the films, and then the XPS spectra were collected at 15° of the take-off angle  $\alpha$  between the sample and the analyzer. The analytical depth  $\lambda_\alpha$  could be decreased by decreasing  $\alpha$  (Figure 3-2), and given by the equation as follows;

$$\lambda_\alpha = \lambda_0 \sin \alpha$$

where  $\lambda_0$  ( $3\lambda$ : 6 nm) is the mean free path of the photoelectrons emitted from the sample. Thus,  $\alpha$  of  $15^\circ$  corresponds to  $\lambda_\alpha$  of 1.55 nm.

No radiation damage was observed during the data collection.

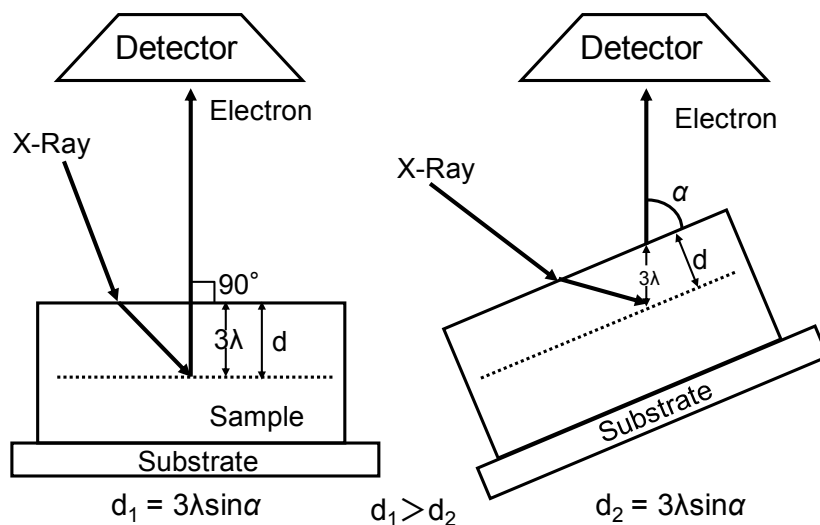


Figure 3-2 Schematic representation of the depth profiling using the XPS measurements.

The dynamic contact angles of distilled water in air were measured with the same method described in Chapter 1. The dynamic contact angle of air bubble in distilled water was measured by sessile bubble method.

To evaluate the adhesive property,  $90^\circ$ -peel test against epoxy resin was performed. First, a sample film was glued to Al plate (the thickness was 0.5 mm) using epoxy resin, commercially available adhesive, Araldite (AR-R30, NICHIBAN Co., Ltd., Tokyo, Japan) followed by being hardened under constant pressure, 270 Pa, for 24 h, at room temperature. After that, the sample film was peeled from the Al plate at the angle of  $90^\circ$ , then the  $90^\circ$ -peel strength was measured by tensile tester, Autograph AGS-1kND (Shimadzu Co., Kyoto, Japan); the peel rate was 50 mm/min. The number of tested specimens was more than five.

For the measurement of macromonomer density, picnometer method, calibrated with distilled water ( $0.996 \text{ g/cm}^3$ ), was performed at  $65^\circ\text{C}$ . The density of the surface modifier was determined by floatation method using the mixtures of methanol ( $0.792 \text{ g/cm}^3$ ) and sodium bromide aqueous solution.

The surface morphology was observed with an atomic force microscope (AFM, NanoNavi Station/E-sweep, Seiko Instruments Inc., Chiba, Japan) in dynamic force mode (DFM). The cantilever was made of Si, whose force constant is  $15 \text{ N/m}$ . The scan area was  $1 \mu\text{m}$  square. The surface roughness was evaluated by the root mean square (RMS) value from the AFM image of the terpolymer modified surface.

### 3. 3. Results and discussion

#### 3. 3. 1. Surface compositions of terpolymer modified surfaces

Figure 3-3 shows the a) wide and b)  $\text{C}_{1s}$  narrow XPS spectra of the surface modified with MMA terpolymer, P(MMA/PFEA-8/PEO-OMe) with  $n = 9$ . The detected depth from the surface is evaluated around  $1.55 \text{ nm}$ ; lower than the conventional depth because of the low incident angle of the X-ray beam [12]. The results of the angular dependence were shown in Figure 3-3c. On the terpolymer modified surface, together with  $\text{C}_{1s}$  and  $\text{O}_{1s}$  peaks, a  $\text{F}_{1s}$  peak was clearly observed around  $680.0 \text{ eV}$ , originating from  $\text{R}_f$  groups. The  $\text{C}_{1s}$  spectra for the terpolymer modified surfaces could be curve-resolved into eight peaks: at  $294.1 \text{ eV}$  ( $-\text{CF}_3$ ),  $291.7 \text{ eV}$  ( $\text{CF}_2-(\text{CF}_2)$ ),  $291.0 \text{ eV}$  ( $\text{CF}_2-(\text{CH}_2)$ ),  $288.8 \text{ eV}$  ( $\text{C}=\text{O}$ ),  $286.5 \text{ eV}$  ( $\text{C}-\text{O}-(\text{C}=\text{O})$ ),  $286.4 \text{ eV}$  ( $\text{C}-\text{O}-(\text{CH}_2)$ ),  $285.5 \text{ eV}$  ( $\text{CH}_2-(\text{CF}_2)$ ), and  $285.0 \text{ eV}$  ( $\text{C}-(\text{CH}_2)$ ). These peak assignments agreed well with the previously reported ones [13, 14]. The curve-resolving was performed under following conditions; the area of the  $\text{C}-\text{O}-(\text{C}=\text{O})$  was equal to that of  $\text{C}=\text{O}$ , and  $\text{C}-(\text{CF}_2)$  was equal to  $\text{CF}_2-(\text{CH}_2)$ , respectively.



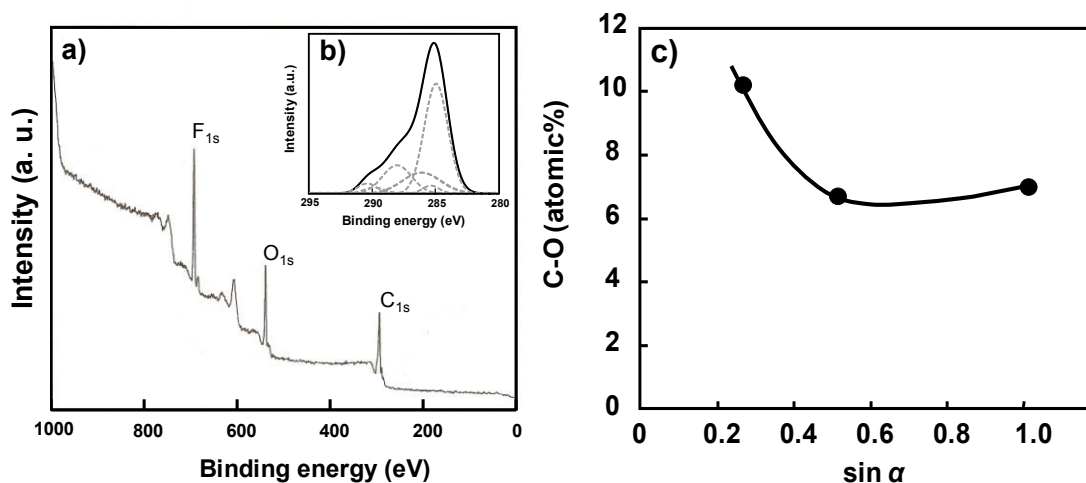


Figure 3-3 XPS a) wide and b) C<sub>1s</sub> narrow spectra of terpolymer (P(MMA/PFEA-8/PEO-OMe) ( $n = 9$ )) modified surfaces. Incident angle of X-ray is 15°. c) Relationship between the C-O atomic% and the depth from the air surface by XPS measurements. The measurements were performed for the P(MMA/PFEA-8/PEO-OMe) films.  $\alpha$ : Take off angle.

Figure 3-4 shows the relationships between the segregations factors of ether (C-O) bond, the fluorine atom and the PEO side chain length of the terpolymer. The segregation factors are here defined as the ratio between the observed (obs.) and calculated (cal.) values. The each value of C-O (obs.) and C-O (cal.) was evaluated by curve-fitting of C<sub>1s</sub> spectra, and the bulk value of surface modifier (calculated from the elemental analyses), respectively. To evaluate the C-O atomic% assigned to the ether bond of PEO side chains, the C-O atomic% from the ester groups were eliminated based on the curve-fitting process. The F/C atomic% (obs.) was also evaluated from the C<sub>1s</sub> spectra. As mentioned above, it is general that the component with the lower  $\gamma_s$  is segregated on the surface. From this view point, surface should be covered with R<sub>f</sub> groups because the  $\gamma_s$  value is 8.5 mJ/m<sup>2</sup> for the homopolymer of PFEA-8 and that of the macromonomer is 44.0 mJ/m<sup>2</sup>. However, the fluorine segregation factor was rather less than the unity. This indicates that the surface fluorine concentration is less than that of the bulk. On the contrary, hydrophilic PEO side chains were predominantly segregated on the surface. The segregation factor of PEO side

chain reached to max.70 times compared with that of the bulk, when PEO side chain length  $n$  of 9. When the terpolymer modified surface was assumed to be totally covered with PEO side chain  $(-(\text{CH}_2\text{CH}_2\text{O})_9\text{-OMe})$ , the segregation factor will reach to ca. 340. In other words, for the terpolymer modified surface, about one fifth as mol ratio of the surface was covered with the surface-segregated PEO side chains. It was speculated that the both PEO side chain and terpolymer main chains existed near the surface because it was random copolymer. However, surface-segregated PEO side chains rather than terpolymer main chain were detectable because of the XPS detected depth. Besides the surface free energy, to explain these phenomena, next, the free volume effect of PEO side chain was investigated.

In general, polymer chain ends are well known to possess high free volume, which brings the surface-segregation of the chain ends because of entropy effect [15]. Bates *et al.* reported that chain with large free volume tends to localize on the surface because of the entropy effect [16]. In the case of using comb-shaped molecule such as macromonomer as used in this study, it is expected that there is also very large free volume attributed to the side chain.

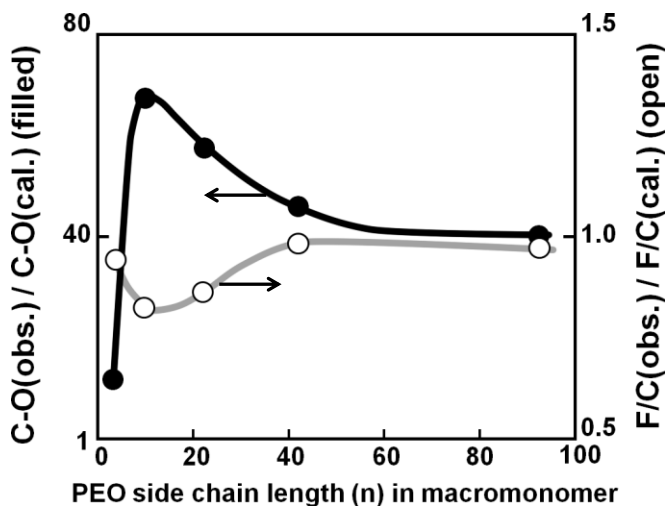


Figure 3-4 Relationships between the segregation factors of C-O, F/C and the PEO side chain length of P(MMA/PFEA-8/PEO-OMe). Matrix resin is composed of PMMA/P(2F-4F) = 40/50.

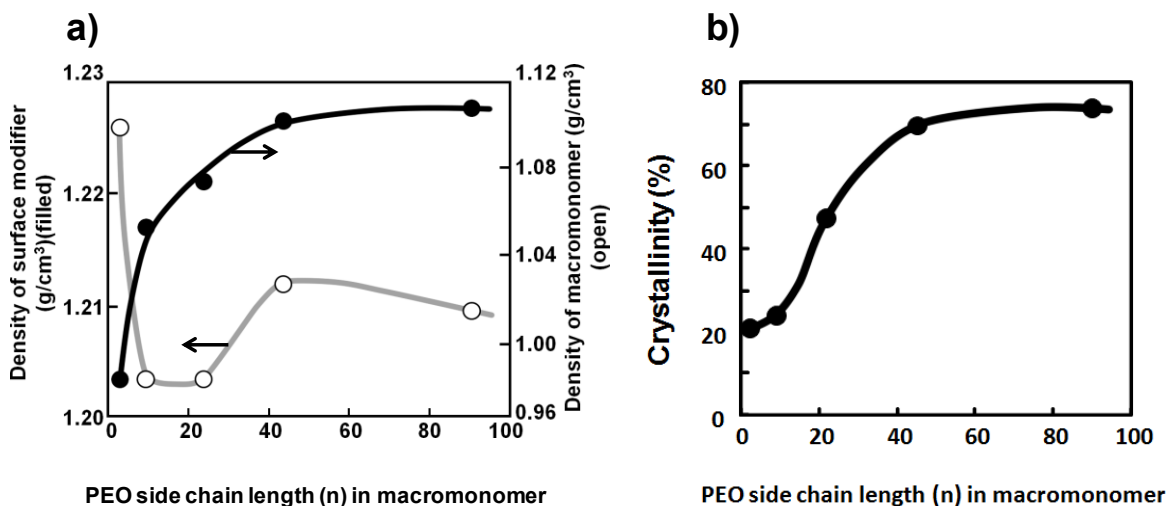


Figure 3-5 a) Effect of the PEO side chain length in macromonomer PEO-OMe on the density of the terpolymer P(MMA/PFEA-8/PEO-OMe), and the macromonomer. b) Effect of the PEO side chain length in macromonomer PEO-OMe on the macromonomer crystallinity. X-ray diffraction (XRD) was carried out using an X-ray diffractometer (RINT2100, Rigaku) equipped with Ni-filtered CuK $\alpha$  radiation, generated at 40 kV, 20 mA. The scanning speed was 2.0 degree/min and the  $2\theta$  scan data were collected at 0.02 degree intervals.

Figure 3-5a shows the effect of the PEO side chain length of macromonomer PEO-OMe on the densities of the terpolymer and the macromonomer itself. Though the density of the macromonomer increased with the PEO side chain length, the density of the terpolymer showed minimum value when  $n = 9$  and  $22$ . The increase of macromonomer density is due to their crystallization (See Figure 3-5b). The macromonomer with long PEO side chain is considered to show low mobility, so the longer PEO side chains were easy to align, then, crystallized and showed high density. For terpolymer, macromonomers were fixed into polymer chain, the crystallization was prohibited due to random sequence, which brought lower density to the terpolymer compared with the macromonomer. The low density suggests that the terpolymers with the PEO side chain ( $n = 9, 22$ ) possesses large free volume. As the results, the large free volume of the PEO side chain stimulates the surface-segregation of the hydrophilic segments due to its entropy effect, which agreed with the results of Figure 3-4. Hereafter, P(MMA/PFEA-8/PEO-OMe) with the PEO side chain

length ( $n$ ) of 22 was used, and the effect of the P(2F-4F) contents of the matrix resin on the surface composition were investigated.

### 3. 3. 2. Effects of P(2F-4F) content on the surface composition

As a matrix resin, P(2F-4F) was used, which was fluorine-containing polymer and possessed higher surface free energy than  $R_f$  group, compatibility with PMMA, in expectations of an interaction between  $R_f$  groups and a matrix resin. Figure 3-6 shows the relationship between the segregation factors of the C-O, F/C and the P(2F-4F) content in the matrix resin. Compared with the bulk composition, fluorine concentrated and no PEO side chain appeared on the surface for just blended the terpolymer with PMMA matrix. This is due to the conventional surface-segregation effect of fluorine based on lowering of surface free energy. On the other hand, instead of fluorine, PEO side chains were segregated on the terpolymer modified surface for the PMMA/P(2F-4F) blended matrix. Especially, in case of 40% wt/wt of P(2F-4F) was blended with PMMA, PEO side chains were largely segregated on the surface. This reveals that the incorporation of P(2F-4F) to the matrix resin promoted the surface-segregation of PEO side chains. It is presumed that the interaction between fluorine segments of the terpolymer and P(2F-4F) of the matrix additionally promotes the surface-segregation of the PEO side chains.

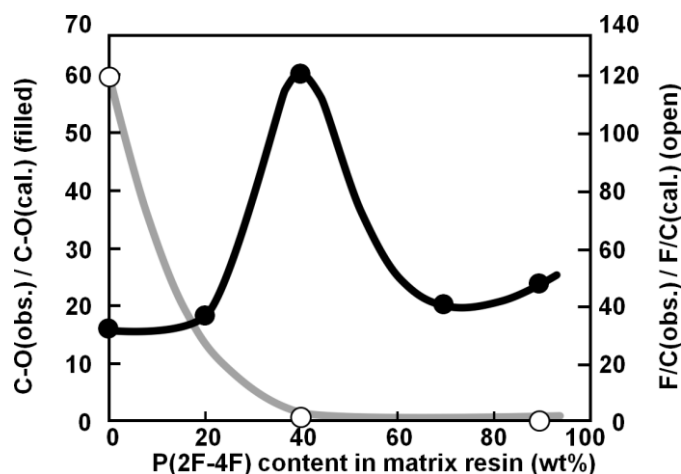


Figure 3-6 Relationship between the segregation factors of C-O, F/C and the P(2F-4F) content in matrix resin on terpolymer modified surfaces ( $n = 22$ ).

From the above results, the mechanism of the segregation of the hydrophilic PEO side chains on the terpolymer modified surface is schematically shown in Figure 3-7. Not only  $R_f$  groups but also PEO side chains are segregated on the surface by balances between three driving forces, *that is*, surface free energy of  $R_f$  group, entropy effect due to free volume of PEO side chain, and interaction between  $R_f$  and P(2F-4F) in the matrix resin. These factors competitively acted, the surface composition can be controlled by the PEO side chain length and compounding ratio of the matrix resin.

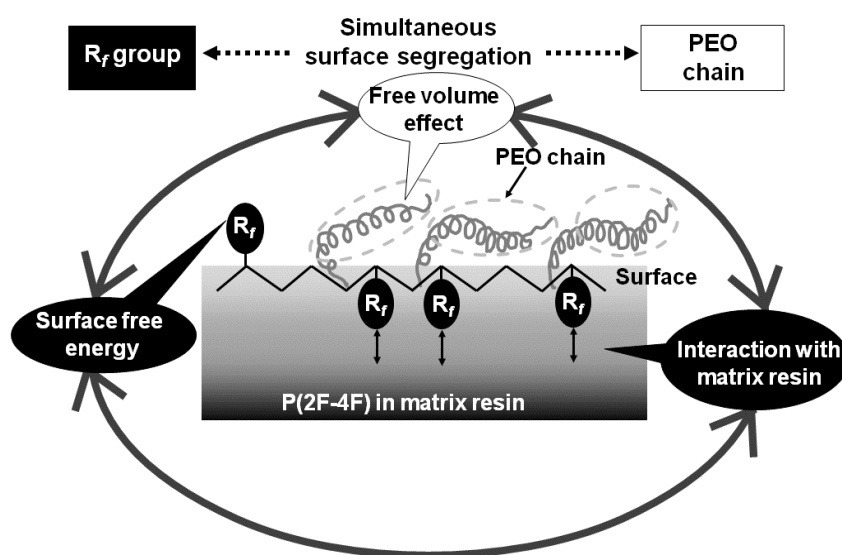


Figure 3-7 Mechanism to explain the segregation of the hydrophilic EO units on the terpolymer modified surface.

### 3. 3. 3. Dynamic contact angle and environment-responsiveness

Figure 3-8 shows the hysteresis of dynamic contact angle of a) water in air and b) air in water on the matrix, P(MMA/PFEA-8/PEO-OMe), and P(MMA/PEO-OMe) surface, where PEO-OMe with  $n = 22$  is used. The  $\theta_a$  and  $\theta_r$  represent advancing contact angle and receding contact angle, respectively. In general, polymer surface shows the hysteresis between  $\theta_a$  and  $\theta_r$ . This phenomenon, as it is called pinning effect [17], can be separated into two types [18, 19]. One is based on physical effect, as famous with Wenzel effect and/or Cassie-Baxter effect, originated from surface roughness. Regarding this matter, the

AFM topographical image of the terpolymer modified surface with P(MMA/PFEA-8/PEO-OMe) and the RMS value by DFM mode operating in air was shown in Figure 3-8c. The terpolymer modified surface possessed a very smooth and flat surface, where the RMS value was 0.5 nm. This indicates that the effect of physical roughness on the dynamic contact angle can be regarded as negligible. The other is chemical pinning effect from chemical heterogeneity/environmental change of the surface during the measurement. A huge variety of studies on the heterogenetic surface about this pinning effect have been performed [20-25].

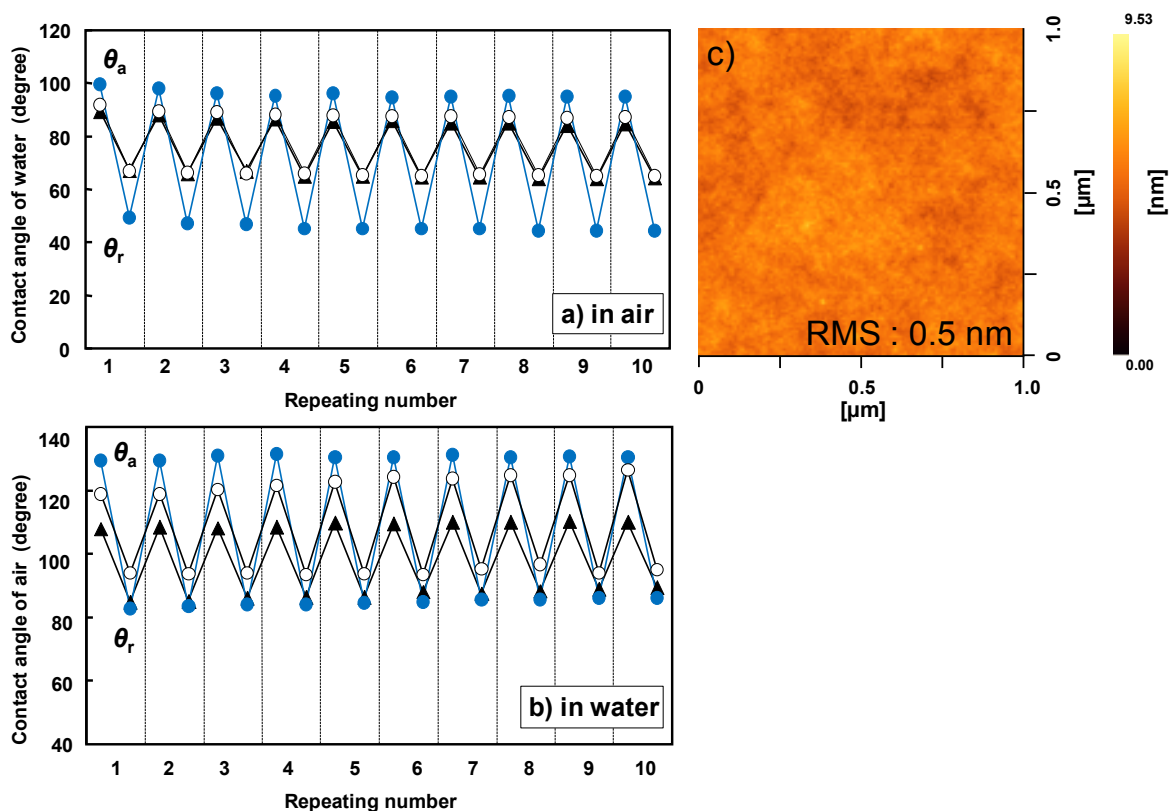


Figure 3-8 Hysteresis of dynamic contact angle of a) water droplet on the terpolymer modified surface in air, b) air bubble on the terpolymer modified surface in water. ●: modified with P(MMA/PFEA-8/PEO-OMe), ○: modified with P(MMA/PEO-OMe) ▲: matrix only. c) AFM Topographical image of the terpolymer modified surface with P(MMA/PFEA-8/PEO-OMe) and the root mean square roughness (RMS) obtained by DFM mode operating in air.

From Figure 3-8a, b, the terpolymer modified surface showed high water repellency due to “chemical pinning effect” of  $R_f$  groups on the surface during the enlargement of water droplet. On the contrary, the surface became hydrophilic during the  $\theta_r$  measurement, because the extended PEO side chains predominated the surface property when water droplet covers the surface. These futures are shown schematically shown in Figure 3-9. Conversely, in water, the terpolymer modified surface is hydrophilic because PEO side chains cover the surface in water, therefore, air bubble shows high  $\theta_a$ , while the  $\theta_r$  of air is low due to spreading of  $R_f$  groups on the surface by contacting with air, *that is*, the terpolymer modified surface showed reverse pinning effect on the air bubble in water. Moreover, through the dynamic contact angle measurements,  $\theta_a$  and  $\theta_r$  were alternatively performed successively at the same point up to repeating number of ten times, these environment-responses were reversible and rapid, which took place within 5 second to change the surface from water repellent one to hydrophilic one, and hydrophilic one to water repellent one, reversely.

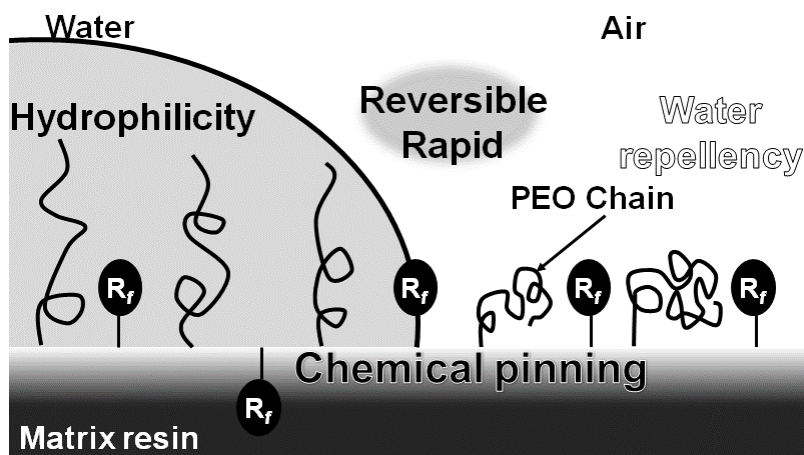


Figure 3-9 Mechanism of high water repellency on terpolymer modified surface.

#### 3. 3. 4. Adhesion property

Figure 3-10 shows the relationship between the  $\theta_a$  value of water on the terpolymer modified surface and the 90°-peel strength against epoxy resin. In general, the surface with

high  $\theta_a$ , value in other words, high water repellent surface shows low peel strength such as PTFE, polyethylene (PE), and *isotactic* polypropylene (PP). This is because the surface possesses poor wettability against adhesive. On the contrary, hydrophilic surface shows low  $\theta_a$  value and high peel strength as poly(vinyl alcohol) (PVA). However, the results in Figure 3-10 indicate the terpolymer modified surfaces showed high  $\theta_a$  and high peel strength simultaneously. On the terpolymer modified surface, high water repellency due to  $R_f$  groups and high wettability against adhesive due to PEO side chains appeared.

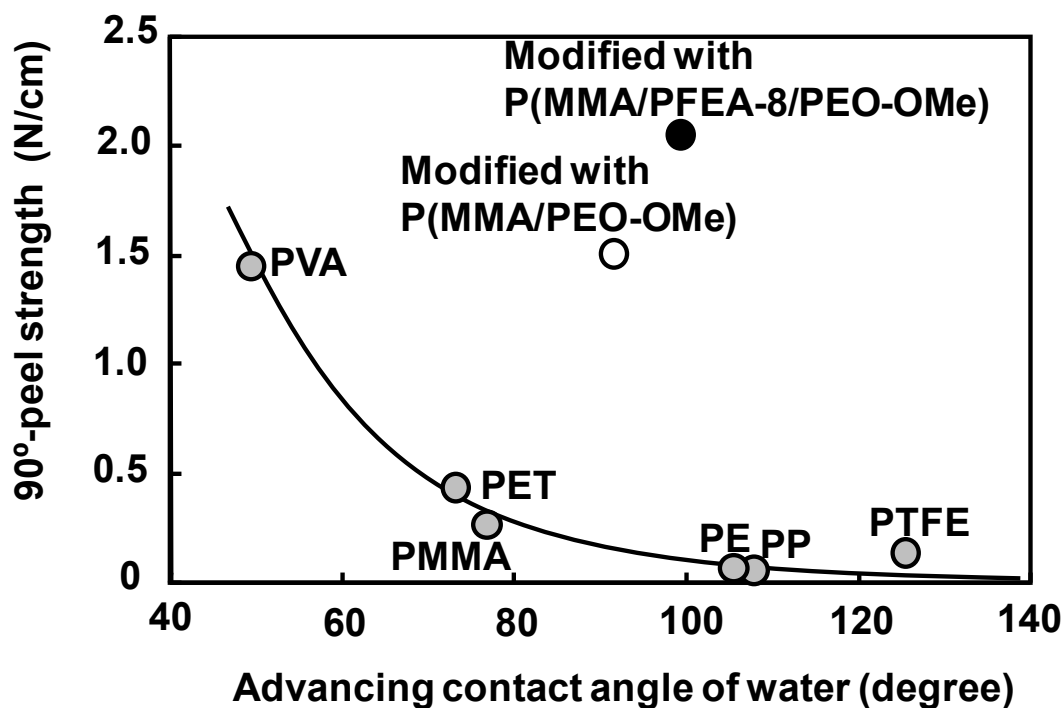


Figure 3-10 Relationship between the 90°-peel strength and the advancing contact angle  $\theta_a$  of water on various polymers.

### 3. 4. Conclusions

The surface modifiers composed of methacrylate-based terpolymer containing both PEO side chains and  $R_f$  groups in a single molecule were prepared, and mixed with PMMA/P(2F-4F) matrix. It was found that not only  $R_f$  groups but also PEO side chains



were segregated on the surface. This is considered to be brought by the balances among the three driving forces, *that is*, surface free energy of  $R_f$  group, entropy effect due to free volume of PEO side chain, and interaction between  $R_f$  and P(2F-4F) in the matrix resin. In the air, the surface showed high water repellency originated from the chemical pinning effect of  $R_f$  group. Instead, in water, the surface is getting very hydrophilic, because the surface is covered with extended PEO side chains. These environment-responses were reversible and rapid, which took place within 5 second. The terpolymer modified surface showed high water repellency due to  $R_f$  groups and high peel strength due to PEO side chains, simultaneously.

### 3. 5. References

- [1] Nishino, T.; Urushihara, Y.; Meguro, M.; Nakamae, K. *J. Colloid Interface Sci.*, 2005, 283, 533.
- [2] Urushihara, Y.; Nishino, T. *Langmuir*, 2005, 21, 2614.
- [3] Wu, D. T.; Fredrickson, G. H. *Macromolecules*, 1996, 29, 7919.
- [4] Wang, J.; Mao, G.; Ober, C. K.; Kramer, E. J. *Macromolecules*, 1997, 30, 1906.
- [5] Katano, Y.; Tomono, H.; Nakajima, T. *Macromolecules*, 1994, 27, 2342.
- [6] Park, I. J.; Lee, S. B.; Choi, C. K. *Macromolecules*, 1998, 31, 7555.
- [7] Hare, E. F.; Shafrin, G. D.; Zisman, W. A. *J.Phys. Chem.*, 1954, 58, 236.
- [8] Nakanishi, H.; Pincus, P. *J. Chem. Phys.* 1983, 79, 997.
- [9] Jannasch, P. *Macromolecules*, 1998, 31, 1341.
- [10] Case, G. S.; Hector, A. L.; Levason, W.; Needs, R. L.; Thomas, M. F.; Weller, M. T. *J. Mater. Chem.* 1999, 9, 2821
- [11] Greenhalgh, R.; Riley, J. P. *Anal. Chim. Acta* 1961, 25, 179.
- [12] Thomas, H. R.; O'Malley, J. J. *Macromolecules*, 1979, 12, 323.
- [13] Park, I. J.; Lee, S. B.; Choi, C. K. *J. Appl. Polym. Sci.*, 1994, 54, 1449.
- [14] Kassis, C. M.; Steehler, J. K.; Betts, D. E.; Guan, Z.; Romack, T. J.; DeSimone, J. M.; Linton, R. W. *Macromolecules*, 1996, 29, 3247.

- [15] Kweskin, S. J.; Komvopoulos, K.; Szomorjai, G. A. *J. Phys Chem.B*, 2005, 109, 23415.
- [16] Sikka, M.; Singh, N.; Karim, A.; Bates, F. S.; Satija, S. K.; Majkrzak, C. F. *Phys. Rev. Lett.*, 1993, 70, 307.
- [17] Quere, D. *Rep. Prog. Phys.* 2005, 68, 2495.
- [18] Johnson, R. E. Jr.; Dettre, R. H. *Surface and Colloid Science*; Matijevic, E, Ed.; Wiley-Interscience: New York, 1969; Vol. 2, pp 85
- [19] Decker, E. L.; Garoff, S. *Langmuir*, 1997, 13, 6321.
- [20] Lv, C.; Yang, C.; Hao, P.; He, F.; Zheng, Q. *Langmuir*, 2010, 26, 8704.
- [21] Bormashenko, E.; Musin, A.; Zinigrad, M. *Colloid Surf. A*, 2011, 385, 235.
- [22] Urata, C.; Masheder, B.; Cheng, D. F.; Hozumi, A. *Langmuir*, 2012, 28, 17681.
- [23] Pilat, D. W.; Papadopoulos, P.; Schaffel, D.; Vollmer, D.; Berger, R.; Butt, H. J. *Langmuir*, 2012, 28, 16812.
- [24] Hong, S. J.; Chang, C. C.; Chou, T. H.; Sheng, Y. J.; Tsao, H. K. *J. Phys. Chem. C*, 2012, 116, 26487.
- [25] Luo, L. X.; Gupta, R.; Frechette, J. *ACS Appl. Mater.Int.*, 2012, 4, 890.



## **Chapter 4**

# **Effect of Poly(ethylene oxide) Side Chains Termini in Surface Modifier on Surface Properties**

#### 4. 1. Introduction

A surface modifier is widely used to change surface properties without losing bulk properties for industrial applications. Fluorinated surface modifiers are used for their unique properties such as oil and water repellency and a low friction property derived from fluorine. Especially, the surface, modified using surface modifier containing perfluoroalkyl ( $R_f$ ) group as side chain or copolymers, shows some property derived from  $R_f$  group when small amount of this surface modifier is added in matrix resin, because  $R_f$  groups are preferentially surface-segregated [1-8]. Although fluorine polymers are expensive, the surface modification can minimize the required amount of fluorine polymers.

As described in Chapter 3, surfaces having unique properties were prepared using surface modifiers which composed of methyl methacrylate (MMA) terpolymers containing both  $R_f$  groups and poly(ethylene oxide) (PEO) side chains in a single molecule. By using these terpolymers as a surface modifier, the terpolymer modified surface was covered with not only  $R_f$  groups but also PEO side chains being against the order of the surface free energy at a certain condition. PEO side chains were found to be surface-segregated by balance of three driving forces as below; free volume of PEO side chains, surface free energy of  $R_f$  groups, and interaction between  $R_f$  groups and fluorine polymer as matrix resin as shown in Chapter 3 [9]. Based on these results, I presumed that controlling surface-segregation of PEO side chains played an important role in broadening the application of surface modifier.

PEO is well known to be a flexible, hydrophilic, neutral polymer and to show resistance to nonspecific protein adsorption and low-toxic property. Then, PEO attracts many attentions in the evolution of polymer materials in the medical field [10-13]. To prepare a PEO rich surface, many methods have been proposed, such as graft copolymerization of PEO macromonomer onto a surface and covalent grafting of PEO, and so on [14].

In this chapter, the preparation of MMA terpolymers containing  $R_f$  groups and PEO side chains in a single molecules was studied. The effect of PEO termini on the terpolymer modified surface was investigated. Moreover, surface properties such as adhesion property and low-fouling property derived from PEO side chain on the terpolymer modified surfaces were also investigated.

## 4. 2. Experimental Section

### 4. 2. 1. Materials

Methyl methacrylate (MMA, Nacalai Tesque, Inc., Kyoto, Japan) was distilled under reduced pressure before use. 2, 2'-Azobis-isobutyronitrile (AIBN, Nacalai Tesque, Inc., Kyoto, Japan) was recrystallized from methanol. The fluorine-containing monomer 2-(perfluoroalkyl) ethyl acrylate (PFEA-8, Clariant Corp., Tokyo, Japan) and several PEO-containing macromonomer (PEO-OH: BLEMMER PE-350D and PEO-OMe: BLEMMER PME-400, NOF Co., Tokyo, Japan) were used as received. Poly(methyl methacrylate) (PMMA) (Acrypet VH, Mitsubishi Rayon Co. Ltd.,  $M_n = 41,100$ , Tokyo, Japan) was purified by reprecipitation by pouring a PMMA/methyl ethyl ketone (MEK, Nacalai Tesque, Inc., Kyoto, Japan) solution into methanol and used as a matrix resin for dip-coating. Vinylidene fluoride-tetrafluoroethylene copolymer ( $(\text{CH}_2\text{CF}_2)_{80}(\text{CF}_2\text{CF}_2)_{20}$ ,  $M_n = 69,300$ , Kynar SL, Atfina Chemicals Inc., Philadelphia, PA, USA) (P(2F-4F)) was also used as matrix resin without further purification. Bovine serum albumin (BSA) and fibrinogen were purchased from Sigma Co (St Louis, MO). Eagle's minimal essential medium containing Kanamycin (Eagle's MEM) and Fetal bovine serum (FBS) were purchased from Nissui Pharmaceutical Co. (Tokyo, Japan) and SIGMA Co. (St Louis, MO), respectively. Other chemicals were purchased from Nacalai Tesque, Inc (Kyoto, Japan).

Fresh human whole blood supplied from a health donor was collected at the medical center for student health, Kobe University. All samples were obtained in accordance with ethical committee regulations of Kobe University.

### 4. 2.2. Sample Preparation

The chemical formulae of the terpolymers used throughout this chapter are shown in Figure 4-1. The preparation of P(MMA/PFEA-8/PEO-OMe) was reported in a previous work (Chapter 3) [9]. In this chapter, the monomer ratios were MMA/PFEA-8/PEO-OMe, OH, and  $R_f = 55/15/30$  w/w/w. P(MMA/PFEA-8/PEO-OH) was free-radical polymerized in ethyl acetate for 7 h at 75°C using AIBN as an initiator. The sum of the monomer concentrations was 30% w/w. The initiator concentrations were 0.5% w/w vs. monomers

for P(MMA/PFEA-8/PEO-OMe) and 5% w/w for P(MMA/PFEA-8/PEO-OH). After the reaction, an excess of *n*-hexane was poured into the reaction solution at room temperature, and then a terpolymer was obtained as precipitate. The terpolymer was dissolved in acetone again and reprecipitated using distilled water. Then, the resultant terpolymer was dried at 40°C under vacuum. P(MMA/PFEA-8/PEO-OH) was dissolved into acetone as 5% w/w solution with keeping at 0°C. Then, triethylamine and perfluorooctylethylsulfonylechloride ( $C_8F_{17}CH_2CH_2SO_2Cl$ ), 1.2 and 1.05-fold the amount of hydroxy groups of PEO side chains, respectively, were added into the solution. Immediately, the flask was sealed and stirred gently for 5 h at 0°C followed by stirring for half a day at room temperature. Next, an excess of *n*-hexane was poured into the reaction solution at room temperature, and the terpolymer was obtained as precipitate. The polymer was purified by reprecipitation in MEK solution for P(MMA/PFEA-8/PEO- $R_f'$ ) in distilled water. Then, the resultant terpolymer was dried at 40°C in air and vacuum.

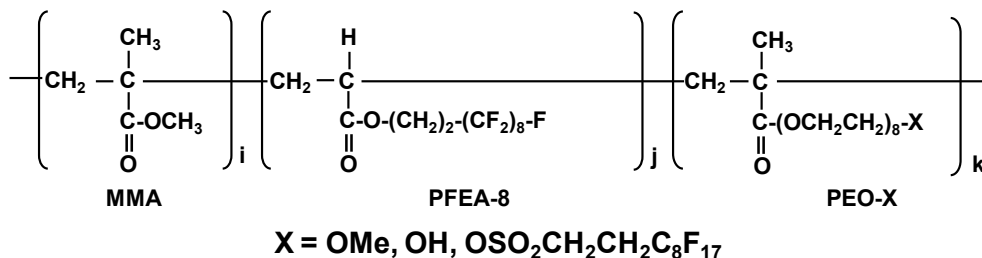


Figure 4-1 Chemical formulae of terpolymers, P(MMA/PFEA-8/PEO-X)s.

The mixture of PMMA, P(2F-4F) and P(MMA/PFEA-8/PEO-OMe), (or P(MMA/PFEA-8/PEO-OH)) were co-dissolved into MEK/methyl isobutyl ketone (MIBK) = 7/3 w/w to prepare 10% w/w clear solution. After stirred overnight, the solution was dip-coated on a poly(ethylene telephthalate) (PET) film, then annealed at 140°C for 1 h. For P(MMA/PFEA-8/PEO- $R_f'$ ), the mixture of matrix resin and P(MMA/PFEA-8/PEO- $R_f'$ ) were co-dissolved into acetone to prepare 5% w/w clear solution. To control the evaporation of acetone, cyclohexanone (5% w/w vs. entire amount) was added to the solution. After stirred for overnight, the coating was performed as described above. The coated surface is hereafter called a terpolymer modified surface.

### 4. 2. 3. Characterization

X-ray photoelectron spectroscopy (XPS) measurements were carried out with the same method described in Chapter 3 and the XPS spectra were collected at 90° of the take-off angle between the sample and the analyzer.

The fluorine content evaluation was performed with the same method described in Chapter 3.

To evaluate the quantity of fluorination, infrared spectroscopy (FT-IR) measurements were carried out using a Perkin–Elmer Spectrum GX FT-IR spectrophotometer with the KBr method. A sample was scanned 10 times at a resolution of 2 cm<sup>-1</sup> over the range of 5000 ~400 cm<sup>-1</sup>.

The dynamic contact angle measurements were performed with the same way described in Chapter 1.

To estimate the adhesive property and surface morphology, 90°-peel tests against epoxy resin and atomic force microscope (AFM) measurements were performed. The methods were the same with those in Chapter 3.

Protein adsorption tests and antithrombogenic tests were performed with in the same way described in Chapter 1, but two different kinds of proteins (BSA and fibrinogen) were used in this chapter. For XPS measurements, films were immersed in each protein solution for 24 h at room temperature and rinsed for three times with distilled water. The XPS N<sub>1s</sub> core level spectra of films were evaluated after drying at room temperature overnight.

Prior to the cell adhesion studies, films were sterilized by immersing in Eagle's MEM containing 60 mg/mL kanamycin for 5 h. L929 fibroblast cells derived from mouse were cultured on the terpolymer modified PET films in Eagle's MEM supplemented with 10% FBS, 1% v/v L-glutamine, and 2% v/v sodium hydrogen carbonate at 37°C in a humidified atmosphere of 95% air and 5% CO<sub>2</sub>. The pH of the medium was adjusted to 7.4. L929 cells were seeded on the sterilized films at a population density of 0.5 × 10<sup>5</sup> cells/mL for the cell-adhesion tests. After culturing, the films were gently rinsed twice with approximately



1.5 mL of PBS to remove cells weakly adhered on the surfaces. The films were observed using a phase-contrast microscope (PM-10AK, Olympus Co., Tokyo). The cell density was evaluated by counting the number of cells attached to unit area from the images. These experiments were performed in triplicate and the data were averaged.

### 4.3. Results and discussion

#### 4.3.1. Composition and reaction of terminal groups of PEO side chain

The actual monomer compositions of terpolymers were shown in Table 4-1. The results show that MMA was preferentially polymerized, and it was difficult for PFEA-8 and PEO macromonomer having long side chains to be copolymerized.

Table 4-1 Monomer compositions of P(MMA/PFEA-8/PEO-X)s.

X		OMe	OH	R <sub>f</sub> '
	MMA	1000	1000	1000
Actual composition (mol ratio)	PFEA-8	12	8	8
	PEO-OMe	81	-	-
	PEO-OH	-	37	33
	PEO-R <sub>f</sub> '	-	-	4
Average molecular weight	$M_n (10^3)$	26.1	5.8	6.4
	$M_w (10^3)$	42.4	22.5	16.9
	$M_w/M_n$	1.6	3.9	2.6

Figure 4-2 shows the FT-IR spectra of P(MMA/PFEA-8/PEO-OH) and P(MMA/PFEA-8/PEO-R<sub>f</sub>'). The absorption bands at 1739 cm<sup>-1</sup> and over 3300 cm<sup>-1</sup> in the spectra of terpolymers were assigned to a carbonyl group and a hydroxy group, respectively. C<sub>8</sub>F<sub>17</sub>CH<sub>2</sub>CH<sub>2</sub>SO<sub>2</sub>Cl reacts with hydroxy groups but not with carboxy groups. The conversion degree in the reaction can be evaluated by the ratio of absorbance of hydroxy

group ( $A_{OH}$ ) and carbonyl group ( $A_{C=O}$ ). After the reaction, the value of  $A_{OH}/A_{C=O}$  changed from 0.0583 to 0.0390 by fluorination. Assuming that there was no side reaction, 33% of terminal hydroxy groups of PEO chains were fluorinated.

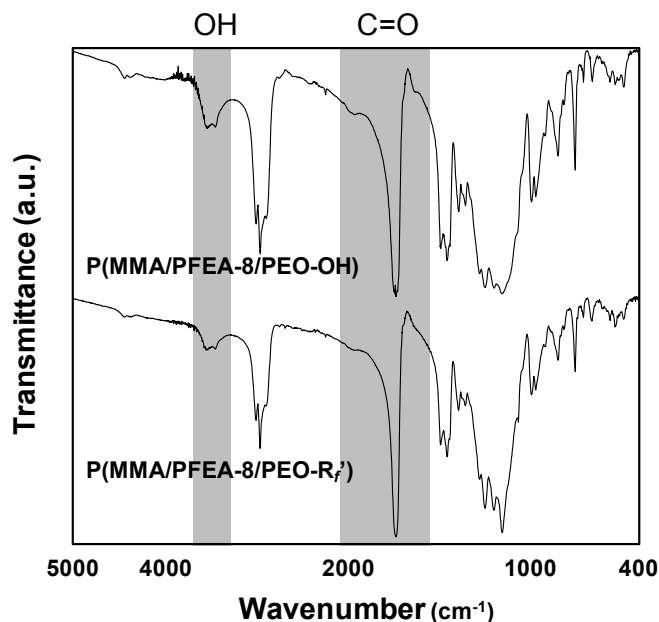


Figure 4-2 FT-IR spectra of P(MMA/PFEA-8/PEO-OH) and P(MMA/PFEA-8/PEO-R<sub>f</sub>).

#### 4. 3. 2. Surface state and wettability

Figure 4-3 shows the typical a) wide and b) C<sub>1s</sub> narrow XPS spectra of the P(MMA/PFEA-8/PEO-OMe) modified surface. For the terpolymer modified surface, a F<sub>1s</sub> peak was clearly found around 680.0 eV, derived from R<sub>f</sub> groups. The C<sub>1s</sub> spectra for the terpolymer modified surfaces were curve-resolved into eight peaks: at 294.1 eV (-CF<sub>3</sub>), 291.7 eV (CF<sub>2</sub>-(CF<sub>2</sub>)), 291.0 eV (CF<sub>2</sub>-(CH<sub>2</sub>)), 288.8 eV (C=O), 286.5 eV (C-O-(C=O)), 286.4 eV (C-O-(CH<sub>2</sub>)), 285.5 eV (C-(CF<sub>2</sub>)), and 285.0 eV (C-(CH<sub>2</sub>)). The peak assignments agreed well with previously reported values [10, 11]. The curve-resolving was performed under following conditions; the area of the C-O-(C=O) was equal to that of C=O, C-(CF<sub>2</sub>) was equal to CF<sub>2</sub>-(CH<sub>2</sub>). Figure 4-3c shows the relationship between PEO termini and C-O atomic% calculated from curve-fitting of C<sub>1s</sub> spectra, the broken line indicates the bulk value. The C-O atomic% was mostly assigned to the ether bond of PEO side chains.

Compared with P(MMA/PFEA-8/PEO-OMe) and P(MMA/PFEA-8/PEO-OH), PEO side chains of P(MMA/PFEA-8/PEO- $R_f'$ ) were much likely to be segregated on the surface because of the introduction of  $R_f'$  groups. As mentioned above, a  $R_f$  group has very low surface energy, therefore,  $R_f'$  groups helped surface-segregation of PEO side chains in a single side chain.

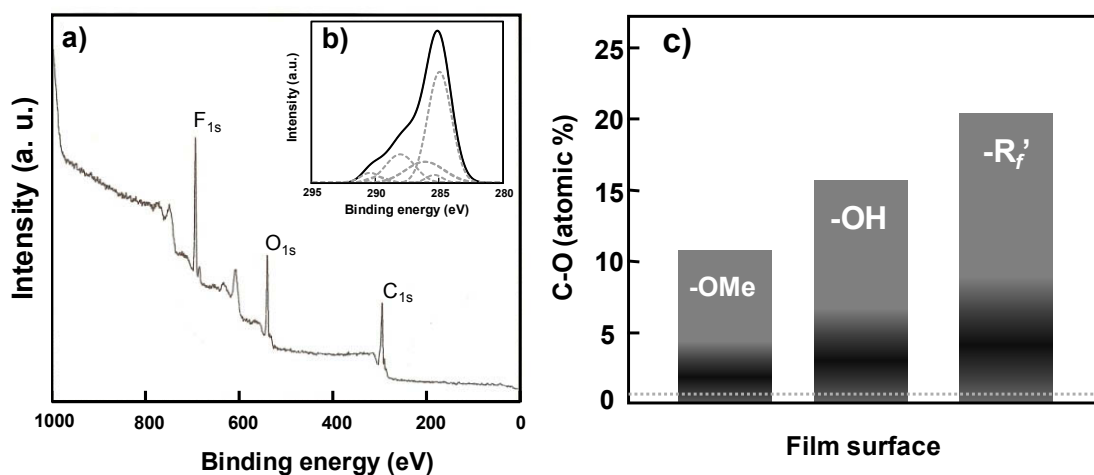


Figure 4-3 XPS a) wide and b)  $C_{1s}$  narrow spectra of MMA terpolymer. c) The surface segregation factor of C-O by the XPS measurements. The broken line is the bulk value calculated from the elemental analysis. The incident angle of X-ray is  $90^\circ$ .

Figure 4-4 shows the hysteresis of dynamic contact angle of water in air on P(MMA/PFEA-8/PEO-OMe), P(MMA/PFEA-8/PEO-OH), and P(MMA/PEO- $R_f'$ ) surfaces. The  $\theta_a$  and  $\theta_r$  represent advancing contact angle and receding contact angle, respectively. Since in air, the terpolymer modified surface is water-repellent because of  $R_f$  groups, therefore, the surface shows high  $\theta_a$  of water. However, the  $\theta_r$  of water was low due to extending PEO side chains by contacting with water. The large difference between  $\theta_a$  and  $\theta_r$  indicates the high environment-responsiveness, which was attributed to the modifier. These behaviors originated from the pinning effect of  $R_f$  groups, being the same as a previous study [9]. These properties were kept when the PEO termini in terpolymer were chemically modified. In particular, for P(MMA/PFEA-8/PEO-OH), the terminal hydroxy groups would

be oriented to water and  $\theta_r$  showed a very low value. Therefore, the surface showed very large hysteresis.

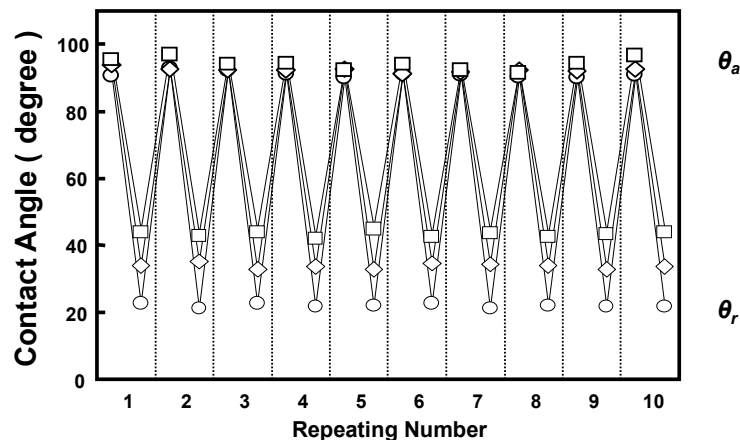


Figure 4-4 Dynamic contact angle of water on the terpolymer modified surfaces in air. The surface modification was carried out using  
 □: P(MMA/PFEA-8/PEO-OMe), ○: P(MMA/PFEA-8/PEO-OH), ◇: P(MMA/PFEA-8/PEO-R<sub>f</sub>' )

A chemical pinning effect is usually observed on surfaces smooth enough. The AFM topographical images of terpolymer modified surfaces in air and water were shown in Figure 4-5. The RMS values are also shown in Figure 4-5. The RMS values indicate that all terpolymer modified surfaces were very smooth enough both in air and in water. In water, the terpolymer modified surfaces showed unique morphologies, which were not observed in air, probably because of highly-swollen PEO side chains. Moreover, RMS values in air were smaller than those in water. These results revealed that surface-segregated PEO side chains might extend in water. In addition, the terpolymer modified surfaces occasionally got a bruise by a cantilever during measurements, which indicates that the terpolymer modified surfaces were soft.

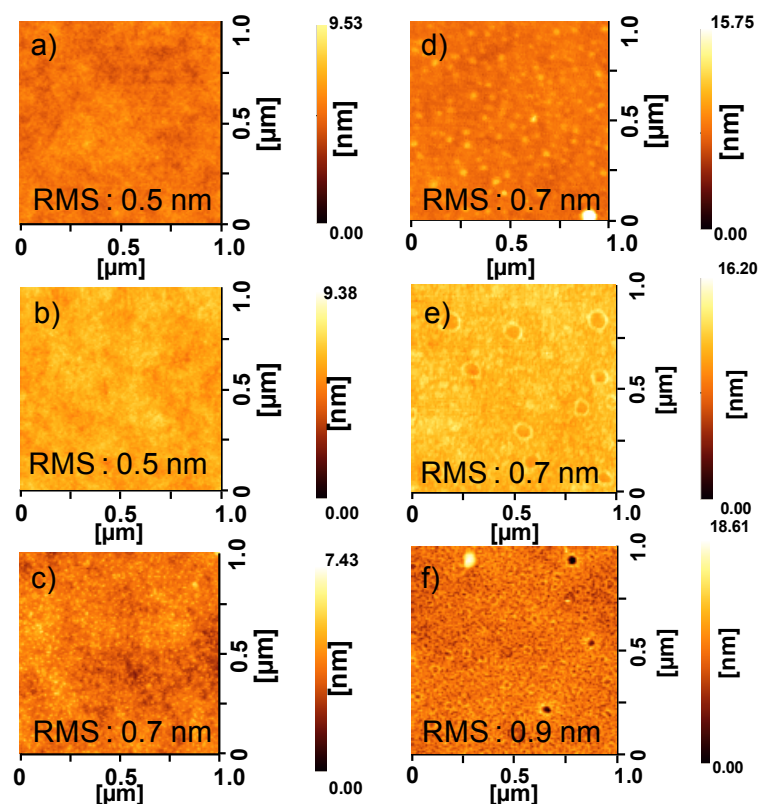


Figure 4-5 AFM topographical images of P(MMA/PFEA-8/PEO-OMe), P(MMA/PFEA-8/PEO-OH), and P(MMA/PFEA-8/PEO-R<sub>f</sub>) modified surfaces obtained by DFM operating in air ((a), (b), (c)) and in water ((d), (e), (f)).

Figure 4-6 shows the relationship between  $\theta_a$  of water and the 90°-peel strength against epoxy resin. In general, a surface with high  $\theta_a$ , in other words, a high water repellent surface shows low peel strength [12-15], because the surface possesses poor wettability with adhesive. On the other hand, a hydrophilic surface, which shows low  $\theta_a$ , has high peel strength. However, terpolymer modified surfaces in this chapter showed high water repellency and high adhesion property, simultaneously [9]. This would be due to both surface-segregated PEO chains and R<sub>f</sub> groups.

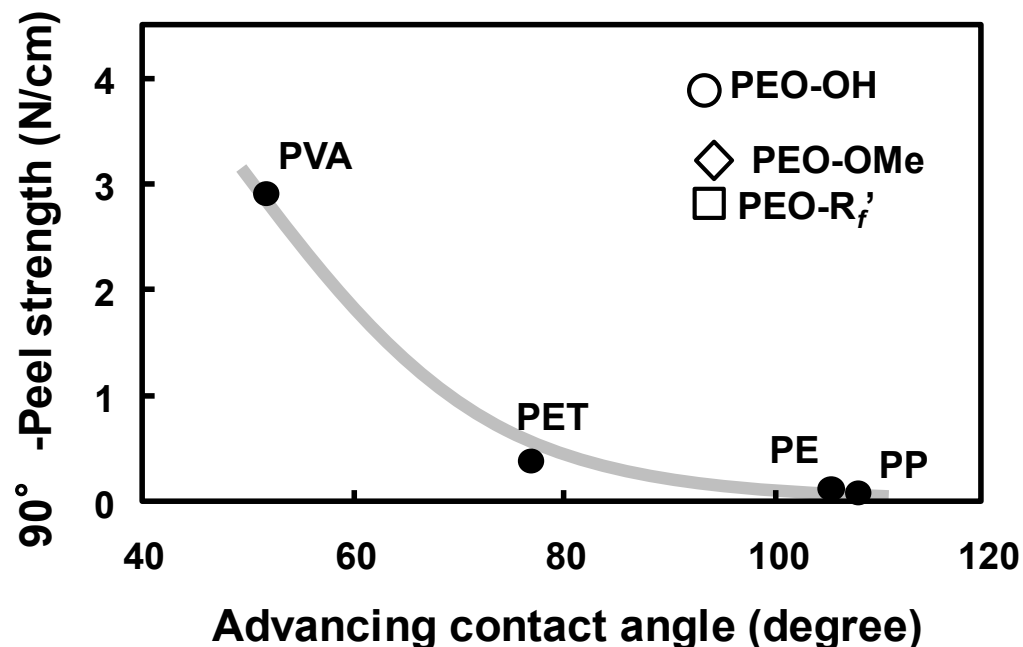


Figure 4-6 Relationship between advancing contact angle of water and the 90°-peel strength on various polymers. PEO-OMe, PEO-OH and PEO-R<sub>f</sub>' represent P(MMA/PFEA-8/PEO-X) modified surface.

Surface-segregated PEO side chains were anticipated to affect the adhesion property. Figure 4-3c reveals that PEO side chains were preferentially segregated on the terpolymer modified surfaces. Especially, on the surface modified with P(MMA/PFEA-8/PEO-R<sub>f</sub>'), surface-segregated PEO chains were one hundred-fold as many as that in the bulk due to R<sub>f</sub>' groups. Even though the PEO side chains were preferentially segregated on the P(MMA/PFEA-8/PEO-R<sub>f</sub>') surface, the peel strength on the P(MMA/PFEA-8/PEO-OH) was the strongest, because R<sub>f</sub>' groups rich surface had poor wettability with the adhesive.

### 3. 3. 3. Low-fouling properties

Figure 4-7 shows the amounts of proteins (BSA and fibrinogen) adsorbed on the terpolymer modified surfaces. These proteins are relatively hydrophobic and are widely used as model fouling proteins in biomedical and bioanalytical fields. While an original PET surface adsorbed about  $0.8 \mu\text{g}/\text{cm}^2$  of BSA, the terpolymer modified surfaces adsorbed reduced amounts of BSA. For example, the adsorbed BSA was only  $0.20 \mu\text{g}/\text{cm}^2$  on a P(MMA/PFEA-8/PEO- $R_f'$ ) modified surface, which was less than one-fourth of that of an original PET surface. On the terpolymer modified surfaces, surface-segregated PEO chains would prevent protein adsorption. The surface modification of a PET surface was also effective for reducing the adsorption amounts of fibrinogen (Figure 4-7b). This resistance would originate from the excluded volume effect and high mobility of PEO side chains in water [16].

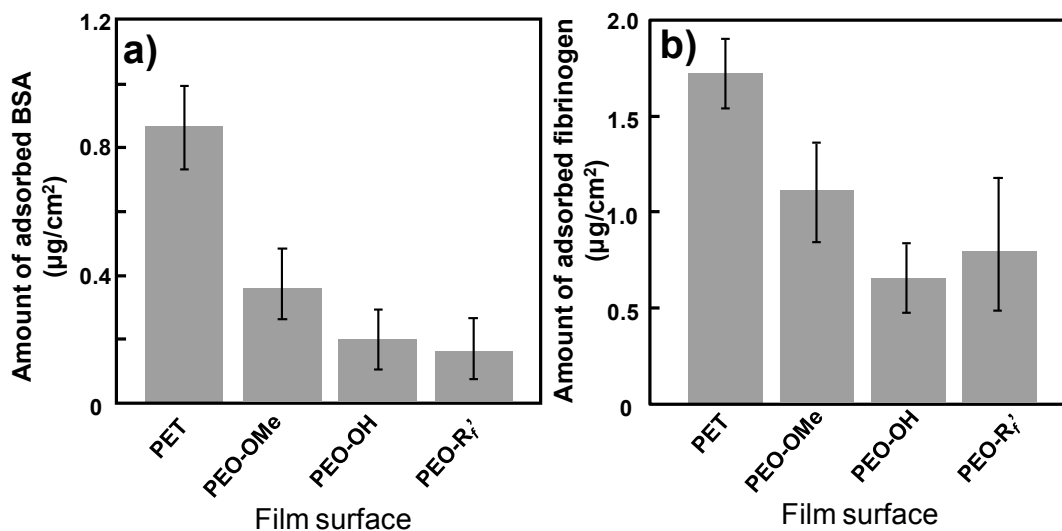


Figure 4-7 Amount of a) BSA, and b) fibrinogen adsorbed on the bare and modified PET films. The surface modification was carried out using P(MMA/PFEA-8/PEO-X).

The  $N_{1s}$  spectra obtained from XPS measurements are shown in Figure 4-8. The nitrogen signal can be used as an indicator of the relative amount of protein adsorbed on the surface [17, 18]. Thus, the significant reduction in protein adsorption was also confirmed from the decrease of the  $N_{1s}$  signal intensity for the terpolymer modified surfaces. These results agreed with the resistance to protein adsorption observed in Figure 4-7.

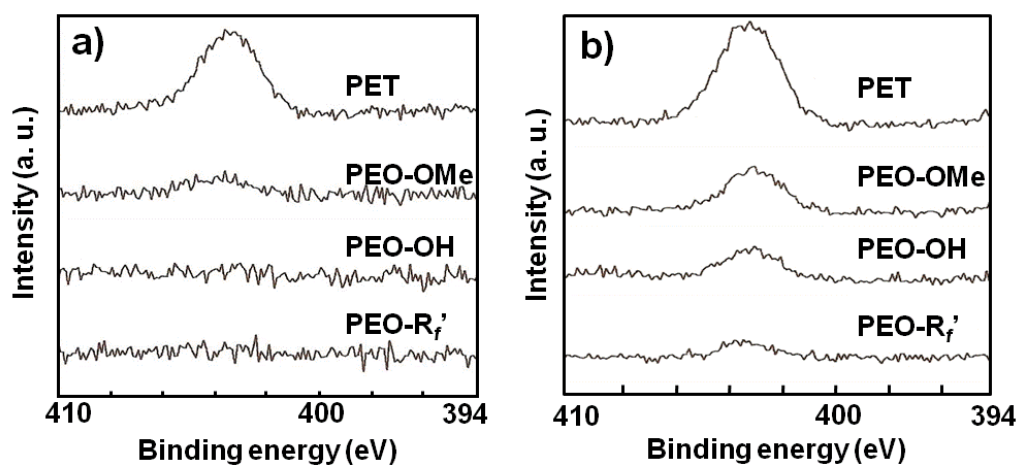


Figure 4-8 XPS  $N_{1s}$  core level spectra of original PET and terpolymer modified surfaces after adsorption of (a) BSA and (b) fibrinogen. PEO-OMe, PEO-OH, and PEO-  $R_f'$  represent PET films coated with P(MMA/PFEA-8/PEO-X).

Figure 4-9 shows the photographs of an original PET film, and the terpolymer modified films after immersed in whole human blood and rinsing. Protein adsorption is a key step of clotting. Blood platelets were adsorbed on the protein and clotting was caused [19, 20]. On the original PET and film coated by only matrix resin clotting took place, while no clots could be observed on the modified surfaces. Especially, P(MMA/PFEA-8/PEO-OH) and P(MMA/PFEA-8/PEO- $R_f'$ ) surfaces were remarkable. These results originated from the protein repellent characteristics of the terpolymer modified surfaces.



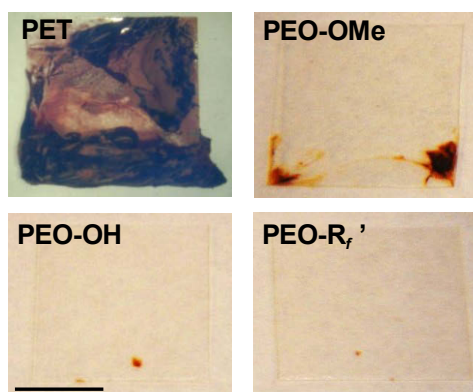


Figure 4-9 Optical photographs of original and surface modified PET films after immersed in whole human blood. PEO-OMe, PEO-OH, and PEO- R<sub>f</sub>' represent PET films coated with P(MMA/PFEA-8/PEO-X). A scale bar represents 5 mm.

Cell adhesion to a material surface is also known to be initiated by protein adsorption to a material surface. The cell adhesion to an original PET surface and terpolymer modified surfaces was investigated using L929 cells. Figure 4-10a, b and c shows the optical micrographs of PET films half-coated with terpolymers after cultivation for 2 days. L929 cells are known to be adherent cells, which grow proliferously with spreading. On the original PET film, the number of the cell attachment was larger than those of the terpolymer modified surfaces. On the terpolymer modified surfaces, there were a few cells attached.

Figure 4-10d shows the relationship between C-O atomic% and the cell density on the surfaces, and C-O atomic% was determined by XPS. Figure 4-10d shows that, as the C-O atomic% became larger, the number of attached cell decreased accordingly. These results reveal that terpolymer modified surfaces can prevent both cell adhesion and propagation. The reduced cell adhesion was probably due to the resistance to protein adsorption by PEO segregated surfaces.

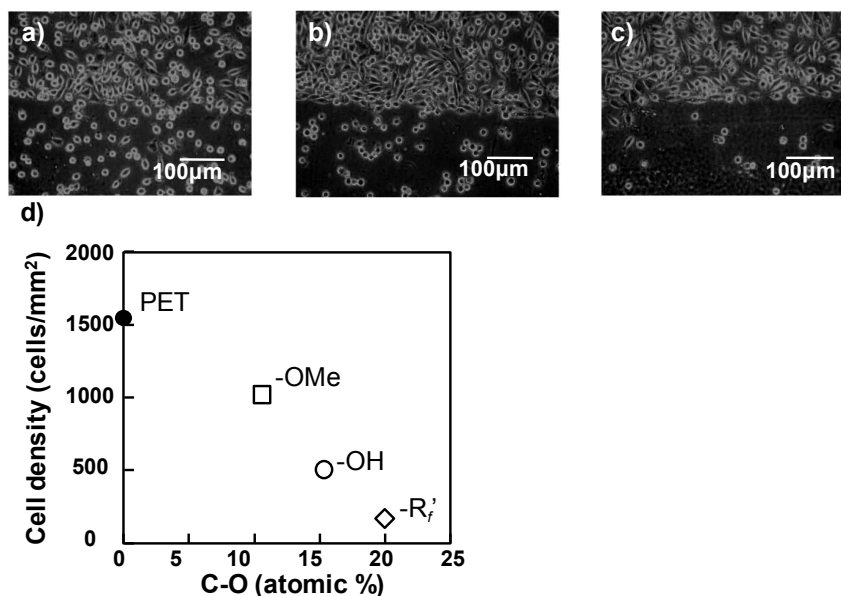


Figure 4-10 Optical micrographs of L929 cells seeded and cultured for 2 day onto films half coated by a) P(MMA/PFEA-8/PEO-OMe), b) P(MMA/PFEA-8/PEO-OH), c) P(MMA/PFEA-8/PEO-R<sub>f</sub>'). d) Relationship between cell density of L929 cells cultured 2 days and the C-O (atomic%) detected by XPS measurement.

#### 4. 4. Conclusions

The terpolymer contained both PEO side chains and R<sub>f</sub> groups in a single molecule was synthesized. The PEO termini were changed. The adhesive properties and low-fouling properties of terpolymer modified surfaces were investigated. On the terpolymer modified surfaces, not only R<sub>f</sub> groups but also PEO chains were segregated, being against the order of surface free energy. These surfaces showed high water repellency and high adhesive property, simultaneously. These surfaces showed resistance to protein adsorption and to cell adhesion derived from surface-segregated PEO side chains. Especially, the P(MMA/PFEA-8/PEO-OH) modified surface showed good adhesion property and low-fouling property.

#### 4. 5. References

[1] Wang, J.; Mao, G.; Ober, C. K.; Kramer, E. J. *Macromolecules*, 1997, 30, 1906.

- [2] Katano, Y.; Tomono, H.; Nakajima, T. *Macromolecules*, 1994, 27, 2342.
- [3] Park, I. J.; Lee, S. B.; Choi, C. K. *Macromolecules*, 1998, 31, 7555.
- [4] Nishino, T.; Urushihara, Y.; Meguro, M.; Nakamae, K. *J. Colloid Interface Sci.*, 2005, 283, 533.
- [5] Urushihara, Y.; Nishino, T. *Langmuir*, 2005, 21, 2614.
- [6] Wu, D. T.; Fredrickson, G. H. *Macromolecules*, 1996, 29, 7919.
- [7] Hare, E. F.; Shafrin, G. D.; Zisman, W. A. *J. Phys. Chem.*, 1954, 58, 236.
- [8] Nakanishi, H.; Pincus, P. *J. Chem. Phys.*, 1983, 79, 997.
- [9] Tokuda, K.; Kawasaki, M.; Kotera, M.; Nishino, T. *Langmuir*, revision required. Resubmission is undergoing.
- [10] Park, I. J.; Lee, S. B.; Choi, C. K. *J. Appl. Polym. Sci.*, 1994, 54, 2538.
- [11] Kassis, C. M.; Steehler, J. K.; Betts, D. E.; Guan, Z.; Romack, T. J.; DeSimone, J. M.; Linton, R. W. *Macromolecules*, 1996, 29, 3247.
- [12] Awaja, F.; Gilbert, M.; Kelly, G.; Fox, B.; Brynolf, R.; Pigram, P. J. *ACS Appl. Mater. Interfaces*, 2010, 2, 1505.
- [13] Morris, H. R.; Turner, J. F.; Munro, B.; Ryntz, R. A.; Treado, P. J. *Langmuir*, 1999, 15, 2961.
- [14] Jung, C. K.; Bae, I. S.; Lee, S. B.; Cho, A. H.; Shin, E. S.; Choi, S. C.; Boo, J. H. *Thin Solid Films*, 2006, 506, 316.
- [15] Pijpers, A. P.; Meier, R. J. *J. Electron. Spectrosc.*, 2001, 121, 299.
- [16] Choi, C.; Hwang, I.; Cho, Y.; Han, S. Y.; Jo, D. H.; Jung, D.; Moon, D. W.; Kim, E. J.; Jeon, C. S.; Kim, J. H.; Chung, T. D.; Lee, T. G. *ACS Appl. Mater. Interfaces*, 2013, 5, 687.
- [17] Pillai, S.; Arpanaei, A.; Rikke, L. M.; Birkedal, V.; Gram, L. *Biomacromolecules*, 2009, 10, 2759.
- [18] Czuhra, M. Jr.; Riggs, W. M. *Anal. Chem.*, 1975, 47, 1836.
- [19] Ratner, B. D.; Hoffman, A. S.; Schoen, F. J.; Lemons, J. E. *Biomaterial Science: An Introduction to Materials in Medicine*, Academic Press, New York 1996, pp133
- [20] Brynda, E.; Houska, M.; Dyr, J. E. *J. Biomed. Mater Res.*, 2000, 51, 249.





## **Chapter 5**

### **Effect of the Carbon numbers of Perfluoroalkyl groups in Surface Modifier on Surface Properties**

## 5. 1. Introduction

A perfluoroalkyl ( $R_f$ ) group is highly fluorinated hydrocarbon, and possesses very low surface free energy derived from fluorine. Polymers with  $R_f$  side chains linked to common thermoplastic polymers [1-7] are widely used for many applications such as biomaterials, coating engineering, and breathable textures, because they show the strong surface-segregation and bring a variety of surface properties. In Chapter 3, the properties of polymer surfaces modified by terpolymers composed of methyl methacrylate (MMA), 2-(perfluorooctyl) ethyl acrylate and several macromonomers (P(MMA/PFEA-8/PEO-OMe)) were investigated. The macromonomers had PEO side chains with different length. Not only  $R_f$  groups but also PEO side chains were found to be segregated on these surfaces, being against the order of the surface free energy. These surfaces showed high water repellency and high adhesive property, simultaneously [8]. Moreover, in Chapter 4, the surface modified by methacrylate-based terpolymers composed of MMA, 2-(perfluorooctyl) ethyl acrylate and three macromonomers having PEO side chains with different termini (P(MMA/PFEA-8/PEO-OMe, OH,  $R_f'$ )) were prepared. Then, factors affecting the surface-segregation were optimized. These surfaces showed good adhesion property and low-fouling properties.

However, a  $R_f$  group with carbon number 8, whose compounds were used in Chapters 3 and 4, has a fear to produce perfluorooctanoic acid (PFOA), which may cause its high bioaccumulation [9].

In this chapter, the carbon numbers of the  $R_f$  group in terpolymers were highlighted to avoid PFOA problem. The effect of carbon numbers of the  $R_f$  group in terpolymers on surface properties were investigated.

## 5. 2. Experimental

### 5. 2. 1. Materials

Methyl methacrylate (MMA, Nacalai Tesque, Inc., Kyoto, Japan) was distilled under reduced pressure before use. 2, 2'-Azobis-isobutyronitrile (AIBN, Nacalai Tesque, Inc., Kyoto, Japan) was recrystallized from methanol. Fluoro-containing monomer, 2-(perfluoroalkyl)ethyl acrylate (PFEA-4, 6, DIC Ltd., Tokyo, Japan and PFEA-8,

Clariant Corp., Tokyo, Japan), in which figures (-4, -6 and -8) represent the carbon numbers of perfluoroalkyl groups, and macromonomer with PEO side chains (PEO-OH: BLEMMER PE-350D, NOF Co., Tokyo, Japan) were used as received. The terminus of the PEO side chain was hydroxy group. Poly(methyl methacrylate) (PMMA) (Acrypet VH, Mitsubishi Rayon Co. Ltd.,  $M_n = 41,100$ , Tokyo, Japan) was purified by reprecipitation from methyl ethyl ketone (MEK) solution into methanol. Vinylidene fluoride (VdF) -tetrafluoroethylene (TFE) copolymer ( $(\text{CH}_2\text{CF}_2)_{80}(\text{CF}_2\text{CF}_2)_{20}$ ,  $M_n = 69,300$ , Kynar SL, Atfina Chemicals Inc., Philadelphia, PA, USA) was used as received. Other chemicals were purchased from Nacalai Tesque, Inc (Kyoto, Japan).

### 5. 2. 2. Sample preparation

The chemical formulae of the terpolymers used throughout this chapter are shown in Figure 5-1. P(MMA/PFEA- $n$ /PEO-OH)s ( $n$  represents the carbon number of the  $R_f$  groups in PFEA monomer,  $n = 4, 6$  and  $8$ ) were synthesized by free-radical polymerization in ethyl acetate at  $75^\circ\text{C}$  for 7 h using AIBN as an initiator (5% w/w vs. monomers). In this chapter, the monomer ratios were MMA/PFEA- $n$ /PEO-OH = 55/15/30 w/w/w. The sum of the monomer concentrations was 30% w/w. An excess of  $n$ -hexane was poured into the reactant solution, and a terpolymer was obtained as precipitate. The polymer was reprecipitated again in acetone solution for P(MMA/PFEA- $n$ /PEO-OH) in distilled water. The resultant terpolymer was used as the surface modifier after being dried at  $40^\circ\text{C}$  in air until no weight change occurred.

To estimate the actual monomer composition of the terpolymer, the elemental analysis was performed with the same method described in Chapter 3. Table 5-1 shows actual monomer compositions of terpolymers.

The mixture of PMMA and P(2F-4F) was used as a matrix resin. PMMA, P(2F-4F) and a terpolymer were co-dissolved into MEK/methyl isobutyl ketone = 7/3 w/w to prepare 10% w/w clear solution. After overnight, the solution was dip-coated on poly(ethylene telephthalate) (PET) film, then annealing at  $140^\circ\text{C}$  for 1 h. The coated surface is hereafter called a terpolymer modified surface.



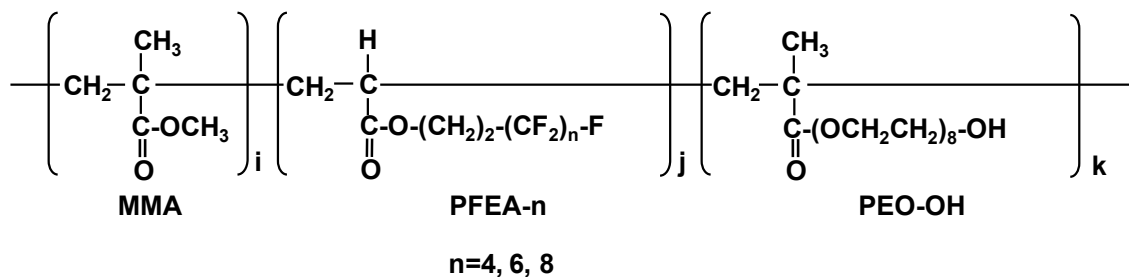


Figure 5-1 Chemical formulae of terpolymer, P(MMA/PFEA-4, 6, 8/PEO-OH)s.

### 5. 2. 3. Characterization

X-ray photoelectron spectroscopy (XPS) and the dynamic contact angle measurements were carried out with the same method described in Chapter 1.

To estimate the adhesive property and surface morphology, 90°-peel test against epoxy resin and an atomic force microscope (AFM) measurement were performed, respectively. The methods were the same with those in Chapter 3.

## 5. 3. Results and discussion

### 5. 3. 1. Polymer compositions and surface state

Table 5-1 shows actual compositions of the monomers in terpolymers. As is clearly seen from the results, the amount of a PFEA monomer introduced into terpolymers decreased with the increase of the carbon numbers of the  $R_f$  group. Longer  $R_f$  group as side chain disturbed the polymerization of PFEA monomers into terpolymers. As mentioned in Chapter 3, a chemically inhomogeneous and smooth surface often shows chemical pinning effect. If P(MMA/PFEA-4, 6, 8/PEO-OH) modified surfaces possess surfaces smooth enough, these modified surfaces would show chemical pinning effect. Figure 5-2 shows the AFM topographical images of P(MMA/PFEA-4, 6, 8/PEO-OH) modified surfaces and RMS values by DFM operating in air. The terpolymer modified surfaces possessed very smooth and flat surfaces similar to the P(MMA/PFEA-8/PEO-OMe) modified surface [8]. These results indicate that the effect of physical roughness on the dynamic contact angle can be negligible.

Table 5-1 Molymer compositions of P(MMA/PFEA-n/PEO-OH), n represents the carbon number of R<sub>f</sub> groups.

n		4	6	8
	MMA	1000	1000	1000
Actual composition (mol ratio)	PFEA-4	69	-	-
	PFEA-6	-	47	-
	PFEA-8	-	-	27
	PEO-OH	90	114	110

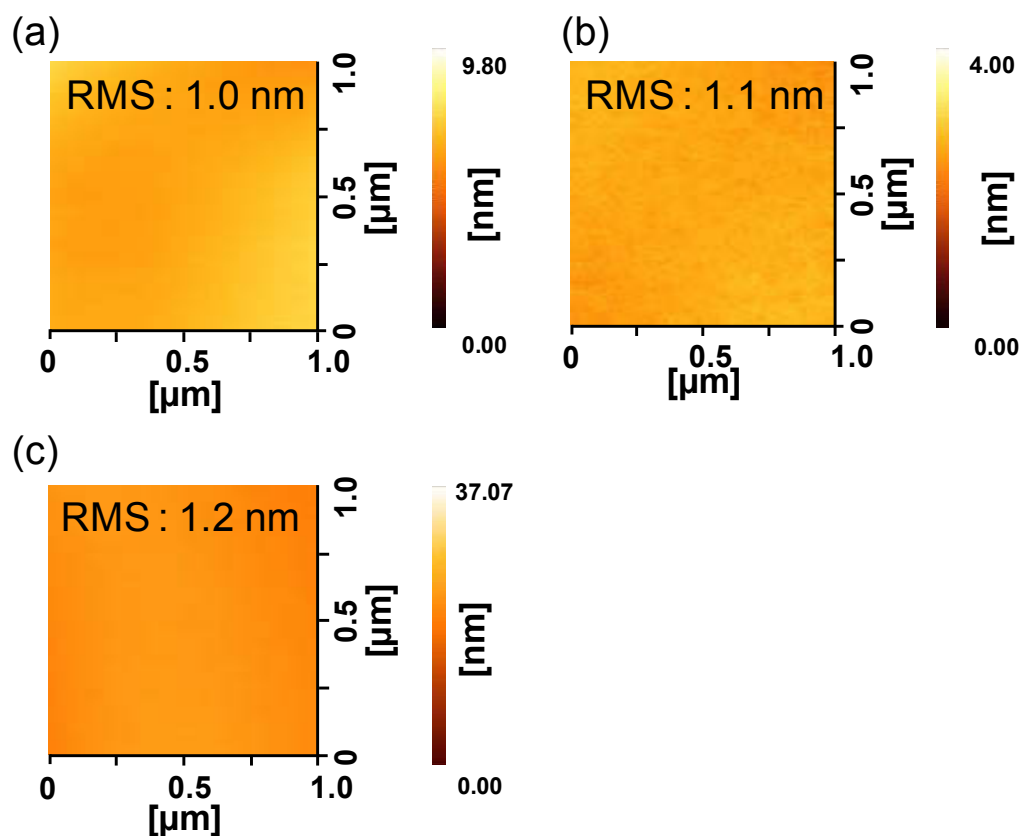


Figure 5-2 AFM topographical images of (a) P(MMA/PFEA-4/PEO-OH), (b) P(MMA/PFEA-6/PEO-OH), and P(MMA/PFEA-8/PEO-OH) modified surfaces obtained by DFM operating in air.

### 3. 3. 2. Adhesion property and environment-response

As well as Chapter 2, the hysteresises of dynamic contact angle of water in air on

terpolymer modified surfaces were investigated. Different from commodity polymer surfaces [10-12], the terpolymer modified surfaces showed high advancing contact angle ( $\theta_a$ ) and low receding contact angle ( $\theta_r$ ) due to the surface-segregated PEO side chains and the pinning effect of the  $R_f$  groups. The changes from water repellent surface to hydrophilic surface and hydrophilic surface to water repellent surface took about several seconds (data not shown). This indicates that response is reversible and rapid. The three terpolymers show similar hysteresis with each other. It is presumed that all terpolymers brought about high environment-responsiveness in all cases.

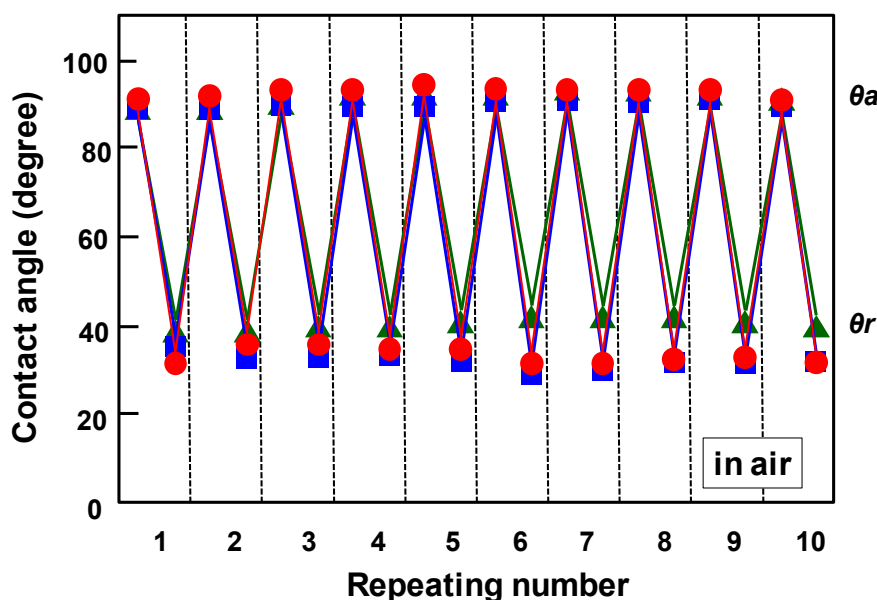


Figure 5-3 Dynamic contact angle of water on the films in air. The surface modification was carried out using

▲: P(MMA/PFEA-4/PEO-OH),    ■: P(MMA/PFEA-6/PEO-OH),    ●: P(MMA/PFEA-8/PEO-OH)

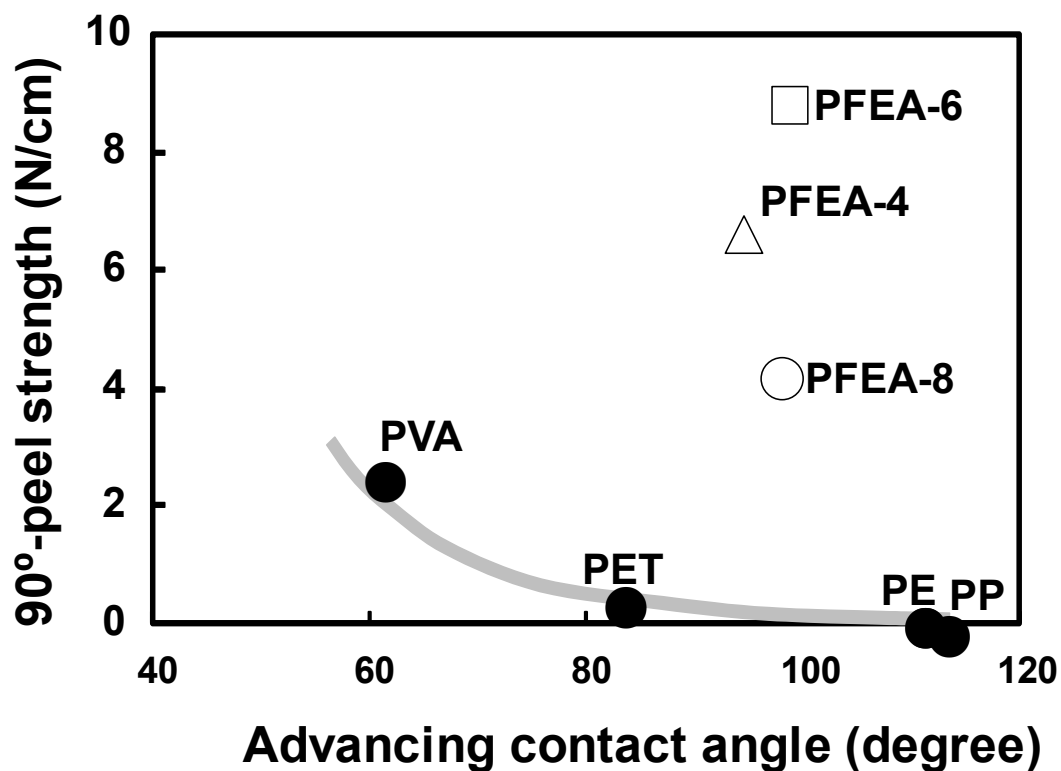


Figure 5-4 Relationship between advancing contact angle of water and the 90°-peel strength on various polymers against epoxy resin. PFEA-4, 6, 8 represent P(MMA/PFEA-4, 6, 8/PEO-OH) modified surfaces.

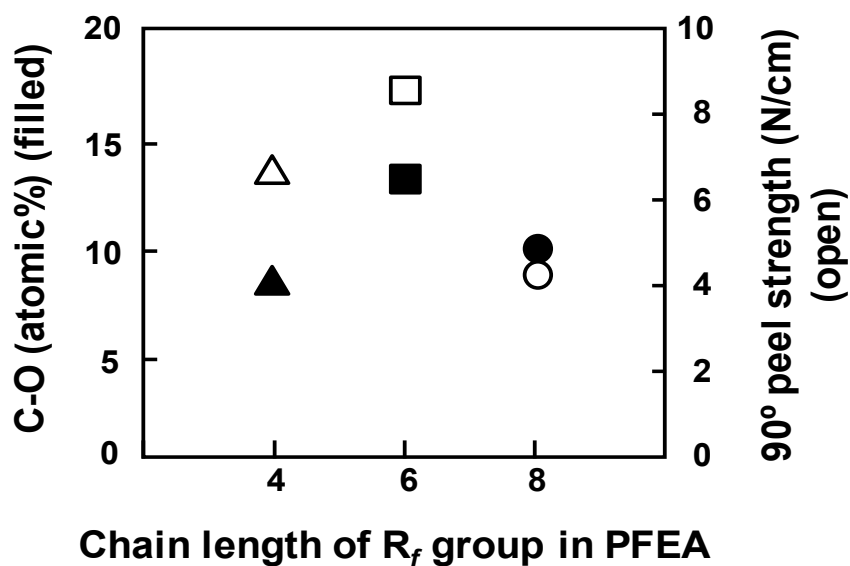


Figure 5-5 Effect of the chain length of R<sub>f</sub> group in PFEA monomer on the C-O atomic% detected by XPS measurement and the 90° peel strength.

These results show that the property of terpolymer modified surface can change due to their responsiveness to contact medium. Then, simultaneous water repellent and high adhesive properties were expected on the terpolymer modified surfaces.

In order to demonstrate these two properties, 90°-peel test was performed. The relationship between the  $\theta_a$  value of water on the terpolymer modified surface and the 90°-peel strength against epoxy resin was shown in Figure 5-4. The terpolymer modified surfaces possessed high  $\theta_a$ , *that is*, high water repellency and high peel strength, simultaneously while surfaces with high  $\theta_a$  such as polytetrafluoroethylene (PTFE), polyethylene (PE), and polypropylene (PP) showed low peel strength. The terpolymer modified surface showed different behavior from commodity polymers, high water repellency derived from the pinning effect of the  $R_f$  groups and high adhesive property derived from surface-segregated PEO side chains, simultaneously.

Compared with the P(MMA/PFEA-8/PEO-OH) modified surface, P(MMA/PFEA-6/PEO-OH) modified surface about showed twice peel strength. After 90°-peel test, on the P(MMA/PFEA-6/PEO-OH) modified surface, cohesive failures between an underside of substrate and a coating polymer appeared to have happened for many specimens. This indicates that the actual 90°-peel strength between an epoxy resin and a modified surface was higher than 9.1 N/cm. To discuss this phenomenon, the terpolymer modified surfaces were investigated using XPS. Chapter 3 revealed that high adhesive property had close relationship with the surface-segregated PEO side chains for these terpolymer modified surfaces. Figure 5-5 shows the effect of the chain length of the  $R_f$  group in a PFEA monomer on the C-O atomic% detected by the XPS measurements and on the 90°-peel strength. The C-O atomic% is mostly assigned to the ether bond of PEO chains. In the bulk, the C-O atomic% (0.6 ~ 0.8 atomic%) were estimated from the elemental analyses. In brief, PEO side chains were found to be segregated on the terpolymer modified surfaces in every case. The 90°-peel strength synchronously changed with the amount of surface-segregated PEO chains. In particular, P(MMA/PFEA-6/PEO-OH) modified surface shows high peel strength and large amount of surface-segregated PEO side chains. Each homopolymer (poly(PFEA-4, 6, 8)) was seemed to have different glass transition point (Tg). Therefore, the carbon number of  $R_f$  group affected the Tg of a surface modifier, *that is*, the mobility of PEO

side chains and  $R_f$  groups.

Figure 5-6 shows the  $\theta_a$  and  $90^\circ$ -peel strength on P(MMA/PFMA-6/PEO-OH) modified surface. P(MMA/PFMA-6/PEO-OH) was synthesized using only methacrylate, and carbon number of  $R_f$  group was 6. Dip-coated samples were prepared in the same way of P(MMA/PFEA-6/PEO-OH). On the P(MMA/PFMA-6/PEO-OH) modified surface, the  $90^\circ$ -peel strength was lower than that on P(MMA/PFEA-6/PEO-OH) modified surface. To achieve the surface-segregation of PEO side chains, it was necessary to optimize the balance of molecular structure.

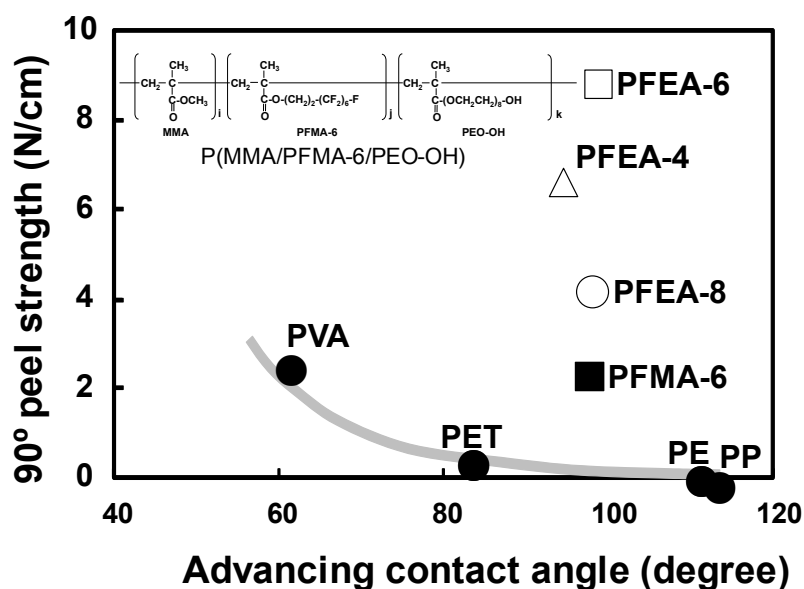


Figure 5-6 Relationship between advancing contact angle of water and the  $90^\circ$ -peel strength on various polymers against epoxy resin. PFMA-6 represents P(MMA/PFMA-6/PEO-OH) modified surface.

#### 5.4. Conclusions

The methacrylate-based terpolymers containing both PEO side chains and  $R_f$  groups, with different carbon numbers, in a single molecule were prepared, and mixed with PMMA/P(2F-4F) matrix. The water wettability and adhesive property on the terpolymer modified surfaces were investigated. The amount of the surface-segregated PEO side chain and peel strength depended on the carbon number of the  $R_f$  groups. These terpolymer modified surfaces showed high water repellency and adhesive property, and

environment-response. Especially, P(MMA/PFEA-6/PEO-OH) modified surface showed good adhesion property while avoiding PFOA problem.

## 5. 5. References

- [1] Tsibouklis, P.; Graham, P.; Eaton, P. J.; Smith, J. R.; Nevell, T. G.; Smart, J. D.; Even, R. J. *Macromolecules*, 2000, 33, 8460.
- [2] Imae, T.; Tabuchi, H.; Funayama, K.; Sato, A.; Nakamura, T.; Amaya, N. *Colloid and Surface A: Physicochem. Eng. Aspects*, 2000, 167, 73.
- [3] Pospiech, D.; Jehnichen, D.; Gottwald, A.; Häußler, L. Kolling, W.; Grundke, K.; Janke, A.; Schmit, S.; Werner, C. *Surface Coatings Int. Part B: Coating Transactions*, 2003, 86, 43.
- [4] Borkar, S.; Jankova, K.; Siesler, H. W.; Hvilsted, S. *Macromolecules*, 2004, 37, 788.
- [5] Bertolucci, M.; Galli, G.; Chiellini, E.; Wynne, K. J. *Macromolecules*, 2004, 37, 3666.
- [6] Gopalan, P.; Andruzzi, L.; Li, X.; Ober, C. K. *Macromol. Chem. Phys.*, 2002, 203, 1573.
- [7] van Ravenstein, L.; Ming, W.; van de Grampel, R. D.; van der Linde, R.; de With, G.; Loontjens, T.; Thüne, P. C.; Niemantsverdriet, J. W. *Macromolecules*, 2004, 37, 408.
- [8] Tokuda, K.; Kawasaki, M.; Kotera, M.; Nishino, T. *Langmuir*, revision required. Resubmission is undergoing.
- [9] Martin, J. W.; White, D. M.; Muir, D. C.G.; Mabury, S. A. *Environ.Sci.Technol.*, 2004, 38, 5379.
- [10] Tretinnikov, O. N.; Ikada, Y. *Langmuir*, 1994, 10, 1606.
- [11] Moraila-Martinez, C. L.; Ruiz-Cabello, F. J. M.; Cabrerizo-Vilchez, M. A. C. *Colloid and Surfaces A:Physicochem. Eng. Aspects*, 2012, 404, 63.
- [12] Hayes, R. A.; Ralston, J. *Colloid and Surfaces A:Physicochem. Eng. Aspects*, 1993, 80, 137.







## **Chapter 6**

**Low-fouling polymer surface prepared by controlled  
segregation of poly(ethylene oxide) and its  
functionalization with biomolecule**

## 6.1. Introduction

Immobilization and conjugation of functional biomolecules, such as antibody and enzyme, on substrate surfaces have been widely studied for detection of specific biomolecules. Preparation of these surfaces is a key step in construction of biosensors and biochips [1-4]. Since antibody reacts with antigen very selectively, antigen-antibody reaction is widely used in medical diagnostics and biosensing fields. However, nonspecific protein adsorption (fouling) on a surface is often a large problem for biosensors and biochips, since the fouling makes the detection inexactitude. It is of great importance to prevent nonspecific protein adsorption on a sensor surface and there have been, to date, a lot of efforts to achieve non-fouling surfaces. For instance, inexpensive and amphiphilic proteins derived from animals, such as bovine serum albumin (BSA), are widely used as a blocking reagent to mask a hydrophobic polymeric surface to prevent protein fouling in a microplate-based immunoassay. A polymer surface blocked by BSA, however, does not show satisfactory resistance to nonspecific protein adsorption and BSA-blocking sometimes interferes with antigen-recognition ability of antibody [5].

Poly(ethylene oxide) (PEO) is well-known to be a flexible, hydrophilic, electrostatically neutral and biocompatible polymer. A PEO-modified surface shows resistance to nonspecific protein adsorption and a low-toxic property [6-9]. To date, many methods have been reported to make PEO chains be segregated on surfaces: graft copolymerization of PEO macromonomer from a surface, covalent grafting of PEO to a surface, and so on [10, 11]. For example, grafting of PEO to hydrophobic surface was performed using argon plasma treatment. The grafting density of PEO was controlled by treating time. These surfaces showed hydrophilicity and low protein adsorption derived from PEO, and had possibilities of improvement by immobilization of biomolecule [12].

In our previous study, the preparation of the methacrylate-based terpolymers containing perfluoroalkyl ( $R_f$ ) groups and PEO side chains in the same molecules as surface modifiers was studied. Using these terpolymers, the surface-segregation of PEO side chains through a very simple method, dip-coating was succeeded. The terpolymer modified surfaces were

covered with  $R_f$  groups and PEO side chains according to the balance among the surface free energy, the free volume effect of PEO side chains and the interaction to matrix resin [13]. The terpolymer modified surface showed high water repellency and high adhesive strength simultaneously.

In this chapter, methacrylate-based terpolymers containing PEO side chains and  $R_f$  groups were synthesized. Terpolymer modified surfaces were prepared by dip-coating polyethylene terephthalate (PET) films with terpolymer solutions. Protein adsorption, anti-thrombogenic tests, and cell adhesion were performed to reveal low-fouling properties of the terpolymer modified surfaces. Moreover, the covalent immobilization of a functional biomolecule on the low-fouling surfaces using the termini of surface-segregated PEO side chains as reactive sites was attempted.

## 6. 2. Experimental

### 6. 2. 1. Materials

Methyl methacrylate (MMA, Nacalai Tesque, Inc., Kyoto, Japan) was distilled under reduced pressure before use. 2,2'-Azobis-isobutyronitrile (AIBN, Nacalai Tesque, Inc., Kyoto, Japan) was recrystallized from methanol. The fluorine-containing monomer 2-(perfluoroalkyl)ethyl acrylate (PFEA-4, 6, DIC Ltd., Tokyo, Japan and PFEA-8, Clariant Corp., Tokyo, Japan) and several PEO-containing macromonomer (PEO-OH: BLEMMEER PE-350D, NOF Co., Tokyo, Japan) were used as received. Poly(methyl methacrylate) (PMMA) (Acrypet VH, Mitsubishi Rayon Co. Ltd.,  $M_n = 41,100$ , Tokyo, Japan) was purified by reprecipitation by pouring a PMMA/methyl ethyl ketone (MEK, Nacalai Tesque, Inc., Kyoto, Japan) solution into methanol and used as a matrix resin for dip-coating. Vinylidene fluoride-tetrafluoroethylene copolymer ( $(\text{CH}_2\text{CF}_2)_{80}(\text{CF}_2\text{CF}_2)_{20}$ ,  $M_n = 69,300$ , Kynar SL, Atfina Chemicals Inc., Philadelphia, PA, USA) P(2F-4F) was used as another matrix resin without further purification. Bovine serum albumin (BSA) and fibrinogen were purchased from Sigma Co (St Louis, MO). Eagle's minimal essential medium containing Kanamycin (Eagle's MEM) was purchased from Nissui Pharmaceutical Co. (Tokyo, Japan).

1-Ethyl-3-(3-dimethylaminopropyl) carbodiimide hydrochloride (EDC) and biotinhydrazide were purchased from Indofine Chemical Company Inc. (Hillsborough, NJ) and Dojindo Molecular Technologies, Inc. (Kumamoto, Japan), respectively. AlexaFluor<sup>®</sup> 488-labeled streptavidin (0.1 mg/mL, Life Technologies Co., Carlsbad, California) and AlexaFluor<sup>®</sup> 647-labeled BSA (0.1 mg/mL, Life Technologies Co.) were used as fluorescence labeled proteins. Other chemicals were purchased from Nacalai Tesque, Inc (Kyoto, Japan).

Fresh human whole blood supplied from a health donor was collected at the medical center for student health, Kobe University. All samples were obtained in accordance with ethical committee regulations of Kobe University.

### 6. 2. 2. Sample preparation

The chemical formulae of the terpolymers used in this study are shown in Figure 6-1. The detailed procedure for the synthesis of terpolymers (P(MMA/PFEA-n/PEO-OH), n = 4, 6 or 8) was described in Chapter 5. Actual monomer compositions of these terpolymers were MMA : PFEA-n : PEO-OH = 1000 : 69 : 90 (n = 4), 1000 : 47 : 114 (n = 6) and 1000 : 27 : 110 (n = 8).

Poly(ethylene telephthalate) (PET) film dip-coated with each surface modifier was prepared with the same way described in Chapter 5.

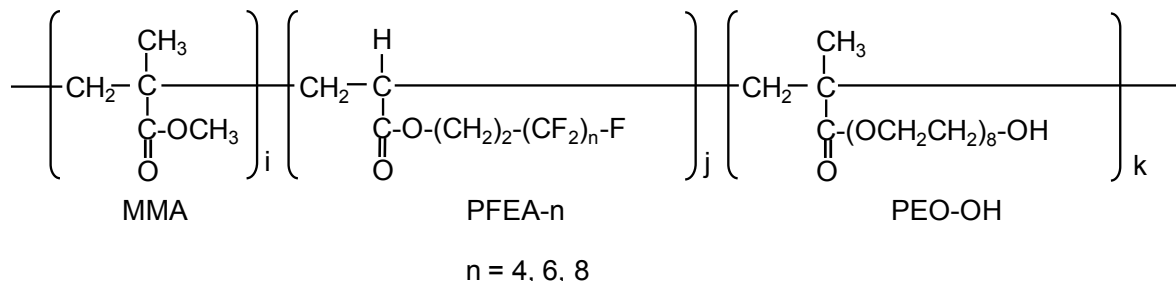


Figure 6-1 Chemical formulae of P(MMA/PFEA-n/PEO-OH). The ratios of I : j : k were 1000 : 69 : 90 for n = 4, 1000 : 47 : 114 for n = 6, and 1000 : 27 : 110 for n = 6.

### 6. 2. 3. Characterization

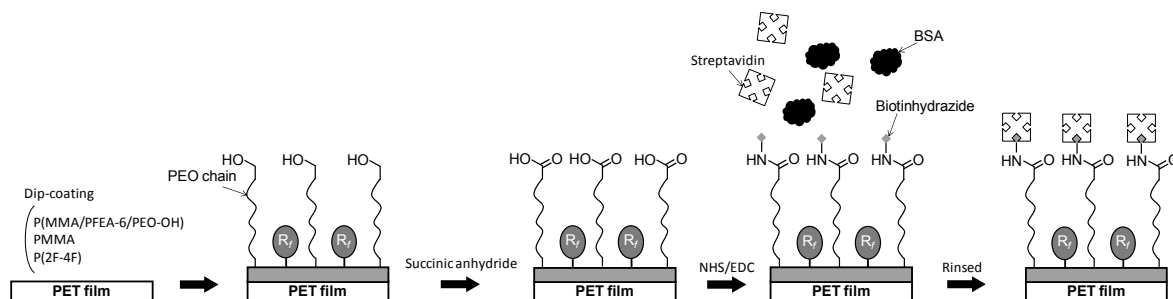
Sample films were immersed in a BSA solution (1 mg/mL, in phosphate buffered saline (PBS)) for 2.5 h at room temperature and rinsed for three times with distilled water to remove BSA weakly adsorbed on surfaces. The amount of BSA adsorbed on the surface was evaluated using the micro bicinchonic acid (BCA) method [14], where the absorbance change of the solution at 562 nm was measured using a UV-vis spectrophotometer (U-2000, Hitachi Ltd. Tokyo, Japan). As a reference, a PET film was used. The number of tested specimens was eight. The adsorption of fibrinogen to film surfaces was also evaluated. To estimate the protein adsorption via another method, XPS measurement for films after immersing in BSA solution was performed in the same way described in Chapter 4.

Antithrombogenic test and cell adhesion test were performed with the same method described in Chapter 1 and 4, respectively.

### 6. 2. 4. Immobilization of fluorescent compounds on terpolymer modified surfaces

PET films ( $0.7 \times 1.5$  cm) modified with a terpolymer (P(MMA/PFEA-6/PEO-OH)) were used for streptavidin immobilization on the surfaces. For surface immobilization experiment, the surface modified with P(MMA/PFEA-6/PEO-OH) is written as “PEO-OH”. To convert the hydroxy group of a PEO side chain in the terpolymer to a carboxy group, the terpolymer modified film was immersed in an ethanol/water (2/8 v/v) solution containing succinic anhydride (20% w/w) and a drop of perchloric acid as a catalyst. After 24 h at room temperature, a sample surface was washed with an excess amount of distilled water. The PET films were dried at room temperature overnight. A terpolymer modified surface was immersed in water containing NHS (100 mM) and EDC (400 mM) for 20 min at room temperature to convert a carboxy group to a reactive NHS ester. Then, a film was immersed in a solution of biontin hydrazide (10 mM in ethanol/water = 2/8 v/v) for 1 h at room temperature. To remove unreacted NHS esters, the films were immersed in a sodium borate buffer (pH 9.0) for 2 h at room temperature. Subsequently, the films were transferred to PBS (pH 7.4) containing AlexaFluor<sup>®</sup> 488-labeled streptavidin (0.1 mg/mL) and AlexaFluor<sup>®</sup> 647-labeled BSA (0.1 mg/mL). A film was washed for two times with PBS

and distilled water, respectively. The fluorescently labeled streptavidin and BSA were visualized  $\lambda_{\text{ex}} = 460 \text{ nm}$ ,  $\lambda_{\text{em}} = 515 \text{ nm}$  and  $\lambda_{\text{ex}} = 630 \text{ nm}$ ,  $\lambda_{\text{em}} = 670 \text{ nm}$ , respectively, using Image Quant LAS 4000 (GE Healthcare, Buckinghamshire, UK). The schematic illustration of preparation of the film surface by dip-coating was shown in Scheme 6-1.



Scheme 6-1 Schematic illustration of preparation of a low-fouling surface using dip-coating and of immobilization of streptavidin on its surface.  $R_f$  represents a perfluoroalkyl group.

### 6.3. Results and discussion

#### 6.3.1. Resistance to protein adsorption

Figure 6-2 shows the amounts of proteins (BSA and fibrinogen) adsorbed on terpolymer modified surfaces. These proteins are relatively hydrophobic and are widely used as model fouling proteins in biomedical and bioanalytical fields. While an original PET surface adsorbed  $1.2 \mu\text{g}/\text{cm}^2$  of BSA, the terpolymer modified surfaces adsorbed reduced amounts of proteins. For example, a PFEA-8-modified surface adsorbed only  $0.40 \mu\text{g}/\text{cm}^2$  of BSA, which was less than one-third of that of an original PET surface. In particular, the terpolymer modification of a PET surface was remarkably effective for reducing the adsorption amounts of fibrinogen. PFEA-4-modification reduced the adsorption amount of fibrinogen to  $0.30 \mu\text{g}/\text{cm}^2$ , while an original PET surface adsorbed  $1.1 \mu\text{g}/\text{cm}^2$ . The difference of the carbon number in  $R_f$  group of the terpolymer gave the variation in the resistance to protein adsorption. As our previous report, dip-coating the terpolymer with PMMA introduced PEO side chains on a surface. The PEO side chains were predominantly segregated on a top surface when the surface contacted with aqueous environment.

Moreover, in Chapter 3, it was found that the incorporation of P(2F-4F) to the dip-coating polymers promoted the surface-segregation of PEO side chains. That is why the terpolymer modified surfaces exhibited resistance to nonspecific protein adsorption. This resistance would originate from the excluded volume effect and high mobility of PEO chains being highly soluble in water.

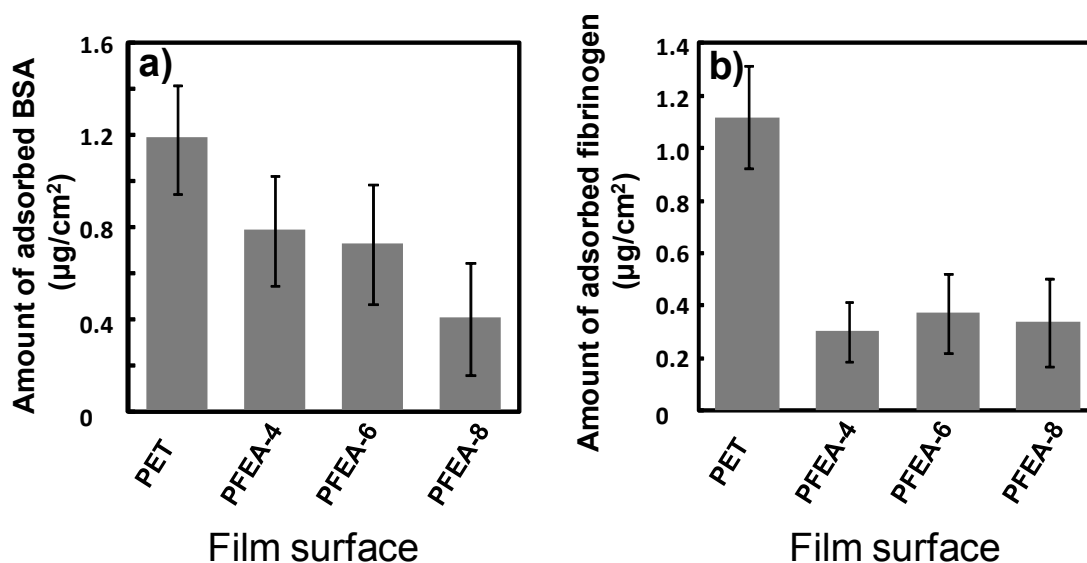


Figure 6-2 Amounts of (a) BSA, and (b) fibrinogen adsorbed on original and modified PET surfaces. The surface modification was performed by dip-coating a mixture of P(MMA/PFEA-*n*/PEO-OH), P(2F-4F), PMMA. Error bars represent standard deviations.

XPS measurement was also used for the detection of protein adsorption [15]. The  $N_{1s}$  spectra from XPS measurements are shown in Figure 6-3. The nitrogen signal can be used as an indicator of the relative amount of proteins adsorbed on the surface [16]. An original PET surface exhibited an  $N_{1s}$  peak around 402 eV, indicating the presence of adsorbed BSA. The terpolymer modification remarkably reduced the  $N_{1s}$  peak, implying the decrease of the BSA adsorption.



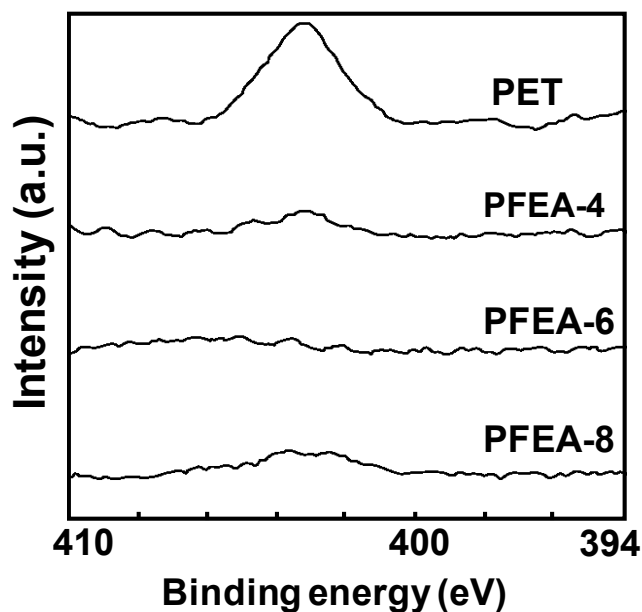


Figure 6-3 XPS N<sub>1s</sub> core level spectra of an original PET surface and terpolymer modified surfaces after BSA adsorption. PFEA-4, PFEA-6 and PFEA-8 represent PET films coated with a mixture of P(MMA/PFEA-n/PEO-OH), P(2F-4F) and PMMA.

### 6. 3. 2. Antithrombogenicity

Above investigations evaluated the adsorption of purified proteins on the terpolymer modified surfaces. In practical terms, a foulant is usually a mixture of proteins, other organic and inorganic compounds. For example, blood contains a wide variety of foulants and they are thought to be cooperatively adsorbed on a polymer surface. Then human whole blood was used to examine the antithrombogenicity of the terpolymer modified surfaces. Figure 6-4 shows that no clots were observed on the terpolymer modified surfaces, while there were obvious blood clots on an original PET surface. Clotting is usually caused by the aggregation and adhesion of platelets. They are triggered by fibrinogen adsorption, which is one of blood proteins. The antithrombogenicity obtained can be explained by the protein repellent characteristics of the terpolymer modified surfaces [17, 18].

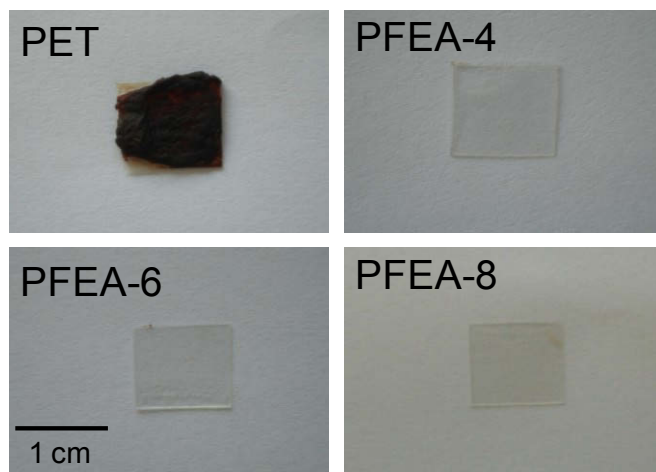


Figure 6-4 Optical photographs of original and surface modified PET films after immersed in whole human blood. PFEA-4, PFEA-6 and PFEA-8 represent PET films coated with a mixture of P(MMA/PFEA-n/PEO-OH), P(2F-4F) and PMMA.

### 6. 3. 3. Resistance to cell adhesion

Cell adhesion to a polymer surface is also known to be initiated by protein adsorption to a polymer surface [19]. The cell adhesion to an original PET surface and terpolymer modified surfaces cells was investigated by using L929 cells. Cell-adhesive proteins play a key role in the adhesion of L929 cells on a polymer surface and the cell propagation [20]. Figure 6-5A shows the cell adhesion on PET film surfaces, lower halves of which were coated with terpolymers. After culturing L929 cells for 2 days on the films, a number of cells adhered on the upper half of the film surfaces (Figure 6-5a-c), meaning the cell adhesion on an original PET surface. The terpolymer modified surfaces (lower halves of the films) exhibited negligible amounts of cell adhesion.

For evaluating the cell adhesion quantitatively, L929 cells that adhered on film surfaces were counted over 3 days. Figure 6-5B shows the effect of culture time on the cell density on an original PET surface and the terpolymer modified surfaces. Cell densities on all kinds

of the terpolymer modified surfaces were only one-eighth of that on an original PET film 3 days after seeded. These results reveal that the surface modification with terpolymers can prevent both cell adhesion and propagation on the surfaces. The reduced cell adhesion was probably due to the resistance to protein adhesion of PEO segregated surfaces. In particular, the PFEA-6-modified surface showed high resistance to the cell adhesion.

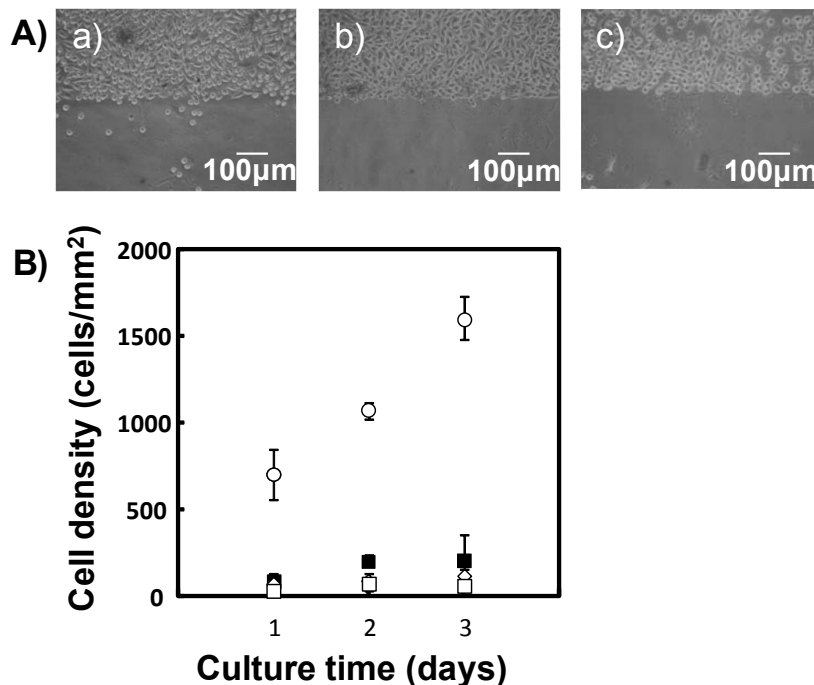


Figure 6-5 A) Optical micrographs of L929 cells seeded and cultured for 2 days on PET films. The lower halves of films were coated with a mixture of P(MMA/PFEA-n/PEO-OH), P(2F-4F) and PMMA. (a) P(MMA/PFEA-4/PEO-OH), (b) P(MMA/PFEA-6/PEO-OH) and (c) P(MMA/PFEA-8/PEO-OH). B) Effect of culture time on cell density of L929 cells on an original PET film and surface modified films. Original PET (○), P(MMA/PFEA-4/PEO-OH) (■), P(MMA/PFEA-6/PEO-OH) (□) and P(MMA/PFEA-8/PEO-OH) (◇).

#### 6. 3. 4. Covalent immobilization of biotin on a low-fouling surface

From the viewpoints of analytical chemistry and of biosensing, covalent immobilization of analytical molecular device (e.g. antibody, enzyme, oligonucleotide, ligand etc) on low-fouling surfaces is of great importance. However, a low-fouling surface is usually less

reactive and does not have reactive functional groups. In the present study, the terpolymer contained hydroxy groups at the termini of PEO side chains. Oxidization of the hydroxy groups of the terpolymer (P(MMA/PFEA-6/PEO-OH)) was performed to produce carboxy groups, and immobilization of a functional molecule (biotin hydrazide) on a terpolymer modified surface was attempted using the carboxy groups. Figure 6-6 shows the fluorescence images of an original PET film and surface modified films after immersed in an aqueous solution containing Alexa Fluor<sup>®</sup>647-labeled BSA (red) and Alexa Fluor<sup>®</sup>488-labeled streptavidin (green). An original PET surface shows strong red fluorescence derived from Alexa Fluor<sup>®</sup>647-labeled BSA, while the terpolymer modified surfaces (PEO-OH, PEO-COOH and PEO-biotin) exhibited weak red fluorescence. This means that the resistance to BSA adsorption derived from PEO chains was maintained even after the carboxylation of the PEO termini and the conjugation of biotinhydrazide to the PEO termini.

Only the biotin-immobilized surface (PEO-biotin) displayed strong green fluorescence derived from Alexa Fluor<sup>®</sup>488-labeled streptavidin, while an original PET surface and other terpolymer modified surfaces did not show green fluorescence. This means the successful carboxylation of the PEO termini and also the successful immobilization of biotin hydrazide. The terpolymer modified surface (PEO-OH) and the carboxylated surface (PEO-COOH) showed resistance to streptavidin adsorption. Streptavidin adsorption was inhibited even on an original PET film. This is possibly due to the blocking effect of adsorbed BSA. BSA molecules were predominantly adsorbed on an original PET film, which would prevent the streptavidin adsorption.

The difference among the results of micro BCA method, XPS, and fluorescence observation was due to the immersing time (micro BCA method: 2.5 h, XPS: 24h, fluorescence observation: 1h). These time conditions could not be unified because of their operation.

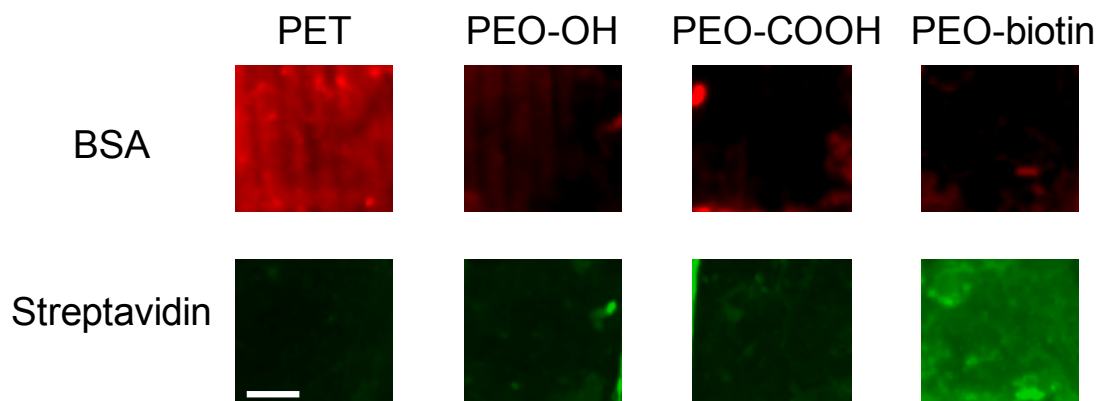


Figure 6-6 Fluorescence images of PET and terpolymer-modified surfaces that were treated with an aqueous solution containing Alexa Fluor<sup>®</sup>647-labeled BSA (red) and Alexa Fluor<sup>®</sup>488-labeled streptavidin (green). A mixture of P(MMA/PFEA-6/PEO-OH), P(2F-4F) and PMMA was used for the modification. PEO-COOH and PEO-biotin represent the terpolymer containing carboxy-terminated PEO and the terpolymer containing biotin-conjugated PEO. PET films were dip-coated with a mixture of P(MMA/PFEA-6/PEO-OH), P(2F-4F) and PMMA (PEO-OH). The hydroxy groups at termini of PEO chains in the terpolymer were carboxylated as illustrated in Scheme 1 (PEO-COOH). Then biotin hydrazide was conjugated with the carboxy groups (PEO-biotin). A scale bar represents 2 mm.

#### 6. 4. Conclusions

In the present study, methacrylate-based terpolymers containing  $R_f$  groups and PEO side chains in the same molecule were used to dip-coat a PET film. The terpolymer modified surfaces showed resistance to protein adsorption, antithrombogenicity and resistance to cell adhesion. These anti-fouling properties were due to the surface-segregated PEO side chains of the terpolymers. Moreover, the carboxylation of the PEO termini and covalent immobilization of biotin on the PEO segregated surface were succeeded. The biotin-functionalized surface recognized streptavidin in the presence of other protein. The present study proposed the simple surface modification via dip-coating synthetic terpolymers to achieve low-fouling properties and ligand-immobilization.

## 6. 5. References

- [1] Bernard, A.; Delamarche, E.; Schmid, H.; Michel, D.; Bosshard, H. R.; Biebuyck, H. *Langmuir*, 1998, 14, 2225.
- [2] Peterbauer, T.; Heiz, J.; Olblich, M.; Hering, S. *Lab. Chip.*, 2006, 6, 857.
- [3] Yates, J. R.; Speicher, S.; Griffin, P. R.; Hunkapiller, T. *Anal. Biochem.*, 1993, 214, 397.
- [4] Schweitzer, B.; Roberts, S.; Grimwade, B.; Shao, W.; Velleca, M.; Kingsmore, S. F. *Nat. Biotechnol.*, 2002, 20, 359.
- [5] Yuan, X.; Yoshimoto, K.; Nagasaki, Y. *Anal. Chem.*, 2009, 81, 1549.
- [6] Holmberg, K.; Bergstorm, K.; Osterberg, E.; Tiberg, F.; Harris, J. M. *J. Adhes. Sci. Technol.*, 1993, 7, 503.
- [7] Ista, L. K.; Fan, H.; Baca, O.; Lopez, G. P. *FEMS Microbiol. Lett.*, 1996, 142, 59.
- [8] Lee, J. H.; Andrade, J. D. *Prog. Polym. Sci.*, 1995, 20, 1043.
- [9] Jo, S.; Park, K. *Biomaterials*, 2000, 21, 605.
- [10] Lee, J. H.; Kopecek, J.; Andrade, J. D. *J. Biomed. Mater. Res.*, 1989, 23, 351
- [11] Lens, J. P.; Harmsen, P. F. H.; Ter Schegget, E. M.; Terlingen, J. G. A.; Engbers, G. H. M.; Feijen, J. *J. Biomater. Sci. Polymer*, 1997, 8, 963.
- [12] Qie, Y. X.; Klee, D.; Pluster, W.; Severich, B.; Hocker, H. *J. Apply. Polym. Sci.*, 1996, 61, 2373.
- [13] Tokuda, K.; Noda, M.; Kotera, M.; Nishino, T. "Multifunctional Polymer Surface with Segregation of Poly(ethylene oxide) Side Chains." Proceedings of ADHESION'13, pp.61-65, Society of Adhesion and Adhesives (SAA), York, United Kingdom (2013).
- [14] Smith, P. K.; Krohn, R. I.; Hermanson, G. T.; Mallia, A. K.; Gartner, F. H.; Provenzano, M. D.; Fujimoto, E. K.; Geoke, N. M.; Olson, B. J.; Klenk, D. C. *Anal. Biochem.*, 1985, 150, 76.

- [15] Pillai, S.; Arpanaei, A.; Meyer, R. L.; Birkedal, V.; Gram, L.; Besenbacher, F.; Kingshott, P. *Biomacromolecules*, 2009, 10, 2759.
- [16] Czuha, M. Jr.; Riggs, W. *Anal. Chem.*, 1975, 47, 1836.
- [17] Tanaka, M.; Motomura, T.; Kawada, M.; Anzai, T.; Kasori, Y.; Shiroya, T.; Shimura, K.; Onishi, M.; Mochizuku, A. *Biomaterials*, 2000, 21, 1471.
- [18] Vroman, L.; Adams, A. L. *J. Biomed. Mater. Res.*, 1969, 3, 43.
- [19] George, P. A.; Donose, B. C.; Cooper-White, J. J. *Biomaterials*, 2009, 30, 2449.
- [20] Yu, Q.; Zhang, Y.; Chen, H.; Zhou, F.; Wu, Z.; Huang, H.; Brash, J. L. *Langmuir*, 2010, 26, 8582.







## **Conclusions**

In this thesis, commodity polymer surfaces were functionalized by the two simple methods using fluorine chemistry. One was direct surface fluorination using a fluorinated reagent (Part I). The other was dip-coating with a fluorine-containing terpolymer as a surface modifier (Part II). Fluorine-containing groups were used not only for giving fluorine-specific properties to a polymer surface, but also for the induction of surface-segregation of other functional group. The properties of the functionalized polymer surfaces were investigated using a combination of various measurements such as dynamic contact angle, 90°-peel test, atomic force microscopy, X-ray diffraction, X-ray photoelectron spectroscopy, micro BCA method, antithrombotic test, and cell adhesion. The results were summarized as shown below.

**Part I** is concerned with the preparation of low energy surface using fluorine-containing groups. Part I is composed of Chapter 1 and Chapter 2.

In **Chapter 1**, properties of fluorinated poly(methyl methacrylate) (PMMA) surface prepared using a reactive fluorinated reagent were evaluated. While a PMMA surface has no functional groups which can be reacted with glycidyl groups of fluorinated reagent, the fluorination used in this thesis was effective. Moreover, the fluorinated PMMA surface was stable under wet and heated conditions. The fluorinated PMMA surface possessed high water repellency, resistance to fingerprint and to protein adsorption derived from fluorine. The fluorinated PMMA surface showed very low surface free energy ( $\gamma_s$ ) value of 10.0 mJ/m<sup>2</sup>, which was lower than that (22 mJ/m<sup>2</sup>) of polytetrafluoroethylene.

In **Chapter 2**, the *n*-perfluoroeicosane (C<sub>20</sub>F<sub>42</sub>) thin films were vapor-deposited on a glass under various conditions. The relationship between  $\gamma_s$  and the orientation of the perfluoroalkyl (R<sub>f</sub>) groups, which were highly fluorinated hydrocarbon, was investigated. For the lowest  $\gamma_s$  value of 6.7 mJ/m<sup>2</sup>, precise control of the surface structure, especially, total coverage of the surface with -CF<sub>3</sub> groups was necessary, while the surface exposure of -CF<sub>2</sub>- group increased the  $\gamma_s$  value. In addition, slightly inclined R<sub>f</sub> groups also increased the  $\gamma_s$  value.

In general, use of fluorine is effective for lowering the  $\gamma_s$ . However, as exemplified by PTFE, many fluorinated surfaces showed the  $\gamma_s$  value down to 10 mJ/m<sup>2</sup> for this reason.

In **Part II**, the R<sub>f</sub> groups were used as a driving force for the surface-segregation of other functional groups. The surface-segregation of poly(ethylene oxide) (PEO) side

chains of a methacrylate-based polymer, which were originally difficult to be segregated on material surfaces, was investigated. The methacrylate-based terpolymers containing both the  $R_f$  group and PEO side chain in a single molecule were synthesized and used as surface modifiers with matrix resin, which was composed of PMMA and fluorine copolymer. A poly(ethylene terephthalate) (PET) film was adopted as a substrate. The effects of the PEO side chain length, compositions of the matrix resin, PEO termini, and the carbon number of the  $R_f$  groups on the surface-segregation of PEO side chains were investigated. Part II is composed of Chapters 3, 4, 5 and 6.

In **Chapter 3**, PET surfaces were modified using methacrylate-based terpolymers containing both the  $R_f$  groups and PEO as side chains in a single molecule. A PET substrate was dip-coated with the terpolymer and a matrix resin composed of PMMA and fluorine copolymer. The morphology and properties of the terpolymer modified surfaces were evaluated by varying the PEO side chain length and the composition of matrix resin. It was found that not only the  $R_f$  groups but also PEO side chains were segregated on the surface. This is considered to be brought by the balances among the three driving forces: surface free energy of the  $R_f$  group, entropy effect due to free volume of PEO side chain, and interaction between the  $R_f$  groups and a fluorine copolymer used as the matrix resin. Under the optimized conditions, the terpolymer modified surface showed high water repellency due to the  $R_f$  groups and high adhesive property due to PEO side chains, simultaneously. These surfaces showed rapid and reversible environment-responsiveness.

In **Chapter 4**, to reveal the effects of PEO termini in the terpolymer on surface properties, the adhesive and low-fouling properties of terpolymer modified surfaces were investigated. The results indicated that large amounts of PEO side chains were surface-segregated when the PEO termini were conjugated with  $R_f$ ' groups. The results also revealed that both an amount of surface-segregated PEO side chains and PEO termini affected on surface properties. When the PEO termini were hydroxy groups, the terpolymer modified surface comprehensively showed good adhesive property and low-fouling properties.

In **Chapter 5**, to reveal the effects of the carbon numbers of the  $R_f$  groups on surface properties, the adhesive property of terpolymer modified surfaces were investigated. It was found that the amount of surface-segregated PEO side chains and 90°-peel strength

against epoxy resin changed depending on the carbon number of the  $R_f$  groups. Especially, when the carbon number was 6, a large amount of PEO side chains were surface-segregated and the surface showed high 90°-peel strength (9.1 N/cm), which was twice as high as that of the terpolymer modified surface with the carbon number of 8. The terpolymer modified surfaces showed high water repellency and adhesive property, and environment-responsiveness. The terpolymers synthesized in Chapters 3, 4, and 5 acted not only as a multifunctional coating agent but also as an effective primer for adhesion to fluorine-containing surface because of their  $R_f$  groups.

In **Chapter 6**, under the conditions in which large amount of PEO side chains were surface-segregated, terpolymer modified surfaces showed low-fouling properties to several foulants. On the terpolymer modified surfaces, forming of clots and cell adhesion triggered by protein adsorption were prevented. The terpolymer modified surfaces were highly effective in reducing protein adsorption, and showed one-third of the amount of protein adsorption for an original PET surface. Moreover, the covalent immobilization of a functional biomolecule on the low-fouling surface was attempted using the terpolymer. As a result, the terpolymer-modified surface showed selective protein adsorption and resistance to nonspecific protein adsorption.

The conditions for surface-segregation of PEO side chains achieved in this thesis were summarized as shown below. Taking account of a bioaccumulation problem and a crystallization of the  $R_f$  groups, the optimized carbon number of the  $R_f$  group was 6. For the PEO side chain length, when it was 9 ~ 22, large amounts of PEO side chains were surface-segregated. The terpolymers with PEO side chain lengths of more than 40 showed scanty surface-segregation. The optimized amount of fluorine copolymer in matrix resin, 40% w/w, did not depend on the carbon numbers of the  $R_f$  groups. This result might be applied other surface modifiers containing the  $R_f$  groups.

In summary, this thesis describes the surface functionalization using fluorine chemistry, which involved two approaches: direct fluorination of a surface and dip-coating with perfluorocarbon-containing terpolymers. While it is already known that fluorine-induction to a surface is effective to obtain low  $\gamma_s$ , this thesis revealed that the precise control of its surface structures (orientation of  $R_f$  groups, surface density and so on) was also important for low  $\gamma_s$ , leading to low-fouling properties, unique adhesive properties and low cell adhesion. In particular, total coverage of the surface with  $-CF_3$

groups was essential for the lowest  $\gamma_s$ . Furthermore, the surface-segregation of the fluorine-containing groups induced a surface-segregation of hydrophilic functional groups in a polymer, which are difficult to be surface-segregated naturally. This work gives the important insights to prepare a low  $\gamma_s$  surface and a multifunctional surface using the  $R_f$  groups. These surface functionalization techniques using fluorine-containing polymers are expected to have great potential for designing and controlling surface properties of solid materials.



# List of Achievements



# Publications

## **Chapter 1**

1. Simple Method for Lowering Poly(methyl methacrylate) Surface Energy with Fluorination

Kaya Tokuda, Tomoya Ogino, Masaru Kotera, Takashi Nishino

*Polymer Journal*, **47**, 66-70, 2015.

## **Chapter 2**

2. Surface Structure to Achieve the Surface Free Energy Lower Than 10 mJ/m<sup>2</sup>

Takashi Nishino, Masashi Meguro, Kaya Tokuda, Yasukiyo Ueda

*The Journal of the Adhesion Society of Japan*, accepted in 29 October 2014.

## **Chapter 3**

3. Highly Water Repellent but Highly Adhesive Surface with Segregation of Poly(ethylene oxide) Side Chains

Kaya Tokuda, Motoko Kawasaki, Masaru Kotera, Takashi Nishino

*Langmuir*, **31**, 209-214, 2015.

## **Chapter 4**

4. 末端を異にするポリエチレンオキシド側鎖の表面偏析を利用した機能性高分子表面の創製

徳田 桂也, 野田 実希, 小寺 賢, 西野 孝, 第 64 回高分子学会年大会, 高分子学会, 札幌, 2015 (発表予定).

## **Chapter 5**

5. Multifunctional Polymer Surface with Segregation of Poly(ethylene oxide) Side Chains

Kaya Tokuda, Miki Noda, Masaru Kotera, Takashi Nishino, Proceedings of ADHESION'13, pp.61-65, Society of Adhesion and Adhesives (SAA), York, United Kingdom, 2013 (to be submitted).

**Chapter 6**

6. A low-fouling polymer surface prepared by controlled segregation of poly(ethylene oxide) and its functionalization with biomolecules

Kaya Tokuda, Miki Noda, Tatsuo Maruyama, Masaru Kotera Takashi Nishino  
*Polymer Journal*, accepted in 12 November 2014.

**The author also contributed to the following paper.**

7. Surfactant-induced Polymer Segregation to Produce Anti-fouling Surfaces via Dip-coating with an Amphiphilic Polymer

Syunsuke Yamamoto, Sigeru Kitahata, Ayane Shimomura, Kaya Tokuda, Takashi Nishino, Tatsuo Maruyama  
*Langmuir*, accepted in 5 December 2014.

## Presentations

1 含フッ素基を利用したポリエチレンオキシド側鎖の表面偏析とその機能

徳田桂也, 河崎元子, 野田実希, 小寺賢, 西野孝

口頭, 第 145 回ポバール会, 京都, 2014

2 ディップコート法によるタンパク質の選択的吸着高分子表面の創製

徳田桂也, 野田実希, 丸山達生, 小寺賢, 西野孝

ポスター, 日本化学会秋季事業第 4 回 CSJ 化学フェスタ 2014, 東京, 2014

3 表面に偏析したポリエチレンオキシド側鎖を利用したタンパク質の選択的吸着

徳田桂也, 野田実希, 丸山達生, 小寺賢, 西野孝

ポスター, 第 63 回高分子学会年次大会, 愛知, 2014

4 含フッ素基を含む多機能高分子表面の創製

徳田桂也

口頭, 神戸大学界面科学研究センターコロキウム「高分子界面」, 兵庫, 2014

5 ポリエチレンオキシド側鎖の表面偏析を利用した多機能表面の創製

徳田桂也, 野田実希, 小寺賢, 西野孝

口頭, 平成 25 年度プラスチック成形加工学会関西支部第 3 回若手セミナー, 京都, 2013

6 ポリエチレンオキシド側鎖の表面偏析を利用した高撥水・高接着性表面の創製

徳田桂也, 野田実希, 小寺賢, 西野孝

ポスター, 平成 25 年度プラスチック成形加工学会関西支部第 3 回若手セミナー, 京都, 2013

7 Multifunctional Polymer Surface with Segregation of Poly(ethylene oxide) Side Chains

Kaya Tokuda, Miki Noda, Masaru Kotera, Takashi, Nishino

英語口頭, ADHESION'13, York, UK, 2013

**8** ポリエチレンオキシド側鎖が偏析した高分子表面の接着性

徳田桂也, 野田実希, 本郷千鶴, 小寺賢, 西野孝

ポスター, 第 59 回高分子研究発表会(神戸), 兵庫, 2013

**9** 表面に偏析したポリエチレンオキシド側鎖を用いた表面改質と機能発現

徳田桂也, 野田実希, 小寺賢, 西野孝

ポスター, 第 20 回クロマトグラフィーシンポジウム, 兵庫, 2013

**10** フッ素化試薬を用いたポリメタクリル酸メチル表面の低表面自由エネルギー化

徳田桂也, 荻野智也, 小寺賢, 西野孝

ポスター, 第 51 回日本接着学会年次大会, 東京, 2013

**11** Multifunctional Polymer Surface Using Segregated Poly(ethylene oxide) Side Chains

Kaya Tokuda, Miki Noda, Masaru Kotera, Takashi Nishino

英語口頭, 第 62 回高分子学会年次大会, 2013

**12** フッ素化試薬を用いた低エネルギー化ポリメタクリル酸メチル表面の創製

徳田桂也, 荻野智也, 小寺賢, 西野孝

ポスター, 第 61 回高分子討論会, 愛知, 2012

**13** ポリエチレンオキシド側鎖が偏析した高分子表面におけるタンパク質の吸着挙動

徳田桂也, 野田実希, 小寺賢, 西野孝

ポスター, 第 8 回日本接着学会関西支部若手の会

**14** 表面に偏析したポリエチレンオキシド側鎖を用いた高撥水・高接着性高分子表面の創製

徳田桂也, 野田実希, 小寺賢, 西野孝

ポスター, 第 50 回日本接着学会年次大会, 福島, 2012

**15** ポリエチレンオキシド側鎖が偏析した機能性高分子表面の創製

徳田桂也, 野田実希, 小寺賢, 西野孝

口頭, 第 60 回高分子討論会, 岡山, 2011

**16** ポリエチレンオキシド側鎖の偏析を利用した多機能表面の創製

徳田桂也, 野田実希, 小寺賢, 西野孝

口頭, 第 57 回高分子研究発表会(神戸), 兵庫, 2011

**17** ポリエチレンオキシド側鎖の偏析を利用した表面改質と機能発現

徳田桂也, 小寺賢, 西野孝

ポスター, 第 49 回日本接着学会年次大会, 愛知, 2011

# Awards

- 1 2013年11月 平成25年度プラスチック成形加工学会関西支部第3回若手セミナー，京都，ポスター発表  
ポスター賞受賞



## Acknowledgement

First of all, I would like to express my deepest gratitude to Professor Dr. Takashi Nishino of Department of Chemical Science and Engineering, Faculty of Engineering in Kobe University, for his continuous encouragement, precious suggestions, helpful discussions and advice through my research life. He is the person who first showed me the attraction of polymer science, and introduced me to the doctoral course. It would have not been possible to continue my experiment and research without his endless patient, deeply expertise guidance and encouragement.

I am very grateful to Assistant professor Dr. Masaru Kotera of Department of Chemical Science and Engineering, Faculty of Engineering in Kobe University, for his fruitful discussions, invaluable feedback, and technical support. I was continually amazed by his broad knowledge and idea.

I am also grateful to Assistant professor Dr. Chizuru Hongo Organization of Advanced Science and Technology in Kobe University, for her helpful guidance and fruitful suggestions.

I would like to express my sincere gratitude to Associate professor Dr. Tatsuo Maruyama of Department of Chemical Science and Engineering, Faculty of Engineering in Kobe University, for his helpful suggestions and instruction of protein adsorption experiments using fluorescence reagents and for reviewing the thesis and for his precious advices in public hearing. I received not only useful advice but also the opportunity to reconsider my study.

We would like to thank Associate professor Dr. Chiaki Ogino of Department of Chemical Science and Engineering, Faculty of Engineering in Kobe University and Specially appointed associate professor Dr. Kiyotaka Hara of Organization of Advanced Science and Technology in Kobe University for allowing us to use Image Quant LAS 4000, and for their great technical assistant.

I wish to express my special thanks to Atsunori Mori and Naoto Omura of Chemical



Science and Engineering, Faculty of Engineering in Kobe University, for reviewing the thesis and for their precious advices in public hearing.

All former and present colleagues in Nishino laboratory at Department of Chemical Science and Engineering, Faculty of Engineering in Kobe University are thankfully acknowledged for the great support. I could not continue my research life without their wonderful collaborative effort, useful discussion, and unending encouragement. Ms. Seira Morimune, Mr. Koji Nobuta, Mr. Makoto Hayasaka, Ms. Maiko Ariyoshi, Ms. Megumi Komada, Mr. Yoshihito, Tanaka, Ms. Yoko Fuke, Mr. Yuki Fujishita, Mr. Motoki Fujimoto, Mr. Chenghui Ho, Mr. Naoyuki Miki are specially thank for their wonderful group organizing efforts. The comfortable workplace was absolutely essential for finishing this thesis. They were friendly, kind and cheerful about everything. It was a great honor to be able to work at such a fulfilling group.

In addition, I am indebted to Ms. Misato Kaishima of Kondo laboratory at Department of Chemical Science and Engineering, Faculty of Engineering in Kobe University. She is my colleague in the doctoral course and good counselor, her warm encouragement and scholarly advice helped my research.

I am grateful to all the staffs in the Department of Chemical Science and Engineering, Faculty of Engineering in Kobe University for their support.

I also would like to express my gratitude to Ms. Yoshimi Ozaki in Nishino laboratory at Department of Chemical Science and Engineering, Faculty of Engineering in Kobe University for her invaluable help and encouragement. KTC are acknowledged for the generous financial support.

Finally, I wish to extend my deepest gratitude to my family, Mamoru Tokuda, Jyunko Tokuda and Akari Tokuda and all relatives for their great patience and warm support.

January, 2015

Kaya Tokuda



Doctor Thesis, Kobe University

“Preparation of Functional Polymer Surface with Fluorine-containing Groups”, 116 pages

Submitted on January, 22, 2015

The date of publication is printed in cover of repository version published in Kobe University Repository  
Kernel.

© Kaya Tokuda  
All Right Reserved, 2015